

University of Louisville

ThinkIR: The University of Louisville's Institutional Repository

Electronic Theses and Dissertations

12-2022

Cadence and range of motion modulate pedal force in a rat model of motorized cycling after spinal cord injury.

Gregory J.R. States
University of Louisville

Follow this and additional works at: <https://ir.library.louisville.edu/etd>

Recommended Citation

States, Gregory J.R., "Cadence and range of motion modulate pedal force in a rat model of motorized cycling after spinal cord injury." (2022). *Electronic Theses and Dissertations*. Paper 4024.
Retrieved from <https://ir.library.louisville.edu/etd/4024>

This Doctoral Dissertation is brought to you for free and open access by ThinkIR: The University of Louisville's Institutional Repository. It has been accepted for inclusion in Electronic Theses and Dissertations by an authorized administrator of ThinkIR: The University of Louisville's Institutional Repository. This title appears here courtesy of the author, who has retained all other copyrights. For more information, please contact thinkir@louisville.edu.

CADENCE AND RANGE OF MOTION MODULATE PEDAL FORCE IN A RAT MODEL
OF MOTORIZED CYCLING AFTER SPINAL CORD INJURY

By

Gregory J.R. States

B.S., University of Louisville, 2013

MEng., University of Louisville, 2016

A Dissertation

Submitted to the Faculty of the
School of Medicine at the University of Louisville

In Partial Fulfillment of the Requirements

for the Degree of

Doctor of Philosophy in Anatomical Sciences and Neurobiology

Department of Anatomical Sciences and Neurobiology

University of Louisville

Louisville, KY

December 2022

Copyright 2022 by Gregory J.R. States

All rights reserved

CADENCE AND RANGE OF MOTION MODULATE PEDAL FORCE IN A RAT MODEL
OF MOTORIZED CYCLING AFTER SPINAL CORD INJURY

By

Gregory J.R. States

B.S., University of Louisville, 2013

MEng., University of Louisville, 2016

A Dissertation Approved on

November 16, 2022

by the following Dissertation Committee:

Dissertation Director – Dr. David Magnuson

Dr. Jeffrey C. Petruska

Dr. David M. Rouffet

Dr. Thomas J. Roussel

Dr. Chad L. Samuelsen

DEDICATION

This thesis is dedicated to my parents – Christopher States and Germaine Russo – who have provided me with love, support, and a balanced appreciation of both arts and sciences.

ACKNOWLEDGMENTS

I would first like to thank Dr. Magnuson, who has been a mentor to me during all phases of my higher education. Starting from my time as a co-op he has led through a combination of insightfulness, dedication, and humility that has guided me to be a better scientist. He is unafraid to tackle hard questions and put his ideas to the test, which has helped me open and challenge myself (even if I still have plenty of work to do in that regard). Next, I would like to thank my committee members. Dr. Roussel has been an excellent teacher, both as my undergraduate professor and committee member. He was instrumental in the design and fabrication of the instrumented pedals by providing expertise and open access to his lab, 3D printers, and tools. His enthusiasm for engineering and science is inspirational. Dr. Rouffet provided a comprehensive knowledge of cycling biomechanics which was instrumental to the completion of the motorized cycling studies. He has pushed me to critically think about all aspects of my projects from study design to clinical relevance. Dr. Petruska consistently developed inventive ideas and challenged me to think outside of the box. He is extremely generous with his time and makes science fun to discuss. Dr. Samuelsen provided an outside perspective and guidance for the next step in my career. He also generously provided access to tools and materials that were necessary for the development of the instrumented cycles.

Thank you to all the members of KSCIRC who have helped me over the years. Alice Shum-Siu provided knowledge of many technical aspects of these studies and was single-handedly responsible for the success of the c-Fos immunohistochemistry. Her

kind, welcoming, and generous attitude helped me grow into the lab as a co-op and never stopped through my PhD. Our team of hardworking technicians and co-cops made this work possible. Danni Oakley, Christian Buckley, and Trevor Clark have greatly contributed to several aspects of this project from animal care to data analysis. Finally, thank you to my fellow graduate students. Morgan Sharp, Greta Cesarz, Carlos Almeida, Brandon Brown, and McKenna Butler have always been willing to help, and are great friends who made the PhD experience more enjoyable. Anastasia Keller, Katie Harman, Katie DeVeau, and Krista Caudle all did fantastic work that my thesis builds upon. I could not have asked for a better group of graduate students to work with. Thank you to the KSCIRC core personnel: Christine Yarberry, Darlene Burke, Johnny Morehouse, and Jason Beare were instrumental in the surgeries, statistical analyses, kinematics acquisition, and microscopy that was involved in this study. I would also like to thank the RRC staff for providing a high level of care to the animals involved in this study.

Finally, thank you to my family and friends who have supported me along the way. My parents have provided me with the support and foundation to succeed. My sister Vanessa will forever be my friend who is always available to help me with my problems and support me even when they are self-inflicted. My wife Chelsea has always been there to love me when I am not my best, and patiently support me through the good and difficult times in our lives.

ABSTRACT

CADENCE AND RANGE OF MOTION MODULATE PEDAL FORCE IN A RAT MODEL OF MOTORIZED CYCLING AFTER SPINAL CORD INJURY

Gregory J.R. States

November 16, 2022

Motorized cycling (MC) can be utilized post-spinal cord injury (SCI) in patients who lack the strength and/or stability to participate in traditional physical exercise interventions. MC has been applied with the goal of improving locomotor function or cardiovascular health in both human and animal models of SCI. However, a discrepancy exists between the results of human and animal studies of MC, particularly regarding cardiovascular outcomes. Despite the abundance of studies in both humans and animals, the mechanism behind the improvements in cardiovascular function following MC are poorly understood.

We posited that increased venous return during MC is likely due to the skeletal muscle pump, where muscle activity during MC would be triggered by stretch reflexes. As stretch reflexes are dependent on both rate and length of muscle stretch, we hypothesized that cycling cadence and crank length could modulate muscle activity and therefore hindlimb loading during cycling. Although this theory implies that more reflex activation during MC might lead to more cardiovascular benefits, previous work from Anastasia Keller in our lab demonstrated that stretching hindlimb muscles disrupted

locomotion, and that this disruption is dependent on nociceptive afferents. The beginning of this thesis is a continuation of this finding, which revealed that naltrexone – primarily a μ -opioid receptor antagonist – exacerbated spasticity during stretching and increased the rate of locomotor decline.

When beginning studies on MC, the goal was to describe the relationship between electromyography (EMG), heart rate (HR)/blood pressure (BP), and pedal force (PF). Several design iterations of a pedal to measure force were produced. Initial studies testing the development of the pedals noted spasticity that was represented in the force traces, and a filtering technique was developed to separate spastic from non-spastic forces. Results from a study using this technique combined with EMG of a knee flexor and extensor suggest that higher cadences (≥ 30 RPM) increased RMS EMG and non-spastic forces, while lower cadences (≤ 15 RPM) increased spastic forces. Muscle activity often occurred during the lengthening phase, although a significant amount of overlap was observed as spasticity caused coactivation of the biceps femoris and vastus lateralis that was most likely to occur from early-mid extension through early flexion. Furthermore, telemetric measurements of HR/BP were recorded with force and hindlimb kinematics during MC using two crank lengths and multiple cadences. The shorter crank length decreased range of motion (ROM) particularly in the hip and knee. The result of lower ROM was a decrease in spastic forces and non-spastic forces in extension, but not flexion. Large spastic events were associated with a brief increase in BP followed by a large decrease, while high cadence cycling with limited spasticity appeared to elevate BP and HR above baseline levels. These results suggest that MC in rats may constitute a mild eccentric training regimen; clinical translation may therefore be dependent on the ability to reflexively generate muscle contraction in patients during cycling.

TABLE OF CONTENTS

DEDICATION	iii
ACKNOWLEDGEMENTS.....	iv
ABSTRACT	vi
LIST OF FIGURES	x
CHAPTER I. PRIMARY AND SECONDARY COMPLICATIONS OF SPINAL CORD INJURY AND POST-RECOVERY REHABILITATION STRATEGIES ¹	
<i>Introduction</i>	1
<i>Secondary Complications: Spasticity</i>	3
<i>Secondary Complications: Pain</i>	5
<i>Secondary Complications: Cardiovascular Dysfunction</i>	6
<i>Rehabilitation Strategies Following Spinal Cord Injury</i>	9
<i>Gait Training</i>	10
<i>Eccentric Training</i>	12
<i>Stretching</i>	13
<i>Functional Electrical Stimulation (FES) Cycling</i>	14
<i>Motorized Cycling (Humans)</i>	16
<i>Motorized Cycling (Rodents)</i>	17
<i>Closing Remarks</i>	19
<i>Specific Aims and Hypothesis</i>	21
CHAPTER II. BROAD OPIOID ANTAGONISM AMPLIFIES DISRUPTION OF LOCOMOTOR FUNCTION FOLLOWING THERAPY-LIKE HINDLIMB STRETCHING IN SPINAL CORD INJURED RATS	23
<i>Introduction</i>	23
<i>Materials and Methods</i>	24
<i>Results</i>	33
<i>Discussion</i>	47
III. CADENCE-MODULATED FORCES AND EMG RESPONSES IN A RAT MODEL OF MOTORIZED CYCLING	52

<i>Introduction</i>	52
<i>Materials and Methods</i>	54
<i>Results</i>	64
<i>Discussion</i>	85
IV. INFLUENCE OF RANGE OF MOTION AND CADENCE ON FORCE AND CARDIOVASCULAR OUTCOMES IN A RAT MODEL OF MOTORIZED CYCLING	91
<i>Introduction</i>	91
<i>Materials and Methods</i>	93
<i>Results</i>	98
<i>Discussion</i>	113
V. OVERALL DISCUSSION	117
<i>Summary</i>	117
<i>Spasticity During Cycling</i>	118
<i>Spastic forces: phasic spasticity?</i>	118
<i>Non-spastic forces: tonic spasticity?</i>	121
<i>Cardiovascular Effects of Motorized Cycling</i>	122
<i>Effects of Transmitter Implant on SCI Recovery</i>	124
<i>Clinical translation: potential hurdles</i>	125
<i>Future Directions and Potential Clinical Translations</i>	129
REFERENCES.....	132
LIST OF ABBREVIATIONS AND SYMBOLS.....	150
CURRICULUM VITA	153

LIST OF FIGURES

FIGURE	PAGE
Figure 1. Timeline indicating the key timepoints for the naltrexone stretching study.	25
Figure 2. Spasticity assessment during the first, second, and third week of stretching. .	33
Figure 3. BBB Open Field Locomotor Scores.	36
Figure 4. Responses to thermal and magnetic tail-stimulation before and after naltrexone.	39
Figure 5. CGRP quantification and analysis of naltrexone and saline treated rats.	42
Figure 6. c-Fos quantification and analysis of naltrexone and saline treated rats.....	44
Figure 7. 3D renderings of various designs used to measure force during motorized cycling.	55
Figure 8. Example trial of EMG analysis.....	62
Figure 9. Comparison of EMG responses in the biceps femoris during motorized cycling using RMS values and percent activation.	65
Figure 10. Comparison of EMG responses in the vastus lateralis during MC using RMS values and percent activation.	66
Figure 11. Example relationship between force and EMG.	68

Figure 12. Average non-spastic forces (normalized AUC) for EMG cycling groups.....	70
Figure 13. Spastic forces over the course of each cycle, pooled and represented as a heatmap.	72
Figure 14. Quantification of trials with spastic forces present.....	74
Figure 15. c-Fos expression in the lumbar spinal cord.....	77
Figure 16. BBB scores during cycling training.....	80
Figure 17. Tail-flick latency during cycling training, normalized to baseline.....	81
Figure 18. Kinematics and range of motion analysis for the hip, knee, and ankle joints.	95
Figure 19. Analysis of non-spastic forces, represent as normalized area under the curve (AUC).	98
Figure 20. Heatmap visualization of spastic forces averaged over one gait cycle.	100
Figure 21. Average heart rate, systolic pressure, and diastolic pressure pre-, during, and post-cycling.	102
Figure 22. Representative trial demonstrating instantaneous cardiovascular effects. ..	105
Figure 23. Line graph representations of HR↔MAP causality pre-, during, and post-cycling for standard and short crank lengths.....	107
Figure 24. Illustration of relative differences in neutral and cycling hip positions of rats and humans.....	121

CHAPTER I

PRIMARY AND SECONDARY COMPLICATIONS OF SPINAL CORD INJURY AND POST-RECOVERY REHABILITATION STRATEGIES

Introduction

Spinal cord injury (SCI) is a devastating condition that greatly affects quality of life in affected individuals. It is estimated that over 90% of SCI cases result from trauma to the cord in incidents such as vehicular accidents, falls, violence, or sports injuries [1]. In addition to the initial insult, blunt force trauma can fracture and dislocate vertebral bodies, causing a compression of the spinal cord that furthers neurologic damage [2]. Current standards of care for a patient acutely post-SCI involves surgical decompression that removes damaged structures to alleviate pressure on the spinal cord [3]. Decompressive surgery performed acutely (24 hours maximum post-injury) improves functional outcomes in patients [4], however they are still left with a variety of neurological impairments depending on the severity/location of injury. Sensory and motor loss occurs below the level of injury, with injuries at the cervical level associated with tetraplegia while lower thoracic/lumbar injuries can result in paraplegia [5].

SCI is generally divided into primary and secondary injury. Primary injury is the acute results caused by the traumatic event, which is most often an impact plus persistent compression type injury that results in an anatomically incomplete injury [6, 7]. The injury disrupts both ascending and descending pathways, damages cells at the site of injury, and ruptures blood vessels causing an imbalance of the blood-brain barrier [8]. This damage causes spinal shock – loss of spinal reflexes and muscle tone below the

level of injury – as well as other effects such as hypoxia and ischemia [9]. Although the primary injury is the immediate result of the trauma, secondary injury begins minutes after the initial insult. This is known as acute secondary injury, which is followed by sub-acute and chronic phases. Acute secondary injury on a larger scale includes disrupted blood flow to the spinal cord that further exacerbates ischemia, resulting from increasing pressure in the cord that obstructs smaller blood vessels and vasospasms in intact vessels [10]. Molecularly, cellular damage causes excitotoxicity by increasing extracellular concentrations of glutamate which binds to a variety of receptors to cause a flood of calcium ions to enter cells. Calcium is trafficked to the mitochondria via mitochondrial calcium uniporter proteins; overaccumulation of calcium overloads the mitochondria leading to cell death [11, 12].

Sub-acute and chronic secondary issues includes phenomena such as Wallerian degeneration [13], apoptosis [14], and the formation of a cystic cavity/glial scar [15]. Our understanding of the temporal mechanisms of injury has increased significantly, however the injury of the spinal cord itself is only one part of a broader picture. SCI is often associated with loss/disruption of sensory and motor functions such as spasticity/contractures, anaphia, and neuropathic pain. Recent evidence suggests that SCI is a whole-body disease that causes a variety of secondary consequences in addition to those mentioned above. These secondary complications include impairments of the autonomic nervous system that controls the cardiovascular, gastrointestinal, and urinary systems [5].

Secondary Complications: Spasticity

Muscle contractures and spasticity are conditions affecting the musculoskeletal system that can affect upper/lower limb as well as trunk musculature depending on the location and severity of the injury [16]. The classic definition of spasticity is “a motor

disorder characterized by a velocity-dependent increase in tonic stretch reflexes resulting from hyperexcitability of the stretch reflex” [17]. In this definition, the stretch reflex is a monosynaptic pathway where afferent information is transmitted from muscle spindles to the spinal cord via Ia afferents [18]. These afferents synapse directly onto alpha motor neurons or associated interneurons; therefore, the result of a muscle spindle stretch is an increase in alpha motor neuron activity that causes a muscle contraction to resist stretch. It should be noted that the sensitivity of a muscle to stretch is modulated by gamma motor neurons that adjust the tension of intrafusal muscle fibers [19]. Gamma motor neurons receive excitatory input from centers in the brain such as the basal ganglia, cerebellum, and cerebral cortex, which are disrupted after SCI [20]. Gamma motor neuron depression is thought to contribute to the lack of stretch reflexes during spinal shock as H-reflexes (that bypass muscle spindles) are present [21], however there is evidence in cats [22] and humans [23] suggesting that enhanced activity of fusimotor drive does not contribute to exaggerated stretch reflexes after SCI. Rather, it is the hyperexcitability of this reflex pathway that is thought to cause spasticity following SCI, however the exact mechanisms are still not fully understood. Afferents themselves undergo changes following SCI, notably sprouting that increases connections in the dorsal spinal laminae [24, 25]. In rats, a T5 spinal cord transection has been shown to increase the density of both myelinated and unmyelinated fibers in the gray matter, with primary afferents increasing inputs onto interneurons in the dorsal horn that modulate hyperreflexia [26]. Although no direct connection from primary afferent to motor neuron was described in this study, a selective ablation of the pyramidal tract in rats was shown to increase the concentration of VGlut1-positive boutons on motor neurons suggesting a sprouting of Ia afferents to motor neurons [27]. This ablation caused an amplification of the H-reflex, suggesting that it may play a role in hyperreflexia.

In addition to morphological changes of sensory afferents, changes in neuronal connections can alter Ia afferent activity. A key modulator of Ia afferents is GABAergic interneurons that are traditionally thought to presynaptically inhibit Ia afferents by forming axoaxonic connections at the afferent terminal [28]. Interestingly, recent evidence suggests that GABAergic synapses may be located less distal on the axon at the Nodes of Ranvier in addition to GABA_A receptors on the sensory afferent itself [29]. Regardless of location, loss of GABAergic tone following SCI is a likely mechanism for spasticity, which is supported by animal models [30] and the use of the GABA agonist baclofen to treat spasticity in patients [31]. The causes of decreased GABAergic tone are likely multifactorial; however, a key factor is the loss of GABAergic neurons following SCI [32, 33]. Genes that modulate apoptosis are either positively upregulated (NF-κB p65/p50) or negatively downregulated (c-Rel) causing cell death of GABAergic interneurons in the upper dorsal horn that modulate inhibition of Ia afferent terminals [34, 35]. In addition to the loss of inhibition from cell death, the action of remaining GABAergic interneurons can be reversed by spinal cord injury, causing them to become excitatory instead of inhibitory. This change is hypothesized to lead to a sensitization of nociceptive circuitry that can cause chronic pain in SCI patients.

Secondary Complications: Pain

Chronic pain is a debilitating consequence of SCI affecting up to 67% of patients [36]. Of particular concern is the development of neuropathic pain, where affected individuals experience chronic pain at or below the level of injury that is difficult to treat with traditional methods [37]. As is the case with spasticity the causes of neuropathic pain are not fully understood, however GABA may also play a role. In the normally developed mature spinal cord, activation of GABA_A receptors causes Cl⁻ ions to flow into the cell causing more negative membrane potentials and an inhibitory effect [38]. This

effect is only possible due to low intracellular concentrations of Cl⁻, which is maintained by the K-Cl co-transporter KCC2 [39]. The concentration of membrane bound KCC2 post-SCI is decreased in cells below the level of injury, causing an increase in intracellular Cl⁻ concentration that reverses the effect of GABA and may cause hypersensitivity associated with neuropathic pain [40]. Specifically, it has been demonstrated that application of 8-Hydroxy-DPAT hydrobromide (5HT-1A receptor antagonist) or lesion of the dorsolateral funiculus can induce an antinociceptive effect from GABA similar to that observed from SCI, suggesting descending serotonergic fibers play a role in this phenomenon [41]. Non-neuronal mechanisms have also been implicated in the development of neuropathic pain, notably glia. SCI causes activation of microglia in the spinal cord, which is associated with production of pro-inflammatory cytokines and activation of p38 MAP-kinase pathways involved with injury response and cell death [42, 43], and the inhibition of members of this pathway have been shown to reduce allodynia in animal models of SCI [44] and peripheral nerve injury [45].

There is currently no universal treatment for neuropathic pain. Traditional pain treatments such as opioids remain controversial; although they have been shown via systematic review to have limited effect on neuropathic pain in patients [46, 47] opioids remain highly prescribed and used in clinical trials [48]. Animal models have hinted at potential causes to the lack of opioid efficacy, as studies have shown reduction of μ -opioid receptor expression in the dorsal horn following both peripheral axotomy [49] and contusive SCI [50]. Additionally, opioid receptors are expressed on glial cells [51] and administration of opioids can activate microglia producing pro-inflammatory cytokines similar to the effects of SCI [52, 53].

As opioids remain controversial, a wide variety of pharmacological [54] and surgical interventions [55] have been administered to treat neuropathic pain with mixed

success. Additionally, a growing body of evidence from work in animals suggests that exercise may play a role in decreasing the development of neuropathic pain. For example, it has been shown that acute forced wheel running is capable of decreasing sprouting of non-peptidergic fibers at the level of injury [56], although the same group also showed that forced wheel running after rats had already developed allodynia was ineffective [57]. Exercise has also been shown to influence the density of peptidergic fibers, as treadmill training was shown to reduce the density of CGRP+ afferents in the dorsal horn [58-60].

Secondary Complications: Cardiovascular Dysfunction

Cardiovascular disease (CVD) is highly prevalent in the SCI population with an estimated 30-50% incidence rate compared to 5-10% in the uninjured population [61]. Cardiovascular complications are more likely to develop when a SCI is at the T5 spinal segment or higher [62] due to the anatomical differences between sympathetic and parasympathetic branches of the autonomic nervous system that are involved in regulating control of the cardiovascular system [63]. While sympathetic preganglionic neurons that innervate the heart are found in the T1-T5 spinal cord, parasympathetic control of the heart is modulated by the vagus nerve which does not enter the spinal cord [64]. This dysregulation between sympathetic and parasympathetic nervous system can result in life threatening consequences such as autonomic dysreflexia (AD), where a stimuli below the level of injury causes sympathetic outflow that is normally modulated by descending vasomotor pathways [65]. Sympathetic outflow to the peripheral vasculature causes hypertension, which reaches life threatening levels in SCI patients as this sympathetic activity is no longer modulated by descending inhibition. In response to hypertension, activity of the vagus nerve increases due to baroreceptor activity which can lead to a counter-acting bradycardia [66].

Autonomic dysreflexia is a severe example of an acute cardiovascular event, however SCI is also linked to sustained changes in risk factors linked to cardiovascular dysfunction. Decreased physical activity plays a large role in the development of CVD, as inactivity causes a decrease in circulating blood volume [67] and is linked to increased risk factors such as increased fat accumulation and diabetes [68]. Furthermore, inactivity combined with a loss of descending excitatory cardiac input causes a decrease in loading of the heart due to a reduction in mean arterial pressure and end-diastolic volume [69]. This unloading leads to a remodeling of the heart that includes reduced left ventricular volume, as well as reduced stroke volume and cardiac output (CO) [70]. The overall effect is a variety of chronic conditions, such as hypertensive/ischemic heart disease [71] and ventricular arrhythmias [72].

Exercise is known to affect cardiovascular health, and the effect of exercise on the heart is multifaceted. Molecularly, exercise releases a variety of signaling molecules such as insulin-like growth factor 1 (IGF-1), neuregulin-1 (NRG-1) and circulating catecholamines that influence heart health [73]. IGF-1 and NRG-1 both activate the phosphoinositide-3 kinase/serine-threonine kinase pathway, which upregulates downstream transcription factors C/EBP β and CITED4 that both play roles in heart weight and cardiomyocyte size [74]. Catecholamines such as epinephrine and norepinephrine activate nitric oxide synthase which has been shown to reduce myocardial fibrosis and modulate vascular tone [75]. On a macro scale, exercise increases stroke volume and CO which places an increased load on the heart that results in hypertrophy. A prevailing – albeit controversial – theory for a mechanism behind increased stroke volume during exercise is the skeletal muscle pump, a mechanism by which rhythmic contraction of lower limb muscles impart kinetic energy to venous capacitance vessels to facilitate its return to the heart [76, 77]. The skeletal

muscle pump has also been theorized to play a role in muscle hyperemia during exercise. Evidence for this theory likely originated with pioneering work which demonstrated that venous pressure at the ankle during exercise initially increased but then progressively decreased until a plateau was reached, then returned to baseline values after approximately 30 seconds after the cessation of exercise [78, 79]. The relationship between blood flow and venous/arterial pressure can be estimated using the Hagen-Poiseuille equation:

$$Q = \frac{\Delta p \pi r^4}{8 \eta l},$$

where Q is blood flow, Δp is the difference between arterial pressure (P_a) and venous pressure (P_v), r is the radius of the blood vessel, η is the viscosity of blood, and l is the length of the blood vessel [80]. Since resistance (R) is given as [81]

$$R = \frac{8 \eta l}{\pi r^4},$$

The equation can be written as

$$Q = \frac{P_a - P_v}{R}$$

and we can see how a decrease in venous pressure leads to an increase in blood flow to the muscle. In summary, the skeletal muscle pump postulates that a muscle contraction pushes blood out of the veins and increases the driving pressure of the blood back to the heart. Upon relaxation, a pressure gradient is created as the venous pressure has been decreased due to the emptied veins, and as a result oxygenated arterial blood can perfuse into the active muscle. However, as R is highly dependent on r, it has been argued that vasodilation – not the skeletal muscle pump – is responsible to exercise induced hyperemia based on evidence that the effects of muscle contraction on limb

blood flow is eliminated when the limb vasculature is dilated using adenosine [76]. However, in vitro analysis of several vasodilators demonstrated that vasodilation occurs over a longer time course compared to the hyperemic effect seen during muscle contraction (>4 seconds compared to 1-2 seconds) [82], suggesting that the skeletal muscle pump likely still plays a role.

Rehabilitation strategies following SCI

Restoration of motor function is often an aim in rehabilitation following SCI, as most injuries are incomplete [83]. Task specific training, such as walking overground or using a treadmill, is thought to provide proprioceptive information that trains central pattern generator (CPG) circuitry in the spinal cord [84]. Although it is sometimes thought of as the primary outcome of rehabilitation, there exist a multitude of rehabilitation techniques to target various functional outcomes. As patients prioritize functions such as bowel/bladder function, pain relief, and spasticity reduction, rehabilitation after SCI has begun to examine these outcomes in addition to locomotor function [85, 86]. Care must also be taken to apply training and exercise in an appropriate manner; exercise can positively affect cardiovascular, metabolic, and mental health, but SCI patients often have reduced cardiovascular capacity and are at risk for complications such as autonomic dysreflexia and bone fractures due to factors such as disrupted autonomic function and reduced bone density, respectively [87].

Gait Training

Gait training is a rehabilitation strategy where a locomotor movement is applied over an extended period with the goal of eliciting a functional benefit such as adaptive changes to neuronal circuitry, increased walking endurance/muscle mass, or reduced pain and/or spasticity [88]. While seemingly straightforward, a variety of factors can be modified such as movement speed, range of motion, body weight support (BWS), and

the degree and manner that physical assistance is applied to aid in the motion of the lower limbs. For example, many gait training procedures involve BWS treadmill training (BWSTT), with manual lower limb assistance provided by physical therapists. This contrasts with overground gait training, where patients must navigate with limited upper body support and aid to the lower limbs [89]. Additionally, semi-recent technological advancements have allowed for strategies such as robot-assisted gait training (RAST) or functional electrical stimulation (FES) gait training.

A prevailing argument in the SCI research community concerns the relative efficacy of various gait training methods. Despite a wealth of clinical trials, no superior technology has emerged. For example, a recent systematic review compared BWSTT, RAST, and overground gait training involving 586 subjects over thirteen controlled trials and found all three training methods increased walking speed and distance, although overground gait training was slightly superior [90]. Similar reviews have found comparable results, with BWSTT and FES training both providing benefits to functional ambulation [91]. Another meta-analysis found no difference in outcome measures such as walking speed/capacity when comparing BWSTT, overground, or RAST, [92] however an updated version [93] noted that in one study the group receiving RAST had significantly worse outcomes compared to BWSTT or overground gait training [94]. However, recent meta-analyses and controlled trials have shown RAST can improve walking ability in SCI patients using outcome measures such as lower extremity motor score and walking ability [95-97], suggesting some functional benefit may be gained using this approach.

Gait training has also been used extensively in animal models of SCI, however clinical translation of these findings has been limited [98]. Methods of gait training have been adapted to rodents, such as treadmill training (both quadrupedal [99] and bipedal

[100]), voluntary walking to mimic overground training [56, 57], and even RAST [101]. Despite the faithful translations of the rehabilitation methods, one of the main limitations is contusion models of SCI in rodents recover locomotion spontaneously, unlike humans [102]. This recovery is thought to be due to CPG circuitry which produces stepping motions that become dependent on afferent information from the periphery [103]. Supporting this claim are studies demonstrating that Egr3 mutant mice that lack normal muscle spindle afferents show diminished locomotor recovery following hemisection injury despite the animals having proficient pre-injury locomotion [104]. This finding was later expanded to parvalbumin expressing neurons that carry proprioceptive information, which were shown to be necessary for initiation and maintenance of spontaneous locomotor recovery using temporal ablation during recovery [105]. Although it has been thought that the afferent information needs to be task specific to train the CPG circuitry, recent evidence from cats suggests that stand training alone may be sufficient to induce locomotor recovery [106].

Eccentric Training

Eccentric muscle contractions – where a muscle is exerting force during the lengthening phase – have been commonly incorporated into fitness regimens in the form of resistance training [107]. Resistance training has a well-documented effect on muscular properties [108, 109], however some controversy exists around eccentric training as it can cause muscle damage and pain when improperly applied [110], likely due at least in part to overextension/disruption of sarcomeres in myofibrils [111]. Although there are risks, a benefit of eccentric training is that it requires less muscle activity and therefore has a lower metabolic demand when compared to force-matched concentric exercise [112]. An increased interest has been placed on eccentric training post-SCI with promising results. Several clinical studies suggest that benefits may be

neurologic in nature, showing eccentric training increased afferent modulation of motor neurons using H-reflex testing [113], improved eccentric strength without altering muscular hypertrophy [114], and induced white-matter plasticity in brain and spinal cord regions measured using myelin water imaging [115]. Similar results have been found in animal studies; downhill locomotion was able to restore a dormant EMG bursting pattern in T8 moderate contusion injury model in rats [116], while improving locomotor outcomes such as hip height and knee range of motion in mice [115]. Interestingly, the latter study associates this recovery with oligodendrocytes despite some controversy regarding their role in recovery of locomotor function [117].

Stretching

Lower-limb stretching is a commonly used clinical practice post-SCI, with the rationale of preventing spasticity and muscle contractures [118]. The rationale for the use of stretching following SCI comes from a mix of human and animal literature, however much of this work was performed in spinally intact populations. Clinically, both static and dynamic stretch have been shown to increase range of motion (ROM) in the range of 4-10° in the knee and ankle [119-121], while in intact rats it was demonstrated that muscle shortening and reduced joint range of motion following cast immobilization can be mitigated with intermittent stretching therapies [122]. Although stretching is a recommended spasticity management tool post SCI, the rationale is still not well described/understood [123-125]. Additionally, stretching provides afferent information to the cord from muscle proprioceptors, which can influence locomotor recovery post-SCI [104, 105]. Work in a rat model of SCI suggests that the effects of this information during stretching may be maladaptive. For example, a static stretching protocol of 30 minutes per day (2 x 1 minute of static stretch per muscle group) has been shown to decrease locomotor function after only one week [126, 127]. These effects are not limited to static

stretching, as rats that underwent dynamic stretching (2 seconds of stretch followed by 1 second of rest for 2 x 1 minute per muscle group) demonstrated similar locomotor deficits [128]. This response appears to be due in part to nociceptive information, as rats that were treated with capsaicin as neonates (thus lacking TRPV1+ C-fiber innervation) retained greater locomotor function following stretching compared to normal stretched animals [129]. Both groups of stretched animals had larger number of c-Fos positive nuclei in the spinal gray matter compared to un-stretched controls, suggesting the effects of stretching are spinally mediated and potentially due to aberrant afferent stimulation.

Although stretching may be thought to “overstimulate” the spinal cord, it should be noted that afferent input delivered with more specific timing can also influence the function of spinal cord circuitry [130]. For example, fully transected rats that receive a shock in relation to an extended hindlimb position learn to keep their leg in a flexed position, while rats that are shocked independent of leg position do not learn this behavior [131, 132]. It should be noted that while these studies describe spinal learning in one limb, the spinal cord holds the ability to modulate stepping bilaterally. This effect has been demonstrated in split-belt treadmill experiments, where animals with fully transected spinal cords are able to independently modulate step-stance cycles on the right and left sides to maintain body position in response to variations in treadmill speed between limbs [133]. Similar results have been demonstrated during human gait [134, 135], suggesting that coordination of the limbs occurs at the spinal level in both quadrupedal and bipedal gait. This synchronization is dependent on afferent sensory information from the limbs, suggesting that the importance of timing on spinal learning could be dependent on the position of one limb relative to the stimulus, as well as its position relative to the opposite limb.

Functional Electrical Stimulation (FES) Cycling

FES cycling is a technique where electrical stimulation is applied via transcutaneous electrodes to paralyzed muscles in a timed fashion to produce a cycling movement. In theory, this technique should mimic voluntary exercise training as muscle contractions are being performed in a coordinated manner. Indeed, patients have anecdotally described benefits of FES cycling that are ascribed to traditional exercise such as muscle function, cardiovascular health, and general improvements in quality of life [136]. As with traditional cycling, a goal of FES cycling is often to improve the overall health and/or power output of lower limb musculature. Although FES cycling is becoming more widely used, it remains expensive and the need for trained personnel further limits availability to individuals with SCI. This issue is reflected in the literature; a recent systematic review on FES cycling found 92 studies meeting eligibility criteria, however a combined assessment of bias [137, 138] revealed only two Level 1 studies (randomized controlled trials with low risk of bias) and seven Level 2 studies (randomized controlled trials with high risk of bias or non-randomized controlled trials with low/moderate risk of bias) [139]. Both Level 1 studies found FES cycling to be safe as assessed by recording adverse events [140] or leg swelling [141], although no improvement in leg swelling was observed. Only one investigated muscle hypertrophy as assessed by cross-sectional area (CSA), which found no effect of training [140], and no significant differences were found in any outcome measures in either study (body composition/quality of life [140], urine output/spasticity using the Ashworth Scale or self-reported [141]). Results from the Level 2 studies are more positive; 3/7 investigated muscle health and all three found significant improvements from FES cycling in thigh muscle volume [142], lean body mass [143], or CSA [144]. Although none of the Level 1 or 2 studies investigated cardiovascular outcomes, 12/17 Level 3 studies and 4/4 Level 4 studies reported

benefits [139] including increased resting CO [145], stroke volume [146], and oxygen pulse [147], suggesting that FES cycling may be a feasible therapy for improving cardiovascular health in the SCI population despite more evidence being needed.

Motorized Cycling (Humans)

The literature on human motorized cycling (MC) is widely varied, as researchers are using MC to approach a variety of health problems using heterogeneous outcome measures. For example, there are a variety of negative health effects associated with modern sedentary lifestyle [148] such as body mass index, triglyceride content, and plasma glucose levels [149, 150]. Researchers have recently investigated the effects of MC on healthy populations, with outcome measures of energy expenditure (measured using indirect calorimetry), heart rate, and oral glucose levels [151]. MC for 30 minutes caused a modest (although significant) increase in energy expenditure and heart rate compared to sitting, although the effects of moderate intensity cycling were significantly more pronounced. The results from this study suggest that, at least in a non-injured population, MC may be capable of inducing a muscular response that can help to reduce cardio-metabolic risk factors. However, it should be noted that cycling frequency in this study was 80 RPM (very high).

The cardiovascular response to passive cycling has been of interest for several decades. An earlier study investigating the differences between active and passive exercise was performed by Norbega et al. [152]. In this study, the cardiovascular responses to passive and active cycling were measured at frequencies of 40 and 60 RPM. CO was increased in both groups, although active cycling elicited a higher CO compared to passive cycling. Interestingly, the mechanisms behind this increased CO were different between active and passive cycling. Active cycling induced an increase in heart rate, while stroke volume (SV) remained unchanged. Conversely, passive cycling

resulted in an elevation of SV while heart rate remained unchanged. The authors speculate that this could be due to peripheral afferent reflexes and increased venous return of blood to the heart resulting from passive movement of muscles. This hypothesis is supported by the work of Figoni and Muraki et al., who demonstrated that MC is capable of increasing CO in patients with SCI [153-155].

As mentioned earlier, the results in cardiovascular outcomes from MC studies are varied and several studies report negative findings. For example, Thomas et al. investigated the effects of passive limb movements on CO and SV in both able-bodied and spinal cord injured subjects, and did not detect significant changes in either group [156]. These results are supported by the work of Ter Woerds et al., who specifically investigated blood flow in the femoral artery using Doppler sonography [157]. The results from this study suggested that neither passive limb movements nor passive cycling are capable of inducing changes in femoral blood flow in either able-bodied or SCI subjects. Contrary to these results, a similar study around the same time demonstrated that peak femoral blood flow velocity was increased following passive cycling in SCI subjects [158]. Although criticisms of this study have suggested that flow changes could be a result of postural changes during the affixation of the probe [159], the authors challenge these criticisms by noting that postural changes were introduced during baseline measurements as well, and that postural changes were performed at least 30 seconds before termination of the cycling exercise.

Passive Hindlimb Cycling (Rodents)

MC has been used to study a variety of issues in rodents other than cardiovascular function. One area of interest is the effects of neuronal plasticity following damage to the nervous system. For example, daily MC has been shown to increase the number of regenerating myelinated fibers following sciatic nerve transection at a similar

rate as forced treadmill walking [160]. Changes following peripheral nerve injury are not limited to the axons in the affected nerve, as passive cycling has also been shown to preserve synapses and perineuronal nets in axotomized motor neurons following sciatic nerve transection [161]. Additionally, recent studies have implied that MC may affect changes in motor neurons following SCI in addition to peripheral nerve injury. Gene expression of motor neurons appears to be affected by passive cycling. Genes involved in neuronal plasticity, such as BDNF, GDNF, and NT-4 are upregulated following MC [162], while a more complex response was seen following MC in genes regulating neuronal excitability, such as serotonin receptors and potassium-chloride cotransporter member 5 [163]. Interestingly, MC has been shown to reduce the sprouting of non-peptidergic c-fibers [56] and reduce hyperexcitability [164, 165] following SCI, implying the possibility of cell-type specific changes resulting from MC. This idea is supported by results demonstrating that MC can induce differential gene expression in motor neurons, DRG neurons, and neurons in the intermediate gray area following SCI [162]. MC has also been shown to affect limb musculature, as one of the earliest studies using a rodent model found that daily training limited muscle atrophy by inducing changes in myofiber size without inducing changes in fiber type [166].

The effects of passive limb cycling on the cardiovascular system are more pronounced in rodent models of SCI compared to humans. A pioneering study by West et al. described the effects of MC on cardiovascular function in a T2 spinal transection model using a variety of outcome measures [69]. SCI rats that received daily passive cycling were able to maintain higher systolic blood pressure and mean arterial pressure compared to SCI controls. Furthermore, the MC group exhibited increased end-systolic/diastolic volume, increased SV, and increased CO compared to SCI controls. These results are supported in a following study from the same group, which

demonstrated that these effects are only maintained in the immediate period following training [167]. These results have been further validated by demonstrating that MC could return SV and CO to control levels, while swim training (purely forelimb exercise) did not [168]. Finally, rodent models of MC have been shown to reduce the severity of autonomic dysreflexia in response to colorectal distension [169]. This muted response is associated with reduced sprouting of CGRP+ afferent fibers in the L3/L4 spinal cord in the MC group.

Closing Remarks

There exists a discrepancy between the results of human and animal studies regarding outcomes from MC interventions. In general, translation of animal work remains a pressing issue in all of science; differences between a human and a rat are numerous both anatomically and physiologically, confounding interpretation. Given these anatomical differences, it is surprising that the biomechanics of passive cycling seem to be rarely considered in both human and animal work. Cycling frequency, body/limb position and crank length (specifically ratio of crank to limb length) can have a drastic effect on the magnitude and rate of muscle stretch. The rate of cycling frequency in human literature is consistently reported but can vary widely between studies. Body position is clearly different between animal and human studies; rats are suspended above an ergometer while humans are often seated with an ergometer in front of a chair. Furthermore, body position is inconsistent from study to study whether animal or human studies. These differences may explain why animal models of passive cycling appear to be capable of eliciting timing-specific bursts of EMG activity [166], while human studies have not [152].

Supraspinal input is either impaired or eliminated following SCI, which causes the spinal circuitry below the lesion to be driven predominately by sensory input from the

periphery. Activation of stretch reflexes is dependent on both rate and length of muscle stretch [170], which would be amplified post-SCI due the loss of descending control that appears as hyperreflexia, spasticity and clonus. Some of the contrasting results between MC studies in humans and MC in animals could then be explained by differences in cycling biomechanics, where different muscles were stretched to different lengths and/or at different rates, thus resulting in different amplitudes and timing of muscle activation and clouding the interpretation of the data.

MC is a unique therapeutic technique that combines aspects of muscle stretch with exercise/eccentric training, as muscle activity elicited by stretching will occur during the lengthening phase. Although rhythmic stretching during MC is considered safe, the results from our lab described earlier indicate that dynamic hindlimb stretching above a certain force threshold post-SCI can cause locomotor deficits, just as tonic stretch-and-hold maneuvers can [128]. As a goal of this project is translation, a first step was to ask if stretch induced deficits in locomotion were mediated by opoidergic circuitry. Next, questions about the rat model of MC could be asked. It should be noted that previous studies of MC in rats have used a transection model of SCI, even though almost 70% of clinical cases are incomplete injuries [83]. This may be due to ease of use, as rats with residual limb function could theoretically break free of the pedal restraints. We proposed that a severe contusion model would be more clinically relevant for studying passive cycling and thus one goal is to compare the pedal reaction forces generated by animals with severe contusions and transections. Can the generated forces be modulated by cycle cadence or range of motion? If so, how does force produced at the pedals relate to EMG in large hindlimb muscles (e.g., knee flexors/extensors)? Finally, are cardiovascular responses to MC based purely on passive movement, or is there a relationship between blood pressure/heart rate and pedal reaction forces? Based on

these questions, the goal of this study was to create a framework for measuring and synchronizing force, hindlimb kinematics, and telemetric data (hindlimb muscle EMG arterial pressure/heart rate) and describe the relationship of these outcomes to crank length and cadence.

Specific Aims and Hypothesis

Aim 1: Determine the effect of an opioid antagonist on stretch-induced locomotor deficits.

Previous work from our lab demonstrates that stretching does not result in a significant reduction in locomotor function in animals that were treated with a systemic injection of capsaicin as neonates, and thus lack TRPV1+ C-fibers [171]. This suggests that nociceptive afferents play a role in stretch-induced locomotor deficits. We hypothesize that administration of naltrexone (opioid antagonist) will mitigate the negative effect of stretching on locomotor function in rats with SCIs.

Aim 2: Describe the relationship of MC parameters (cycle frequency and crank length) with EMG responses of knee flexor and extensor muscles, and pedal reaction forces in a rat model of high-thoracic severe, but incomplete SCI.

As mentioned previously, it has been demonstrated that the stretch reflex is dependent on the rate and length of muscle stretch [170]. However, muscle force can also be generated passively when muscles are stretched past their resting length [172]. Therefore, it is necessary that we describe the activity of the muscles during cycling, as well as how muscle activity and force output are altered by varying cycling parameters. We hypothesize that EMG activity during cycling will be induced during the lengthening phase at a rate corresponding to length and rate of muscle stretch. Furthermore, EMG activity will correspond with PF such that muscle contraction will primarily be eccentric.

Aim 3: Describe the relationship of force generation during MC and instantaneous cardiac function in a rat model of incomplete SCI.

Higher forces generated during MC suggest increased venous return to the heart from the skeletal muscle pump and increased arterial pressure and reduced heart rate. We hypothesize that systolic pressure and heart rate will be elevated during cycling, and that sharp increases in arterial blood pressure will be associated with higher forces.

CHAPTER II

BROAD OPIOID ANTAGONISM AMPLIFIES DISRUPTION OF LOCOMOTOR FUNCTION FOLLOWING THERAPY-LIKE HINDLIMB STRETCHING IN SPINAL CORD INJURED RATS

Introduction

Stretching is a widely applied therapy for preventing and reducing spasticity and contractures resulting from spinal cord injury (SCI) while attempting to maintain or increase joint range of motion in this population [118]. The rationale for the use of stretching following SCI is largely based on studies in intact rats demonstrating that muscle shortening and reduced joint range of motion following cast immobilization can be mitigated with intermittent stretching therapies [122]. While increased range of motion has been seen in spinally intact animals, studies from our lab indicate that daily hindlimb stretching does not improve joint contractures following contusive SCI, and furthermore, it results in deficits in locomotor function compared to unstretched SCI control animals [126]. These deficits are present when stretching is applied at acute or chronic timepoints [127] using either static or dynamic stretching protocols [128] without overt signs of muscle damage. Although the mechanisms behind this dysfunction are not entirely clear, we found that SCI animals depleted of TRPV1+ unmyelinated primary afferents (predominantly nociceptors) are less affected by daily stretching compared to SCI controls [171], showing that nociceptors contribute to stretch-induced locomotor deficits, likely by their activation.

We therefore sought to address the mechanisms by which this presumed nociceptive input may be acting on locomotor capacity. We considered the endogenous opioid system due to its known role in pain control, effects on locomotor output, and common clinical use after SCI. Opioid receptors (μ , δ , and κ) are expressed in DRG neurons and second-order neurons, with the highest levels expressed in the substantia gelatinosa of the dorsal horn [173]. All classes of opioid receptors are coupled to inhibitory G proteins which depress neuronal firing rates by affecting downstream targets such as adenylate cyclase and pre/post-synaptic ion channel properties [174]. Following SCI or any severe tissue injury, opioid systems in the spinal cord and brain facilitate an adaptive compensatory response to inhibit pain [175]. Additionally, SCI can result in sensitization of the nociceptive response below the level of injury by several methods, including disruption of descending pathways, reduced spinal GABA levels, and altered Cl⁻ equilibrium potential [176]. It has been suggested that endogenous opioids may counteract or mask a nociceptor hyperfunctional state, as the opioid antagonist naltrexone was shown to reinstate pain-like behaviors when administered months after nociceptor activation and sensitization by peripheral administration of complete Freund's adjuvant [177]. Based on this background, we chose to use naltrexone to investigate the role of endogenous opioids in the stretching phenomenon. Naltrexone is a long-lasting antagonist of μ - and κ -opioid receptors, which are primarily located on peptidergic afferents and associated nociceptive circuitry [178, 179].

Materials and Methods

Experimental design

A summary of the experimental design is shown in Figure 1. Eight adult female Sprague-Dawley rats (225-250 g, Envigo, Indianapolis, IN) were acclimated in their home cages for two weeks then divided into two groups: drug-treated (n=4) and vehicle-treated (n=4). We performed stretching on weekdays during post-SCI weeks 6, 8, and 11. No stretching was performed during post-SCI weeks 7, 9, and 10. Stretch and non-stretch weeks were intercalated to assess the effect of drug on the known post-stretch recovery of locomotor function, as well as allow for sensory measurements in the absence of an acute effect of stretching.

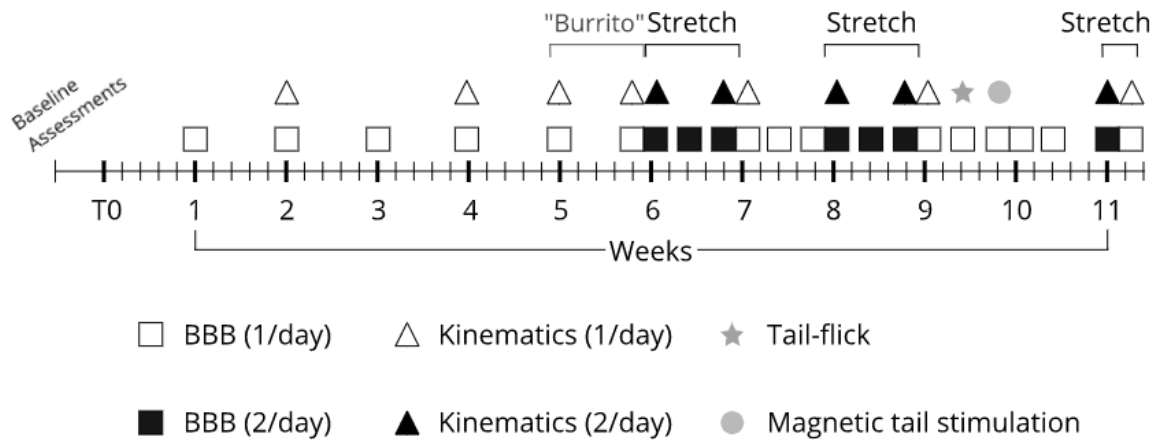


Figure 1. Timeline indicating the key timepoints for the naltrexone stretching study.

Spinal cord injuries are performed at T0. "Burrito" refers to wrapping animals in towels for the duration of a normal stretch session without applying stretch to control for possible stress. BBB, Basso Beattie Bresnehan Open Field Locomotor Scale.

Spinal cord injury

Animals were anesthetized with a ketamine (50 mg/kg)/xylazine (0.024mg/kg) cocktail to provide a surgical level of anesthesia as confirmed by the absence of paw withdrawal reflexes in response to toe pinch. The back of each animal was shaved and treated to produce an aseptic incision area. Next, a midline incision was made over the lower thoracic spine, followed by a laminectomy of the T9 vertebra. A spinal cord contusion was delivered using the NYU Impactor set to 25g-cm as previously described [180]. This magnitude of injury is generally considered to be “moderately-severe” and is selected for these studies because it is incomplete and spares a meaningful degree of motor function like many clinical injuries.

Drug dosing and administration

Naltrexone hydrochloride (Sigma-Aldrich Corporation, St. Louis, MO) was dissolved in saline and aliquoted for use in coded vials such that experimenters performing stretching, assessments, and analysis were blinded to the drug group. Prior to stretching or other sensory evaluations, experimental rats were given subcutaneous injections of the naltrexone-saline mixture (15 mg/kg) while control rats were given an equivalent volume of saline. Drug dose was selected based on its efficacy in other studies examining the impact of nociceptive sensory input on spinal motor function [181]. Drug/vehicle was given at least 15 minutes prior to stretching or evaluations based on evidence that the drug would be present in plasma at this time [182].

Stretching protocol and evaluation

Our daily stretching protocol has been thoroughly described previously [126-128, 171, 183]. The protocol consists of stretches applied to the 6 major hindlimb muscle groups bilaterally: an ankle extension (tibialis anterior), an ankle flexion/knee extension

(triceps suare), knee extension/hip flexion (posterior biceps femoris/semitendinosus), knee flexion/hip extension (vastus lateralis/intermedius/medialis and recuts femoris), hip abduction (adductors brevis, longus, magnus, minimus, pectineus, gracilis, and obturator), and adduction (gluteus, iliopsoas). Each stretch was held at the end of range-of-motion for 1 minute and repeated once for a total of ~24 minutes of stretching/day. During the stretching sessions, 4 researchers (blinded to experimental groups) were assigned such that the number of times a researcher stretched each rat was minimized while maintaining an approximately even distribution of rats from each experimental group that were stretched by an individual. Responses displayed after each stretch such as kicking, clonic-like spasticity, or withdrawal were noted. Responses were given a score of 1, 2, or 3 for mild/infrequent, moderate/frequent, and severe/very often as previously described [171]. To control for the effects of handling on locomotor function, animals were wrapped in a towel daily for 24 minutes, but not stretched, for 5 days (week 5 post-injury) when locomotor function had plateaued.

Locomotor assessments

Locomotor function was assessed using the BBB Open Field Locomotor Scale [184]. Baseline measurements were taken pre-injury followed by weekly post-injury assessments (weeks 1-4) to describe recovery. During week 5 (no stretching, towel wrapping), BBB scores were assessed Monday (pre-towel wrapping) and Friday (post-towel wrapping). During week 6, BBB scores were assessed 3 times per week at three daily time-points (Monday, Wednesday, and Friday) as follows: point 1 (pre-stretching, pre-injection), point 2 (pre-stretching, post-injection), and point 3 (post-stretching, post-injection). During week 8, BBB scores were assessed 3 times per week at two daily time-points as follows: point 1 (pre-stretching, pre-injection) and point 2 (post-stretching,

post-injection). During week 11, animals were evaluated before stretching, and once after each stretching session.

Sensory assessments

Two sensory tests were employed to investigate the role of naltrexone on sensorimotor function. First, a tail-flick assay was employed to assess thermal sensitivity using a radiant heat tail-flick device (Columbus Instruments, Columbus, Ohio, USA). A rat was placed on the platform and gently restrained, while the base of the tail was placed above the photocell for thermal stimulation. Intensity of the heat source was set to 10 out of 25, with a maximum duration of 10 seconds for each trial to avoid tissue damage. For each rat, a baseline tail-flick latency was measured three times with 30 seconds between measurements. Following baseline testing, each rat was administered a naltrexone dose (or saline) and re-tested 30 minutes later.

Secondly, magnetic stimulation-evoked EMG responses were assessed in the gastrocnemius as previously described [126, 180]. Briefly, each rat was restrained onto a solid flat board using a cloth stockinette. 26-G needle electrodes were inserted into the lateral gastrocnemius muscles bilaterally. A figure eight magnetic transducer coil (MagStim 1165-00, Magstim Inc., Eden Prairie, MN) was placed at the base of the tail to directly stimulate afferent nerves. A stimulus amplitude of 80% output was used to induce a maximal response while avoiding direct stimulation of the spinal cord or muscles, which can be identified by a reduced latency. EMGs were elicited using a MagStim 200 Mono Pulse (Magstim Inc., Eden Prairie, MN), and recorded using a Cadwell Sierra II EMG system (Cadwell Industries Inc., Kennewick, WA). Following the baseline test, rats were given the drug or vehicle and re-tested 30 minutes later. Each sensory assessment was performed during week 9 post-injury when no stretching occurred.

Euthanasia and tissue histology

Animals were sacrificed approximately 4 hours after the last stretching session using a ketamine (50 mg/kg)/xylazine (0.024mg/kg) cocktail and transcardially perfused with 4% PFA. Spinal cords were dissected and post-fixed in 4% PFA for 2 hours, then transferred to 30% sucrose for cryoprotection. The L1-L5 segments were separated from the rest of the spinal cord under a dissecting microscope and blocked in O.C.T. compound. Transverse sections were cut at 20 μ m on a cryostat for immunohistochemical analysis into 6 blocks. For CGRP analysis, sections of L3 spinal cord were warmed and washed with PBS and 0.3% PBS-Triton (PBST). Slides were then blocked for 1 hour with PBST, 5% bovine serum albumin (BSA), and 10% normal donkey serum (NDS). After blocking, slides were washed and incubated overnight with CGRP primary antibody (guinea pig polyclonal anti-CGRP, 1:1000, 20R-CP007, lot #P17101902, Fitzgerald), 5% BSA, and 5% NDS at 4°C. Following incubation, sections were washed and incubated with a secondary antibody (Alexa Fluor 594-conjugated Donkey anti guinea pig, 1:200, 706-585-148, Lot #129041, Jackson ImmunoResearch Laboratories) for 1 hour. Slides were coverslipped using Fluoromount.

For c-Fos analysis, sections of L2-L5 spinal cord were warmed and washed with PBS and 0.3% PBST for 30 minutes at room temperature. Sections were then incubated in antibody diluent reagent (Invitrogen # 00-3218, Lot1966331A) with c-Fos primary antibody (mouse monoclonal anti-c-Fos, 1:1000, cat#ab208942, Abcam) overnight at 4°C. The next day, sections were washed once with 0.1% PBST and twice with PBS (10 minutes/wash at room temperature). Secondary antibody (donkey anti-mouse FITC, 1:250, cat#715-096-151, Jackson ImmunoResearch Laboratories) was combined with antibody diluent reagent (Invitrogen # 00-3218, Lot1966331A) for 1 hour at room temperature. Following incubation, slides were washed once with 0.1% PBST and twice

with PBS for 10 minutes/wash at room temperature. A secondary amplification process was performed using AlexaFluor 488 (mouse anti-FITC, 1:500, cat#200-542-037, Jackson ImmunoResearch Laboratories) in antibody diluent reagent (Invitrogen # 00-3218, Lot1966331A) for 1 hour at room temperature. Sections were then washed once with 0.1% PBST for 10 minutes at room temperature, and once with Hoechst (1:1000) in PBST for 5 minutes. After a set of 3 washes (PBS for 10 minutes/wash at room temperature), Sudan Black B was dissolved (1mg/ml) in 70% EtOH and applied for 15 minutes at room temperature. Slides were coverslipped using fluromount after a final set of 6 washes (PBS for 5 minutes/wash at room temperature).

Image analysis

Images of each section were acquired on an inverted microscope using a 20x objective for all histological analyses (resolution 0.33 μm / pixel). For CGRP analysis, a threshold was chosen based on control images, then applied to each image to quantify the CGRP-positive area of spinal cord cross section; the same threshold was applied to images from all animals. Total CGRP area was quantified for each dorsal horn excluding the dorsal root entry zones, which were removed manually from each image. Analysis of images was conducted using MatLab (MathWorks, Natick, MA).

For c-Fos analysis, a control brightness was established for c-Fos and DAPI, then this threshold was applied to each image using NIS-Elements (Nikon Corporation, Tokyo, Japan). Each c-Fos positive nucleus was manually identified and marked based on overlap between c-Fos and DAPI. Neuron locations were displayed as heatmaps using a custom MatLab program. To generate contour plots, neurons were first marked using Nikon Elements software. A custom-made MatLab program was then developed to reconstruct and normalize the position of labelled neurons across sections. A reference axis was created for each image with the origin centered on the central canal, the y-axis

parallel to the spinal cord midline, and the x-axis orthogonal to the y-axis.

Contour/scatter plots were constructed using R. Distribution contours were created by calculating the two-dimensional kernel density (using the `kde2d` function in the MASS library), then connecting points of equal density values between 30-100% of the estimated density range in increments of 10%.

Statistical analyses

Data were analyzed using SPSS (IBM SPSS Statistics for Windows, Versions 26/27. IBM, Armonk, NY). The BBB locomotor scores, tail flick response latency, stretching spasticity and CGRP data were analyzed using repeated measures ANOVA. While this was a pilot study with a smaller sample size per group, overall the distributions were generally normal and when the variances were not equal both degrees of freedom were adjusted accordingly and strict post hoc t-tests (Bonferroni t-test for multiple comparisons) were employed. Nonparametric analysis of c-fos data were compared between independent groups using Mann-Whitney U tests. No exclusion criteria were set *a priori*, and no animals or data points were removed from analysis.

Results

Acute response to stretching

Consistent with previous results [183], rats in both groups exhibited clonic-like responses and spasms in their hindlimbs during stretching. Upon the release of stretch, spasticity, air-stepping, and kicking again reemerge with greater intensity but usually last for only one or two seconds. It was noted that some rats in the current study exhibited stronger reactions during initial limb positioning and during stretch. In the final analysis stage, it was determined that those animals belong to the naltrexone group. Naltrexone treated animals also exhibited unusually prolonged spastic responses right after the

release of a stretch and a writhing phenotype in the hindlimbs and tail that could last for almost a minute post-stretching. The most robust responses were seen following knee and hip stretches, although differences could be seen in ankle stretches as well. These reactions were evident during the first day of stretching, and the intensity of the responses persisted throughout all stretching sessions. Analysis of variance showed significant group differences in all stretches (Tibialis Anterior: $F_{(1,22)}=11.7$, $p=.002$, Gastrocnemius: $F_{(1,30)}=63.6$, $p<.001$, Hamstring: $F_{(1,33)}=112.24$, $p<.001$, Rectus Femoris: $F_{(1,26)}=78.9$, $p<.001$, Hip Abduction: $F_{(1,32.2)}=67.7$, $p<.001$, Hip Adduction: $F_{(1,28)}=74.9$, $p<.001$). Pairwise comparisons are shown in Figure 2A-F.

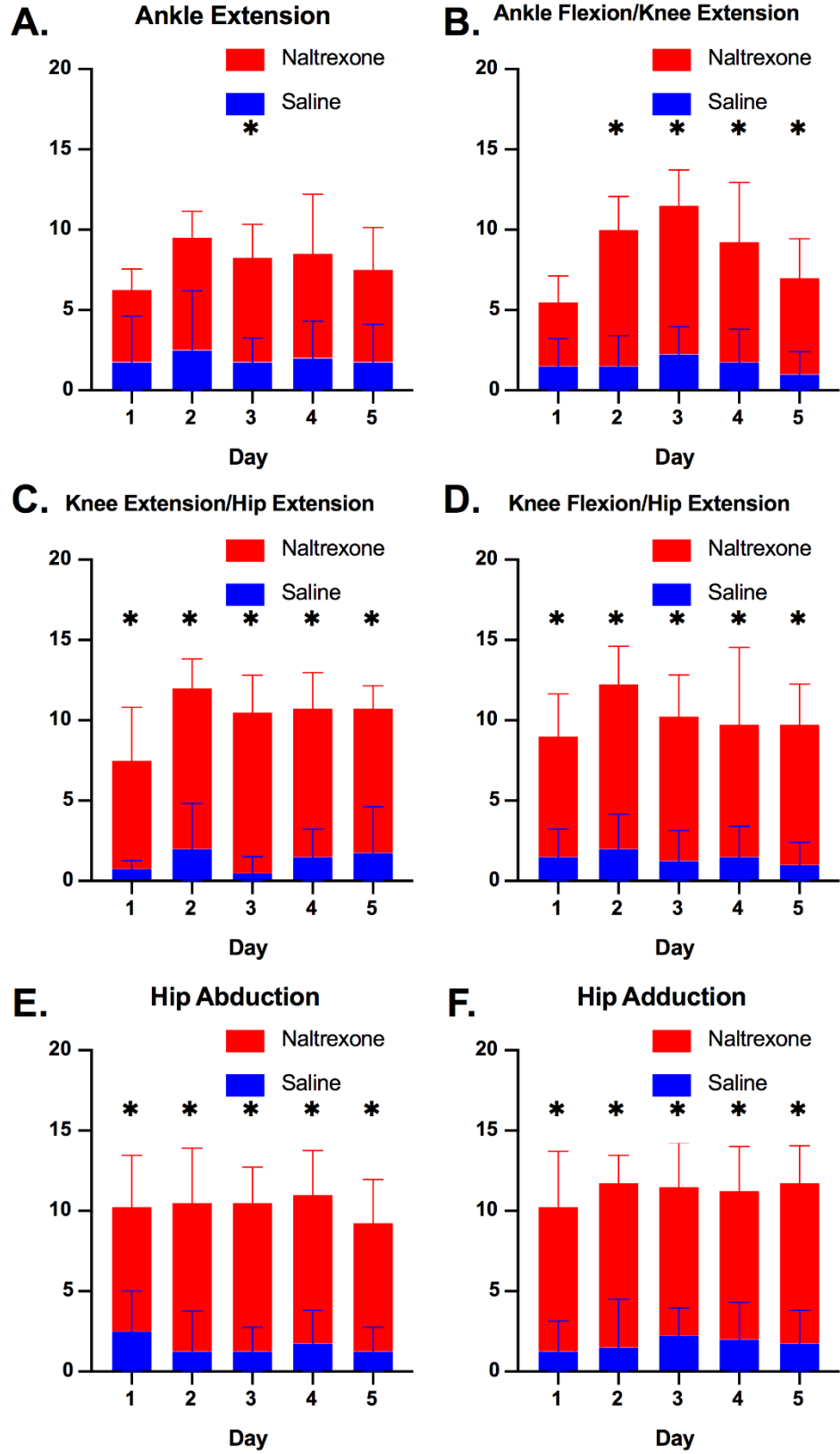


Figure 2. Spasticity assessment during the (A) first, (B) second, and (C) third week of stretching.

Spasticity was quantified on a scale of 1-3 during each stretch. Total scores are shown for each day (2 stretches x 2 limbs x 3, for a maximum score of 12) for stretch of tibialis anterior (TA), gastrocnemius (Gastroc), hamstring (Hamstring), rectus femoris (RF), hip abduction (HAb), and hip adduction (Had) for naltrexone and saline groups. Data were analyzed using a RMANOVA, with Bonferroni corrected post-hoc t-tests. * $p < 0.05$, naltrexone vs. saline groups.

Locomotor function

Locomotor function as assessed by BBB scores plateaued at the beginning of week 5 post injury with no significant differences observed between groups. Any stress induced by wrapping the animals in towels alone (burrito) was insufficient to induce changes in locomotor function (Figure 3A). Administration of naltrexone alone (without stretching) did not alter locomotor function at any timepoint tested. Analysis of variance confirmed significant differences between groups ($F_{(1,91)}=3282.7$, $p<.001$). There were no significant differences between the naltrexone and saline groups at any timepoint tested during the first week of stretching (Figure 3B). However, naltrexone-treated animals had a significantly lower BBB scores following stretching during weeks 8 and 11 (Figures 3C and 3D).

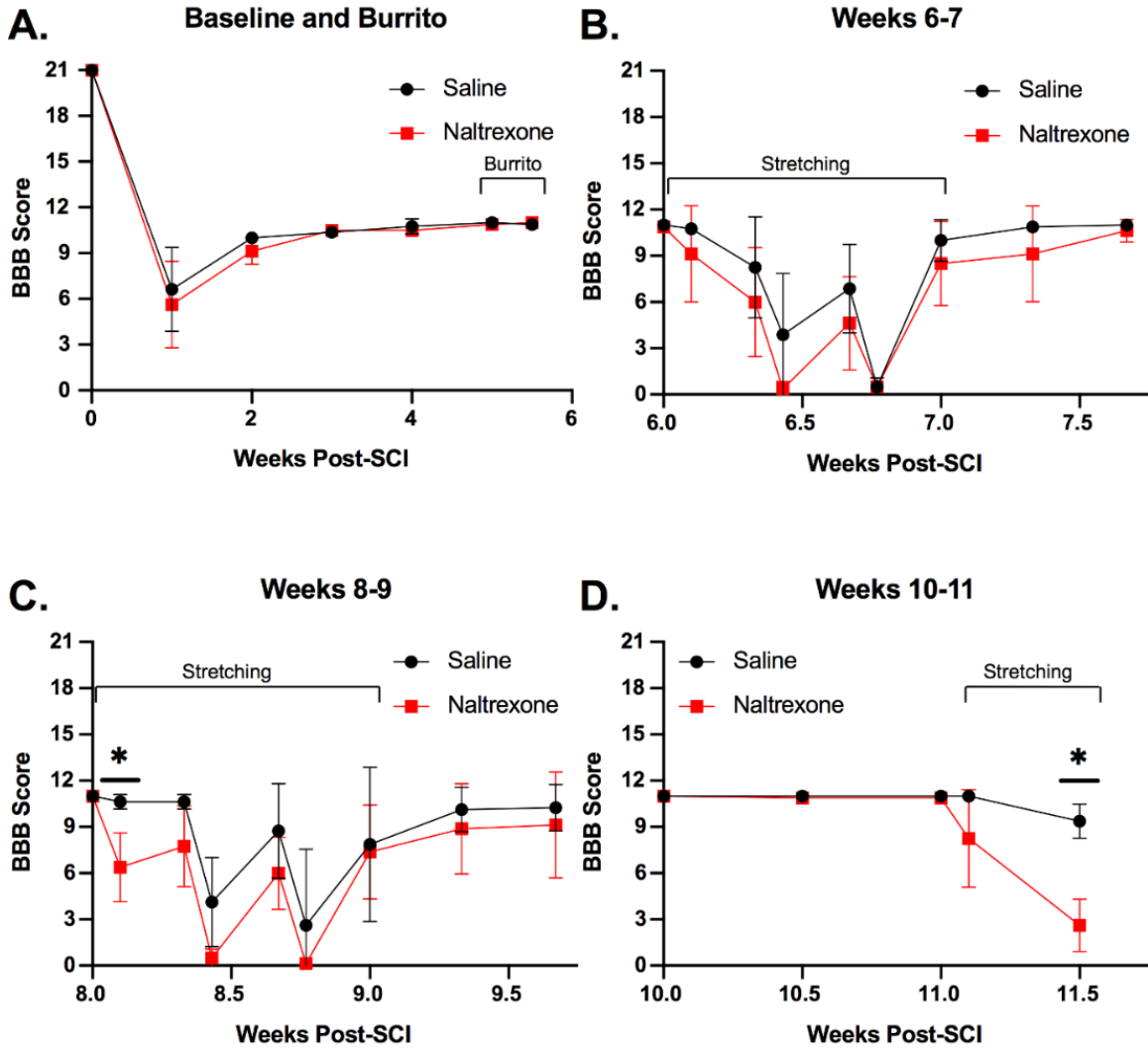


Figure 3. BBB Open Field Locomotor Scores.

Stretching causes a decrease in locomotor function following SCI. The locomotor dysfunction is accelerated following administration of naltrexone. **A)** Baseline BBB measurements, as well as BBB measurements before and after the towel wrapping session without stretching. The first, second, and third weeks of stretching are shown in panels **B**, **C**, and **D**, respectively. Significant differences were seen following 1 day of stretching during the second week of stretching (**C**) and following 2 days of stretching during the third week of stretching (**D**). Data are displayed as group mean (solid/dashed line) and individual values. All data were analyzed using a mixed model ANOVA between each time point, * $p < .05$

Response to afferent stimulation

Analysis of variance revealed a difference between saline and naltrexone groups ($F_{(1,11)}=6.8$, $p=0.024$). However, post-hoc analysis showed no significant difference in tail-flick response latency between groups before and after drug/saline injections (Figure 4A $p>0.05$). Furthermore, there were no significant differences in onset latency, peak-trough amplitude, and response duration of gastrocnemius EMG following magnetic stimulation of the tail between groups or following administration of naltrexone (Figure 4B-D).

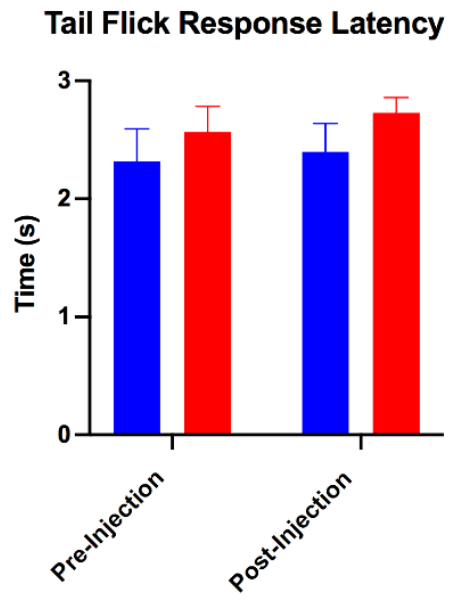
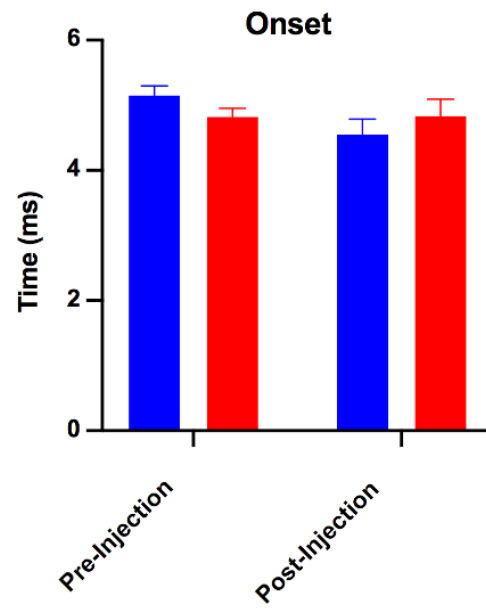
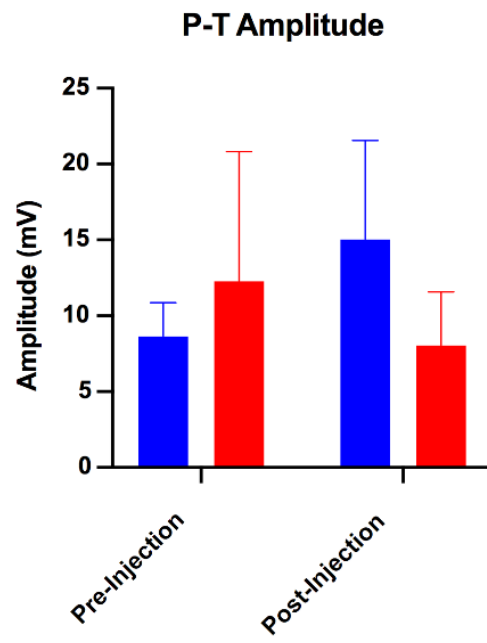
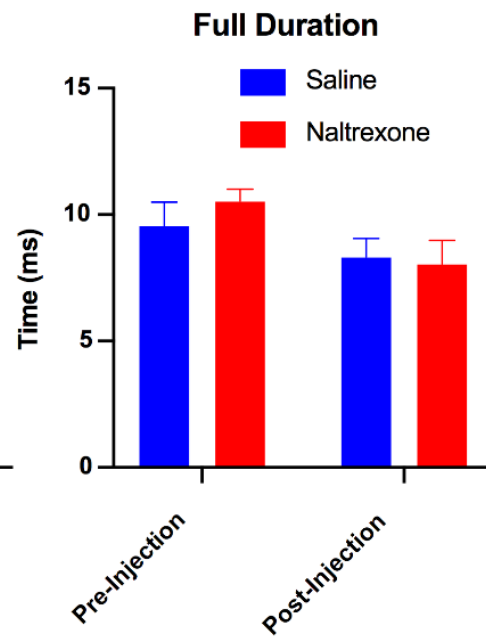
A.**B.****C.****D.**

Figure 4. Responses to thermal and magnetic tail-stimulation before and after naltrexone.

(A) Response latency measured by tail-flick assessment. (B) Time between initial tail-stimulation and gastrocnemius EMG response. (C) Peak-trough amplitude of gastrocnemius EMG response to tail-stimulation (D) Duration of gastrocnemius EMG response to tail-stimulation. Data is displayed as group mean +/- SD. All data were analyzed using a mixed model ANOVA. No significant differences were found between groups at any measured point.

Immunohistochemistry

Representative images of CGRP immunohistochemistry are shown for naltrexone-treated and control animals in Figures 5A and 5B, respectively, while the CGRP+ area used for calculations is shown in Figures 5C and 5D. There were no differences in CGRP-positive area between groups as demonstrated in Figures 5E and 5F ($F_{(1,36)}=0.058$, $p>0.05$).

Representative images of c-Fos immunohistochemistry are shown for control and naltrexone-treated animals in Figure 6A and 6B, respectively. Heatmap visualizations of total neuron distribution from spinal L2-L5 (Figure 6C and 6D) demonstrate the spatial arrangement of the number of c-Fos positive nuclei (groupwise comparisons are in Figure 6E and 6F). Due to differences between left and right sides, counts were split for Mann-Whitney analysis ($n_1 = n_2 = 12$, two-tailed significance for all tests). On the left side, differences were seen between groups at spinal segments L2 ($U = 7$, $p<0.001$), L3 ($U = 3$, $p<0.001$), L4 ($U = 33.5$, $p<0.05$), while right sided differences were seen at spinal segments L2 ($U = 20$, $p<0.005$), L3 ($U = 22.5$, $p<0.005$), L4 ($U = 13.5$, $p<0.001$), and L5 ($U = 31.5$, $p<0.05$). Neuron distributions appear similar between both groups (Figure 6G-N), although higher concentrations are seen in the naltrexone-treated group.

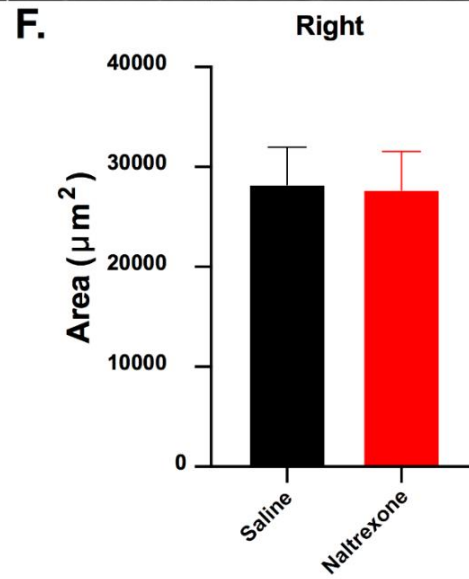
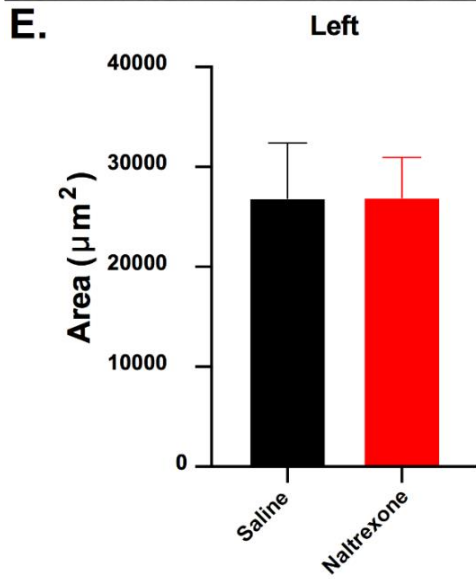
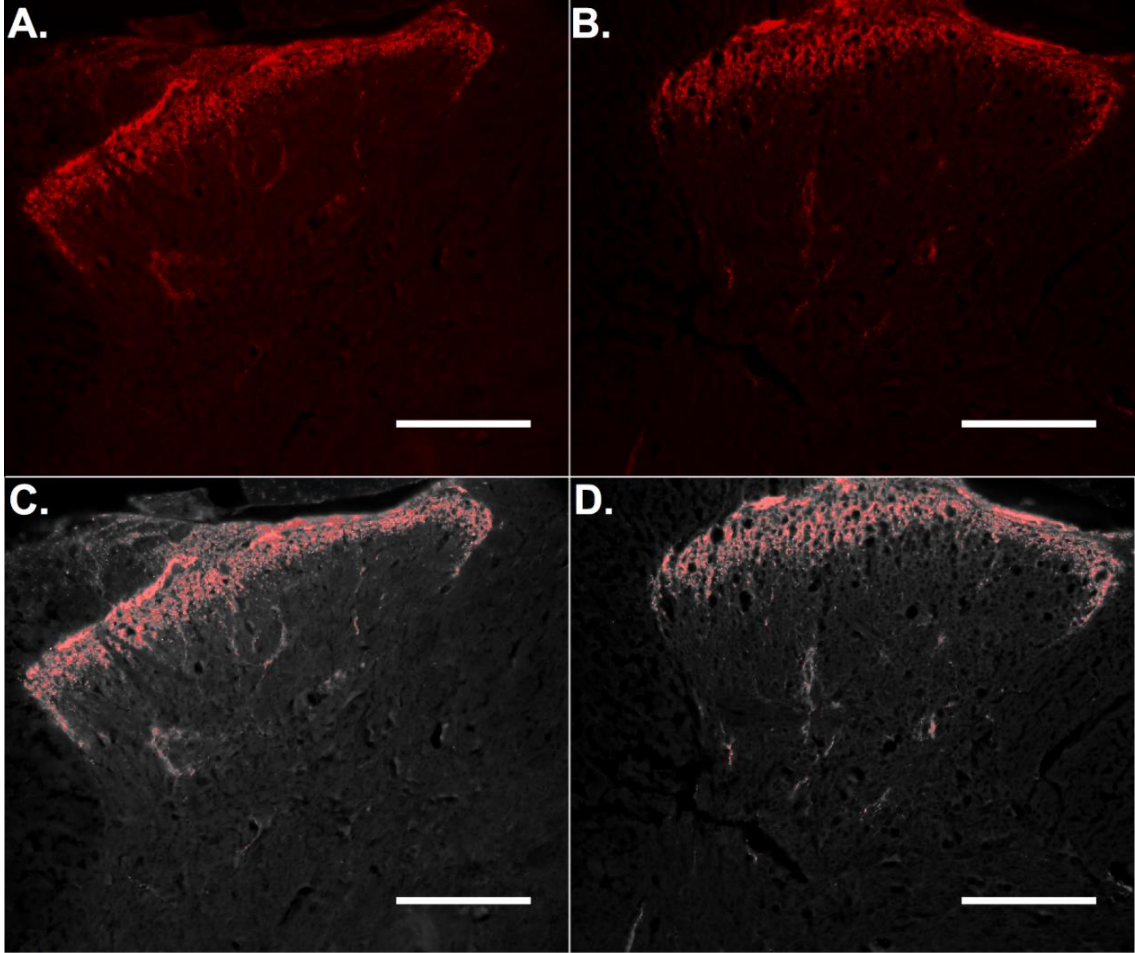


Figure 5. CGRP quantification and analysis of naltrexone and saline treated rats.

A&B) show representative images from naltrexone and control animals, respectively.

C&D) CGRP immunohistochemistry in the dorsal horn of the spinal cord (L3 segment).

Data shown as means + standard deviation (One-way ANOVA, Tukey HSD post hoc).

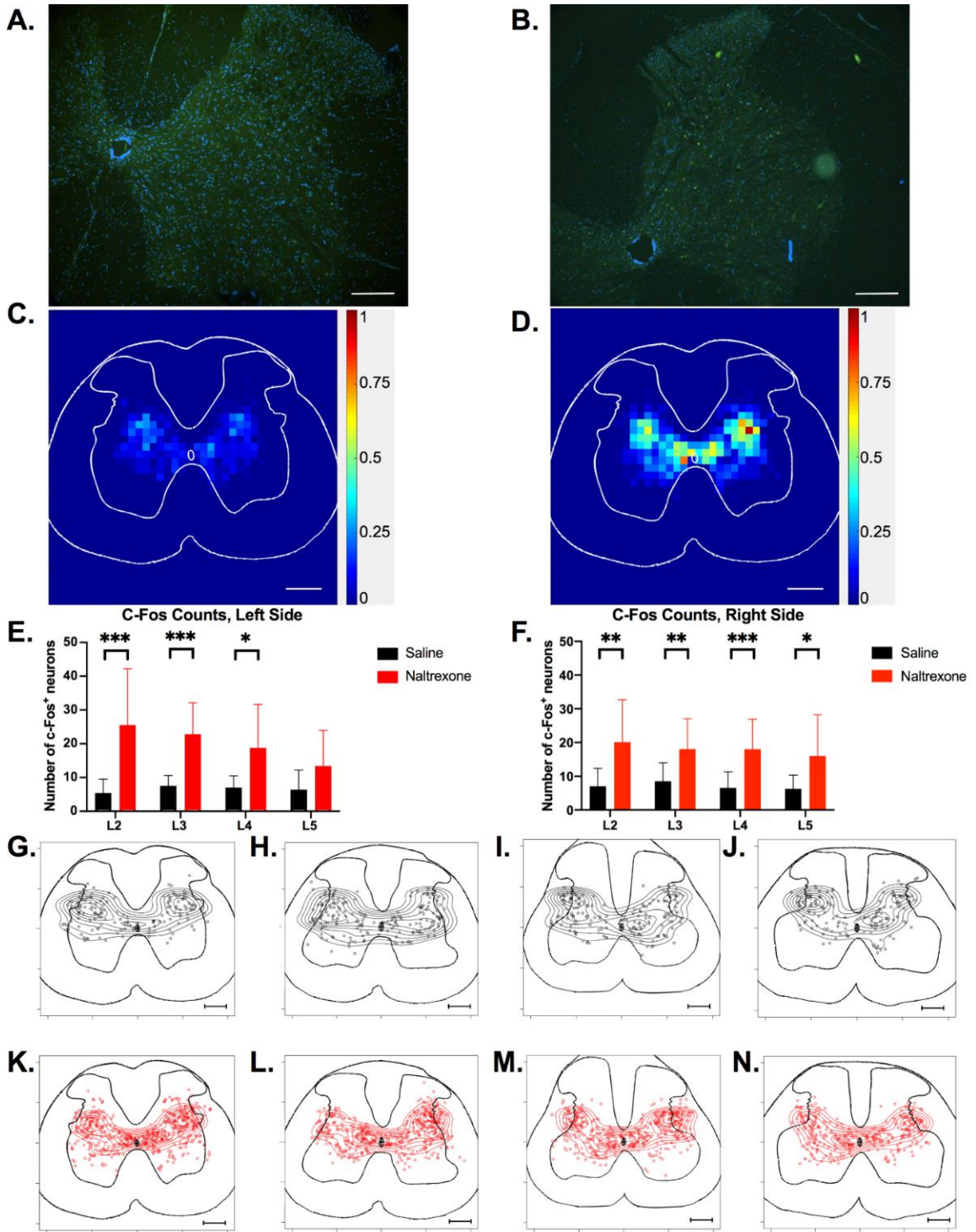


Figure 6. c-Fos quantification and analysis of naltrexone and saline treated rats.

A&B) Representative images from control and naltrexone animals (scale bar = 100 μm), respectively while **C&D)** show heatmaps representing the overall distribution of neurons from L2-L5 (each “pixel-bin”:100x100 μm). **E&F)** quantifications of neurons divided into spinal level, where each bar represents an average number of c-Fos positive neurons from 3 sections at each level. Data is displayed as group mean +/- SD. All data were analyzed using a Mann-Whitney test, * $P < .05$, ** $P < .01$, *** $P < .001$. **G-N)** Scatter-contour plots of for L2-L5 c-Fos neurons of control animals (**G-J**) and naltrexone animals (**K-N**), (scale bar = 500 μm).

Discussion

Based on evidence that ablation of C-fibers reduces the detrimental locomotor effects of stretching after SCI [171], the goal of this study was to use a pharmacological approach to further elucidate the role of the nociceptive system in this phenomenon. Opioid receptors are widely distributed throughout nociceptive circuitry in the spinal cord as well as directly on sensory afferents, therefore endogenous opioids could play a role in modulating the information conveyed from nociceptors to populations of locomotor related interneurons. Consistent with previous studies, daily stretching led to a progressive decrease in locomotor function over the course of a single week. Additionally, typical stretch responses such as air stepping, spasms, and kicking were present following stretching as seen in previous studies [183]. Administration of naltrexone prior to stretching increased the rate of locomotor decline following stretching and greatly increased the spasticity and spastic hindlimb responses during and following stretch. Previously, we found that nociceptor-depleted animals had significantly reduced clonic-like hindlimb responses to stretch as compared to nociceptor-intact stretched rats. In addition, the latter group of animals had a significant correlation between the number of c-Fos+ neurons in the intermediate and ventral horn gray matter and the clonic-like hindlimb response severity scores [171]. These data suggest that endogenous opioids mitigate the inhibitory effect on locomotion induced by clinically modeled hindlimb stretching.

Application of naltrexone in this study was systemic and could therefore be acting at multiple targets in the nociceptive circuitry, although the majority of μ -opioid receptors are expressed on central terminals of nociceptive afferents that primarily synapse in laminae I and II [185]. Endogenous opioid peptides activate μ -opioid receptors on these terminals and decrease neurotransmitter release by shortening repolarization time and

duration of action potentials via inhibition of adenylyl cyclase/reductions of cAMP and decreasing conductance of Ca²⁺ channels [186]. Blocking this effect with naltrexone would result in greater synaptic efficacy, therefore amplifying the effects of stretching. However, if this were the sole mechanism of action the nociceptors involved in the tail-flick reflex would also be altered and should lead to decreased response time, which was not the case. This discrepancy could simply be due to the difference in stimulus duration and scope; stretching is a prolonged, presumed-nociceptive stimulation over the course of two minutes for an entire muscle group, whereas the tail flick assay uses a brief and localized stimulus (2-3 seconds) with a pause between tests. This theory is supported by evidence demonstrating that opioid antagonists can modulate the response of deep dorsal horn interneurons to repetitive electrical stimulation of C-fibers, emphasizing the importance of timing and duration [187]. In addition, the dosage of naltrexone used here would antagonize not only μ -opioid receptors but also κ -opioid receptors. It has been demonstrated that κ -opioid receptors exert their effects postsynaptically by inhibiting NMDAR synaptic currents [188], which could provide an additional mechanistic difference between stretch and tail-flick induced changes. Furthermore, specific antagonism of κ -2 opioid receptors is sufficient to inhibit the sensory-dependent modification of motor output in a model of instrumental learning in the spinal cord [189].

Despite the robust increase in spasticity following stretching, administration of naltrexone did not alter the response in our tail flick assay or change EMG responses to stimulation of large diameter afferents at the base of the tail. Expression of opioid receptors on primary afferents is almost entirely restricted to small-diameter unmyelinated c-fibers [19], with only scarce expression demonstrated on large diameter axons [20]. Based on this expression pattern, it was not surprising that magnetic

stimulation – recruiting primarily large diameter afferents – was unchanged following administration of naltrexone.

Increased expression of c-Fos positive neurons in the naltrexone animals after two days of stretching corresponds with the quicker decrease in locomotor function seen in this group. The distribution of these neurons appears to be concentrated in the deep dorsal horn, intermediate gray matter, and ventral horn. This distribution of is similar to previous stretching induced expression of c-Fos [171], suggesting activation of the same circuitry. However, despite the increase in c-Fos positive neurons, administration of naltrexone prior to stretching did not appear to influence sprouting of peptidergic C-fibers below the level of injury compared to stretching without naltrexone. These results are in apparent contrast to our earlier findings showing that increases in c-Fos+ nuclei and CGRP+ afferent processes were both present in the lumbar dorsal horns of stretched animals [171]. It is possible that the naltrexone-exacerbated stretching effect was insufficient to cause a change in sprouting, or that the sprouting observed previously was only indirectly related to muscle stretching. For example, it has been demonstrated that forced exercise can reduce nonpeptidergic C-fiber sprouting [56], suggesting a likely role for inactivity in sprouting. Additionally, the severity of injury has been shown to play a role in the amount of sprouting both rostral and caudal to the site of injury [190]. Further investigation into the relationship between nociceptor sprouting and the effects on the spinal circuitry following stretching are warranted. Emphasis should be placed on the action of specific opioid receptor subtypes (e.g., μ vs κ) and how their effects differ on pre- and post-synaptic nociceptive circuitry.

In conclusion, we have described the locomotor, behavioral, and histological effects of acutely blocking opioid receptors before hindlimb stretching post-SCI. Given generally negative effects associated with nociceptive afferent signaling following SCI,

the evidence in the current study suggests that endogenous opioids play an important role in modulating nociceptive inflow and/or processing. Interestingly, in a clinical trial, patients with SCI who received naloxone infusions experienced increased frequency and duration of spasticity during the period of infusion and these effects were not seen in able-bodied subjects [191]. While we did not observe spontaneous spasticity in response to naltrexone over the course of this study, the responses to stretch following administration of naltrexone are like those described in humans. These findings highlight physiologically similar responses in human patients and animal models of SCI to opioid receptor blockade and thus emphasize the potential clinical relevance of our observations.

Whereas opioid receptor antagonism in the current study enhanced stretch-induced locomotor dysfunction, it is important to note that exogenous administration of opioid agonists post-SCI can also have a detrimental effect on locomotor recovery [48]. A potential physiological mechanism underlying this agonist-induced phenomenon is kappa opioid-mediated central sensitization resulting in excitotoxicity [192]. Other evidence suggests that endogenous opioids play a mixed role following SCI: pharmacological blockade can improve spinal cord perfusion and neurological function following SCI [193], however, endogenous opioids also play an important role to counter maladaptive hyperexcitability and states of hyperalgesia. While many of these published results appear contradictory, they highlight the complexity of the opioid system and our limited knowledge of the mechanisms of action, particularly in conditions like SCI which can broadly alter circuitry, receptor expression, and cell physiology.

CHAPTER III

CADENCE-MODULATED FORCES AND EMG RESPONSES IN A RAT MODEL OF MOTORIZED CYCLING

Introduction

Exercise and MC are used to target central nervous system plasticity and/or cardiovascular health post-SCI. Despite its use, clinical studies of MC have shown limited effects on spasticity [194, 195] and arterial peripheral circulation [157, 196]. Conversely, a rat model of MC has demonstrated effects on H-reflex habituation [197], wind-up of stretch reflexes [198], and electrophysiological properties of motoneurons [165]. These contradicting results suggest a fundamental difference between the animal model and clinical practice.

A potential source of variability is the magnitude of muscle activation that occurs during MC. Although often termed “passive”, MC was shown to elicit rhythmic electromyography (EMG) activity in the soleus of a spinalized rat that corresponded with the flexion of the ankle [166]. This pattern suggests that spinally mediated muscle activation during MC is caused by reflex arcs below the level of lesion, potentially by muscle stretch reflexes. Because muscle spindles are responsive to length and rate of stretch [199], differences in biomechanics and/or cadence during MC could cause varying magnitudes and patterns of muscle activation between species or even individuals. This theory suggests that greater muscle activation could be achieved by

altering parameters such as range of motion or cadence, however any modifications must be considered in the context of SCI.

Spasticity is a common issue in the SCI population that could be induced during MC due to its dependence on velocity and limb position [200, 201]. Although limb position during cycling is generally aimed to not overstretch muscle, increases in cycling cadence would increase muscle stretch velocity. Furthermore, maladaptive afferent input from hindlimb stretching has been shown to include eccentric muscle contractions [183] and reduce locomotor function in a rat model of SCI [171], even when applied in a phasic pattern [128]. The reduction in locomotor function was associated with an increased density of CGRP+ afferents in the dorsal horn [171], suggesting that maladaptive plasticity may play a role. While exercise has been shown to reduce the density of CGRP+ afferents in the dorsal horn [56], this is thought to be because of task specific training. Muscle contractions during MC would not only be eccentric but would be opposite of those seen in overground locomotion or active cycling. Furthermore, activity dependent plasticity can be increased by MC training by modifying PTEN/mTOR signaling [202], however whether these changes are adaptive or maladaptive are unknown. It is possible that the effects of mistimed afferent information from MC may have a negative effect on locomotion like stretching, as spinal learning is dependent on afferent input that is coordinated with limb position [203]. The significance of this effect has not yet been studied as the rat model typically utilizes a complete transection.

It was the goal of this study to characterize the effects of daily MC training on EMG, cycling load, and locomotor/ sensory function in both a contusion and transection rat model. We hypothesized that EMG and cycling load would correspond to limb position and would increase with cycling cadence. Furthermore, we hypothesized that daily training would reduce hypersensitivity while having no effect on locomotor function.

Materials and Methods

Experimental design

This goal of this study was to describe the biomechanics of a rat model of MC, and how these mechanics affect the magnitude and timing of EMG activity and force production during cycling. We furthermore sought to understand how daily cycle training affects locomotor and sensory function, and if these changes are reflected in the spinal cord. Cycling began one-week post-SCI and consisted of both training and evaluation cycling paradigms. Training was performed Tuesday-Thursday (30 min/day at 45 RPM), while evaluations were performed Monday and Friday (8-9 minutes). Other outcome measures were performed throughout the week before cycling began. Animals in the transection group were euthanized at 4 weeks post-injury, while animals in the contusion group were euthanized 5 weeks post-injury. This difference was due to time constraints, as animals had to be euthanized ~1 hour after their final cycling session for histological outcome measures (cFos).

Animals, EMG transmitter implantation, and spinal cord injury

Twenty-three adult female Sprague-Dawley rats (225 ± 16 g, Envigo, Indianapolis, IN) were used for this experiment. All procedures involving animals were approved by the Institutional Animal Care and Use Committee at the University of Louisville. Animals were acclimated in their home cages, then handled and exposed to all testing devices used in the study for two weeks before evaluations. Handling was continued throughout the experiment on days when the animals did not receive cycling. Following acclimation, animals were divided into four groups: contusion/cycling (n=9), contusion/no cycling (n=4), transection/cycling (n=6), and transection/no cycling (n=4). Of the contusion/cycling group, four animals were randomly selected to be implanted with EMG

transmitters three weeks before spinal cord injury. Animals were anesthetized for all surgeries using a ketamine (50 mg/kg)/xylazine (0.024mg/kg) cocktail to provide a surgical level of anesthesia as confirmed by the absence of paw withdrawal reflexes in response to a strong toe pinch. The upper back of each animal was shaved and treated to produce an aseptic incision area. A small skin incision was made between the shoulder blades to allow placement of the transmitter (HD-X02, DSI, St. Paul, MN). The transmitter wires were tunneled subcutaneously to the left hindlimb by separating the skin from the muscle layer using blunt dissection. A small incision was made over the thigh of the animal allowing the electrodes to be inserted into the main belly of the vastus lateralis and biceps femoris muscles. Sutures were used to hold the electrodes in place. The incisions were closed using sutures and animals were allowed to recover, receiving our standard post-operative care. Three weeks after this surgery the animals received either a moderate-severe spinal cord contusion injury (25 g/cm, NYU Mascis Impactor) or complete transection at the T10 level as previously described [180]. The animals were allowed to recover for seven days before cycling.

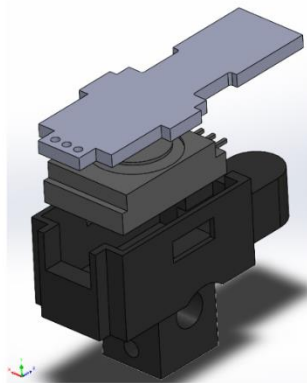
Pedal design

A custom pedal was designed to measure forces during cycling. The goal of this design was to reliably measure the forces seen during MC, while keeping the foot position and trajectory as similar as possible to the pedals received with the purchase of the cycles. Various designs were tested based on these criteria. A progression of these designs can be seen in Figure 7. The first design featured a unidirectional force sensor that only detected forces in compression (Figure 7A). After testing various minor iterations of the design on anesthetized and awake rats it became evident that the design would not be suitable for two reasons. First, rats exhibited significant pulling forces that were not being captured by the force sensor. The foot plate was floating from

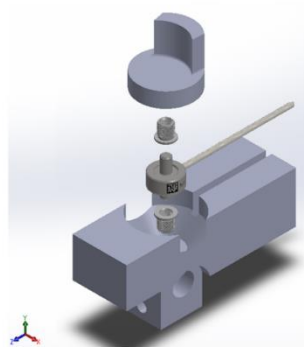
the force sensor to prevent rats from applying enough tension to break the sensor, however this had an unwanted effect of movement between the foot plate and sensor that created unreliable force readings. Second, the metatarsals of the rat were attached using a Velcro strap that proved to be incapable of securing the foot for the duration of a recording session.

The second design (Figure 7B) overcame these limitations by first using a sensor that measured forces in tension and compression (LCM100, FUTEK Advanced Sensor Technology, Irvine CA). Aluminum threaded ends were firmly secured in the new footplate and base, creating a reliable connection. Additionally, the new footplate allowed the metatarsals to be secured vertically to the sensor using tape, which was more reliable at keeping the paw secured during cycling. This design was improved upon in the final iteration (Figure 7C), which incorporated a tri-axial, multi-directional force sensor (Nano17 SI-12-0.12, ATI Industrial Automation, Apex, NC). Three hemispheres forming a right angle were added to the outside of the pedal, which could be tracked alongside other kinematic markers to calculate the point and direction of force. It should be noted that all designs were 3D printed using polylactic acid (PLA) filament (Hatchbox 3D, Pomona, CA) at 30% density, which was sufficient to not deform under the loads being applied.

A. **Design 1**
Single direction force sensor



B. **Design 2**
Single axis, bi-directional force sensor



C. **Design 3**
Tri-axial, multi-directional force sensor

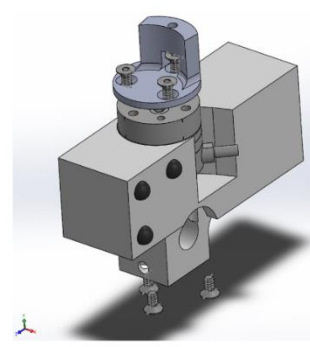


Figure 7. 3D renderings of various designs used to measure force during motorized cycling.

Kinematic recordings, locomotor assessments, and pedal forces

Locomotor function was assessed using the BBB locomotor scale [184]. Baseline measurements were taken pre-injury (pre- and post-transmitter implant), then bi-weekly on Monday and Friday.

Hindlimb kinematics were recorded using two sagittal-oriented cameras (Basler AG, Ahrensburg, Germany) at 100Hz in a custom LabView program. Animals were marked using 3mm OptiTrack hemispherical reflective markers (Planar Systems, Beaverton, OR) placed on the skin over the iliac crest (anterior rim of the pelvis), hip (head of the greater trochanter), ankle (lateral malleolus), and toe (fifth metatarsophalangeal joint). Videos were digitized and converted into 3D coordinates using the MaxTraQ software package (Innovision Systems Inc; Columbiaville, MI). It should be noted that the knee was not marked since excessive movement of the skin relative to the joint results in inaccurate information [204]. To account for this, the femur and tibia of each rat was dissected and measured postmortem. These measurements were used to scale custom models of each rat [205] in the OpenSim platform [206]. Inverse kinematics were calculated using the measured marker locations, which were then analyzed using custom MATLAB scripts (MathWorks, Natick, MA). Cycling kinematics were recorded during the evaluation cycling protocol, which consists of twenty cycles at six cadences (5, 10, 15, 30, 45, and 60 RPM) applied in a random order. Hindlimb cycling kinematics were collected in synchrony with EMG (described below) and forces (1000Hz) using a custom LabView script weekly on Monday and Friday. After applying markers as described, the hindpaws of the rat were attached to the pedals (Figure 7C) using tape and the rat was secured in place by a strap with velcro.

Electromyographic (EMG) recordings

EMGs were recorded at 1000Hz using LabChart 8 (ADInstruments, Sydney, Australia) during cycling evaluations and exported for further analysis to MATLAB. Kinematic recordings synchronized to the EMG recordings were used to divide EMG into gait cycles for further analysis.

Forces

Forces were processed before analysis using a custom MATLAB script. Briefly, a second order zero-lag lowpass filter with a cutoff frequency of 6 Hz was applied to the raw data. The data was then separated into individual cadences and the fundamental frequency (f_0) was identified at each cadence. A notch filter was applied at f_0 , then the subsequent two harmonics ($2*f_0$ and $3*f_0$). The resultant force was used as the spastic force, while the non-spastic force was calculated as the difference between the original and spastic forces.

Non-spastic forces were divided into flexion and extension phases, and the normalized area under the curve (AUC) was used for analysis (total AUC/cycle length). This process was performed on the cycling rats under isoflurane pre-injury; these normalized values (greatest normalized AUC from each cycling cadence) were subtracted from awake cycling to approximate the effects of limb inertia and gravity. Spastic forces were also divided into flexion and extension, however peak values were used for analysis. Peaks $>20\%$ body weight were detected, and trials containing a spasm were identified as a trial that contained one or more peak. Heatmaps were created by defining the onset and termination of each spasm (individual spasms were defined as a gap > 1 s between peaks) and representing activity as either “on” or “off”.

EMG

After collection, the raw EMG signal was high pass filtered at 50 Hz to remove movement artifacts, then separated into flexion and extension phases for analysis. Root mean square values were calculated for each cycle to allow analysis of EMG magnitude. This technique was limited to analysis between cadences in individual animals at discrete timepoints due to non-physiologically relevant variations in EMG magnitude. As obtaining maximum voluntary activations in rats is not possible, EMG was instead normalized using the Teager-Kaiser Energy (TKE) operator combined with morphological operators as described by [207, 208]. The TKE operator is defined as

$$\psi(n) = x^2(n) - x(n+1)x(n-1)$$

for the original EMG signal (x) where n is the sample number [208]. A period of muscle inactivity was recorded before each trial and used to set a threshold (T), defined as

$$T = \mu_0 + j * \delta_0,$$

where μ_0 and δ_0 are the mean and standard deviation, respectively and j is a scale factor [208]. This method then detects and classifies bursts of EMG activity as “on”, with periods of inactivity classified as “off”. The resultant signal is therefore classified on a scale of 0 to 1, where 0 represents no muscle activity and 1 represents muscle activity throughout the duration of the cycle.

Sensory assessments

A tail-flick assay was employed to assess thermal sensitivity using a radiant heat tail-flick device (Columbus Instruments, Columbus, Ohio, USA). A rat was placed on the platform and gently restrained, while the base of the tail was placed above the photocell for thermal stimulation. Intensity of the heat source was set to 10 out of 25, with a maximum duration of 10 s for each trial to avoid tissue damage. For each rat, tail-flick latency was measured three times with at least two minutes between measurements. A baseline

assessment was performed pre-injury, and subsequent tests were performed weekly on Tuesday.

Euthanasia and tissue histology

Animals were sacrificed 1-2 h after the last cycling evaluation using a ketamine (50 mg/kg)/xylazine (0.024 mg/kg) cocktail and transcardially perfused with 4% PFA. Spinal cords were dissected and post-fixed in 4% PFA for 2 h, then transferred to 30% sucrose for cryoprotection. The injury epicenter was separated from the contusion animals, while the L1–L5 segments were separated from the rest of the spinal cord of all animals under a dissecting microscope and blocked in O.C.T. compound. The injury epicenter of the transected rats was determined complete by visual inspection. For the injury epicenters, transverse sections were cut at 50 μm on a cryostat.

Transverse sections were cut at 20 μm on a cryostat for immunohistochemical analysis into 6 blocks. Immunohistochemistry was performed using CGRP and c-Fos antibodies as previously described [209]. Briefly, sections of L3 spinal cord were warmed and washed with PBS and 0.3% PBS-Triton (PBST), then blocked for 1 h with PBST, 5% bovine serum albumin (BSA), and 10% normal donkey serum (NDS). After blocking, slides were washed and incubated overnight with CGRP primary antibody (guinea pig polyclonal anti-CGRP, 1:1000, 20R-CP007, lot #P17101902, Fitzgerald), 5% BSA, and 5% NDS at 4 °C. Following incubation, sections were washed and incubated with a secondary antibody (Alexa Fluor 594-conjugated Donkey anti guinea pig, 1:200, 706–585–148, Lot #129041, Jackson ImmunoResearch Laboratories) for 1 h. For c-Fos, sections of L2–L4 spinal cord were warmed and washed with PBS and PBST. Sections were then incubated in antibody diluent reagent (Invitrogen # 00-3218, Lot1966331A) with c-Fos primary antibody (mouse monoclonal anti-c-Fos, 1:1000, cat#ab208942, Abcam) overnight at 4 °C. The next day, sections were washed and a secondary

antibody (donkey anti-mouse FITC, 1:250, cat#715-096-151, Jackson ImmunoResearch Laboratories) was combined with antibody diluent reagent for 1 h at room temperature. Following incubation, slides were washed and a secondary amplification process was performed using AlexaFluor 488 (mouse anti-FITC, 1:500, cat#200-542-037, Jackson ImmunoResearch Laboratories) in antibody diluent reagent for 1 h at room temperature. Sections were then washed with DAPI (1:1000) in PBST for 5 min. After a set of 3 washes, Sudan Black B was dissolved (1 mg/ml) in 70% EtOH and applied for 15 min at room temperature. Slides were coverslipped using fluomount after a final set of washes.

Image analysis

Images of each section were acquired using a Nikon Ti2 microscope (Nikon Corporation, Tokyo, Japan) using a 20x objective for all histological analyses (resolution 0.32 $\mu\text{m}/\text{pixel}$). An area encompassing each section was defined, and images were stitched such that the entire section was represented in one image. Image analysis of c-Fos and CGRP was performed as previously described [209]. Briefly, CGRP area was quantified in the dorsal horns excluding the dorsal root entry zones, which were removed manually from each image. Analysis of images was conducted using MATLAB (MathWorks, Natick, MA). For c-Fos analysis, each c-Fos positive nucleus was manually identified and marked based on overlap between c-Fos and DAPI using Nikon Elements software. To generate contour plots and heatmaps, previously marked neurons were exported from Nikon Elements. A custom-made MATLAB program was then developed to reconstruct and normalize the position of labeled neurons across sections. A reference axis was created for each image with the origin centered on the central canal, the y axis parallel to the spinal cord midline, and the x axis orthogonal to the y axis. Contour/scatter plots were constructed using R. Distribution contours were created by calculating the two-dimensional kernel density (using the `kde2d` function in the MASS

library), then connecting points of equal density values between 30% and 100% of the estimated density range in increments of 10%.

Statistical analyses

Data were analyzed using SPSS (IBM SPSS Statistics for Windows, Versions 26/27. IBM, Armonk, NY) except for the linear regressions shown in Figure XB&D, which were created using Prism, Version 9 (GraphPad Software, San Diego, CA). Distributions were checked for normality; if data were normal a repeated-measures analysis of variance (RMANOVA) was used for analysis, with strict post hoc t tests (Bonferroni t test for multiple comparisons). For these analyses, independent variables of group, cadence, week, and day were used. Group refers to the injury and cycling condition (e.g., cycle trained transection vs. non-cycled contusion). Cadences were divided into low (5, 10, and 15) and high (30, 45, and 60); significant effects in cadence represent a low-high difference. Week signifies the timepoint post-injury the evaluation occurred, whereas day refers to either the Monday or Friday that the evaluation was performed. In instances where data were not normal (c-Fos), a Mann-Whitney U test was used. Finally, RMS EMG values could not be compared between subjects and were therefore analyzed on a trial-by-trial basis using the sign test.

Results

Muscle activity during motorized cycling

An example trial is illustrated in Figure 8, where rectified EMG data for each cadence is shown in (8A), and EMG normalized using the Teager-Kaiser energy (TKE) operator is shown in (8B).

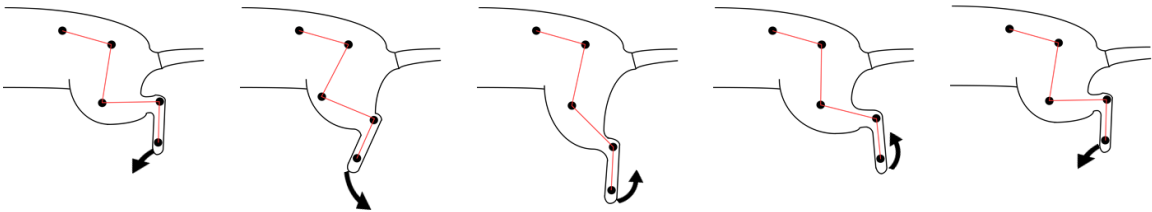
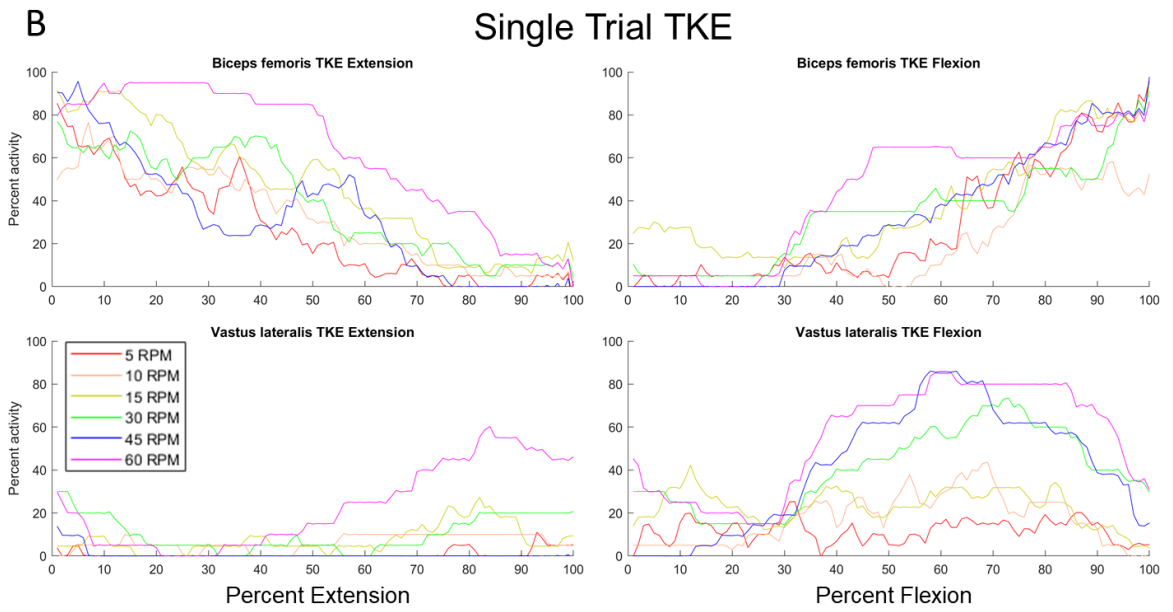
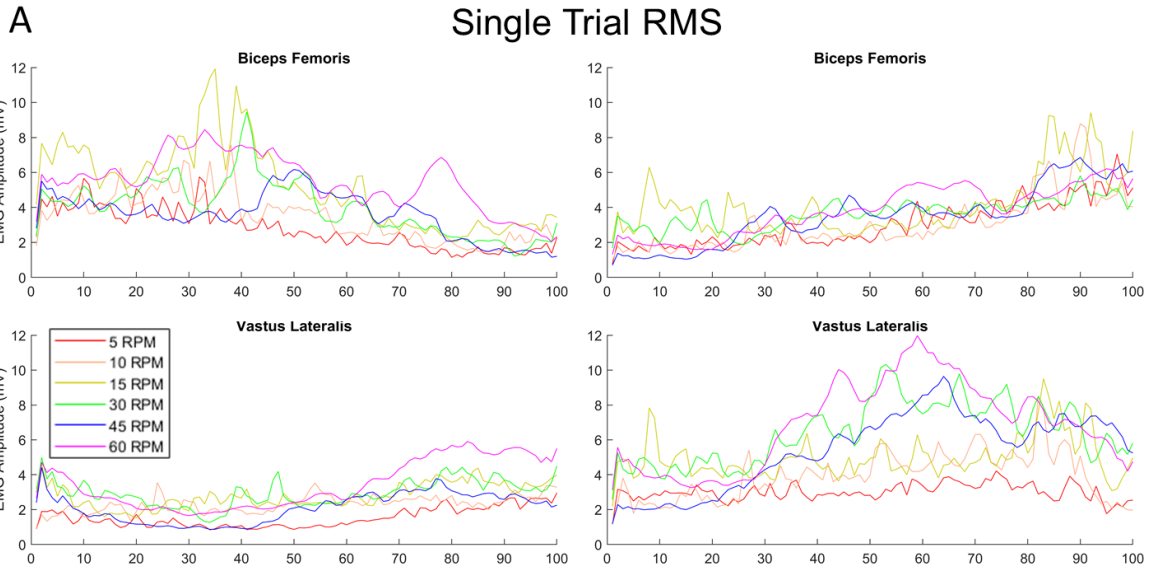


Figure 8. Example trial of EMG analysis.

(A) Raw EMG data was high-pass filtered and rectified using a moving average filter (window size = 23ms); plots represent the average of 20 trials at each cadence. (B) Filtered EMG data was analyzed using a TKE operator algorithm (see Methods). This algorithm detects bursts of EMG and reinterprets the signal as “on” or “off”. Plots represent the average of 20 trials at each cadence, where a value of 0 represents no activity and 100 represents complete activity.

EMG analysis of the biceps femoris is shown in Figure 9. Sign test analysis of individual trials revealed significant differences in 13/27 trials (10/13 high>low cadence) in extension, and 14/27 trials (14/14 high>low cadence) in flexion (Figure 9A). EMG analysis of the vastus lateralis is shown in Figure 10. Sign test analysis of individual trials revealed significant differences in 12/27 trials (9/12 high>low cadence) in extension, and 15/27 trials (14/15 high>low cadence) in flexion (Figure 10A). Percent activation evaluated using TKE was evaluated for biceps femoris and vastus lateralis at each week to examine the effect of phase (flexion vs. extension) and cadence (low vs. high) using RM ANOVA. In the biceps femoris, significant effects of cadence were found at weeks two ($F_{1,8}=8.1$, $p<0.05$), three ($F_{1,7}=9.1$, $p<0.05$), and five ($F_{1,12}=16.0$, $p<0.01$), although no effects were found for phase. Similarly, significant effects of cadence were found in the vastus lateralis at weeks two ($F_{1,9}=10.9$, $p<0.01$), three ($F_{1,11}=12.3$, $p<0.01$), and five ($F_{1,11}=28.7$, $p<0.001$), however significant effects of phase were also found at weeks two ($F_{1,9}=7.0$, $p<0.05$), three ($F_{1,11}=7.0$, $p<0.01$), four ($F_{1,5}=8.0$, $p<0.05$), and five ($F_{1,9}=9.4$, $p<0.05$). Average TKE values with significant post-hoc values for the biceps femoris and vastus lateralis are shown in Figures 9B and 10B, respectively. Although the sample size is small ($n=3$), the data suggest that activation of both muscles occurs more on average for both the BF and VL at higher cadences, with more differences seen during extension. However, it appears as though the VL is preferentially activated during flexion, although an increased sample is warranted before definitive conclusions can be drawn.

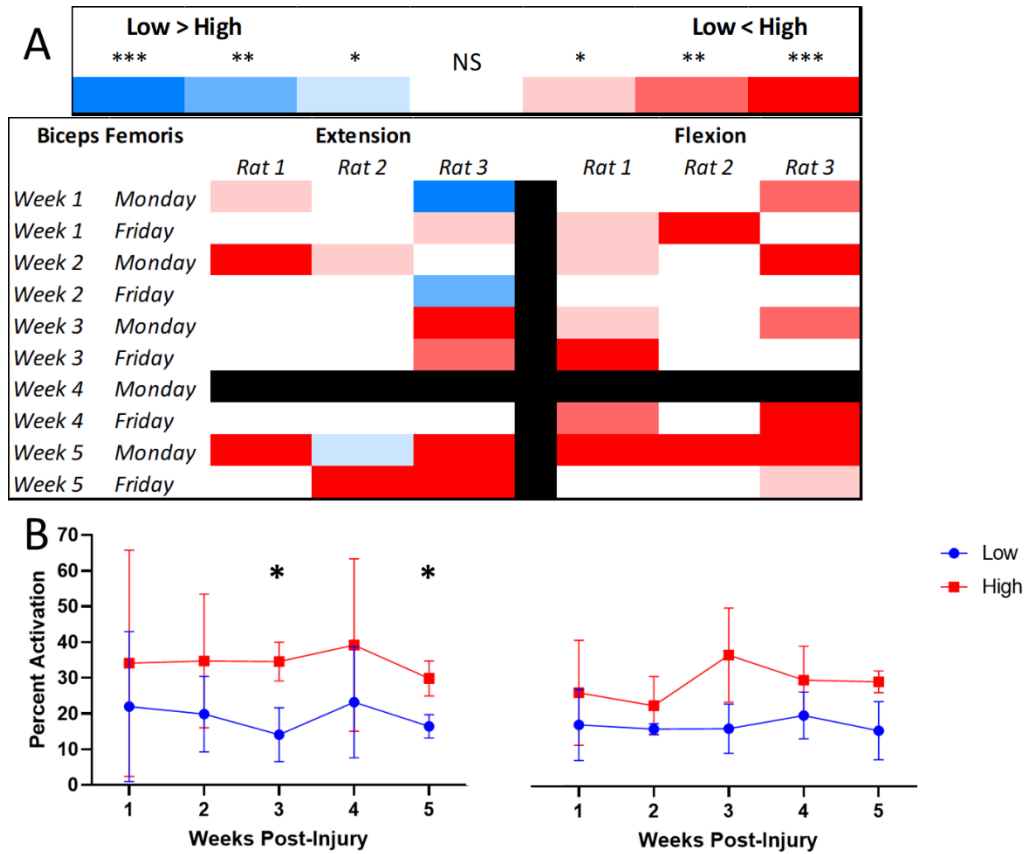


Figure 9. Comparison of EMG responses in the biceps femoris during motorized cycling using RMS values and percent activation.

A) Low and high values were compared for each rat at individual timepoints using the sign test. Values are represented as a heatmap according to the statistical significance found for each day. **B)** Average activation values calculated using the TKE algorithm (n=3) during extension and flexion. Data are displayed as group mean \pm SD. Significant differences from Bonferroni corrected post-hoc t-tests are shown, *p<0.05.

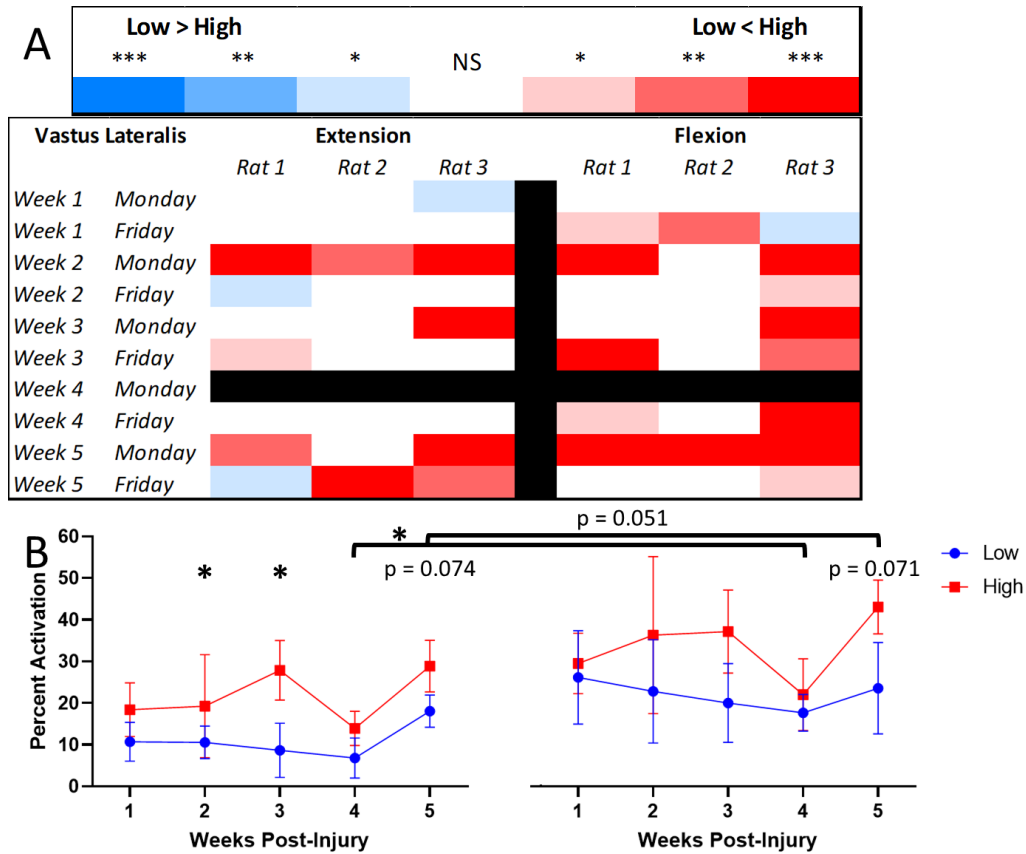


Figure 10. Comparison of EMG responses in the vastus lateralis during MC using RMS values and percent activation.

A) Low and high values were compared for each rat at individual timepoints using the sign test. Values are represented as a heatmap according to the statistical significance found for each day. **B)** Average activation values calculated using the TKE algorithm (n=3) during extension and flexion. Significant differences were found between cadences (low<high) and weeks (flexion>extension). Differences between cadences approached significance at week 5 during flexion and extension, while the difference between flexion and extension approached significance at week 5. Data are displayed as group mean \pm SD. Significant differences from Bonferroni corrected post-hoc t-tests are shown, *p<0.05.

Spastic and non-spastic forces during motorized cycling

An example of the relationship between force (spastic and non-spastic) and EMG is shown in Figure 11 for high and low cadences. Figure 11A&C contain example force traces along with EMG activity in the VL and BF obtained during the same cycling session, with the flexion phase indicated by the gray box. During high cadence cycling, bursts of EMG in the VL are seen during flexion, which result in mild non-spastic force. EMG increases until a spasm is seen, however the muscle activity still appears to be primarily during flexion. This is reflected in the force trace, which contains both a spastic and non-spastic component. In contrast, the spasms during low cadence cycling (Figure 11C, arrows) begin around the point of peak extension and are characterized by co-activation of the BF and VL with high frequency (5-8 Hz) spikes in the EMG. Scatterplots between EMG and force are shown for this trial in Figure 11B&D, where forces are divided into non-spastic and spastic in the left and right columns, respectively. A relationship between the non-spastic force and EMG is seen for the VL at high cadences ($R^2=0.41$) but at no other conditions. In contrast, a relationship between spastic forces and EMG is seen for the BF at high cadences ($R^2=0.52$), but also for the VL and BF at low cadences ($R^2=0.33$ and 0.51 , respectively).

A quantification of the average non-spastic forces is shown in Figure 12. During the flexion phase, RM ANOVA of non-spastic forces revealed an effect of GROUP ($F_{2,130}=6.5$, $p<0.005$), CADENCE ($F_{1,115}=12.3$, $p<0.001$), and WEEK ($F_{4,56}=22.8$, $p<0.001$), but not DAY (Monday vs. Friday). Similarly, an effect of GROUP ($F_{2,67}=5.6$, $p<0.001$), CADENCE ($F_{1,61}=9.0$, $p<0.01$), and WEEK ($F_{4,40}=33.9$, $p<0.001$), but not DAY was found during extension.

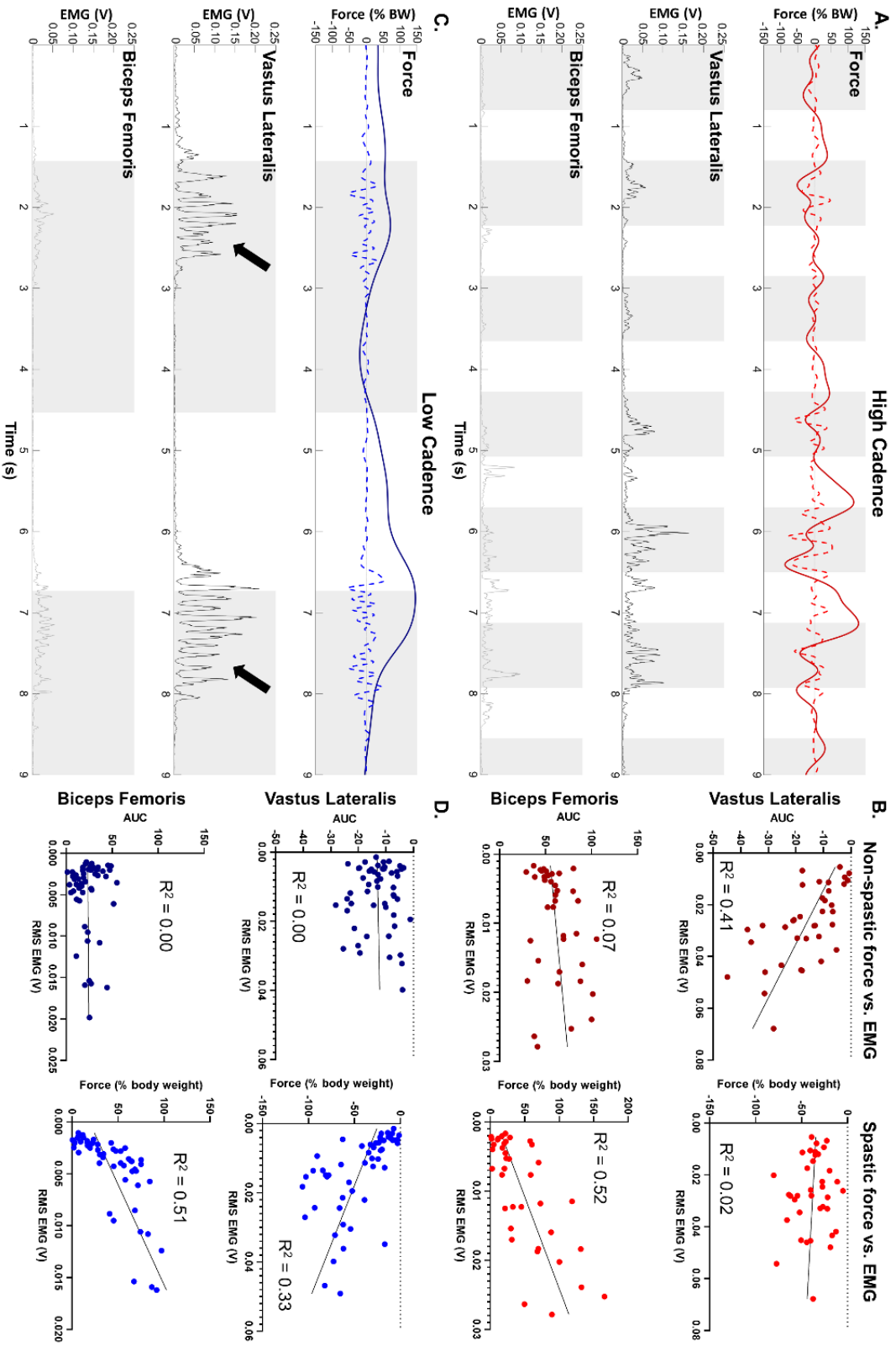


Figure 11. Example relationship between force and EMG.

A) Spastic (red, dashed) and non-spastic (dark red, solid) forces are shown with EMG from the VL and BF during 45 RPM cycling. **B)** Scatterplots of RMS EMG vs. non-spastic (dark red, left) and spastic (red, right) per cycle are shown for the VL and BF. **C)** Spastic (blue, dashed) and non-spastic (dark blue, solid) forces are shown with EMG from the VL and BF during 5 RPM cycling. Arrows indicate spasm with a high frequency component (~8 Hz) **D)** Scatterplots of RMS EMG vs. non-spastic (dark blue, left) and spastic (blue, right) per cycle are shown for the VL and BF.

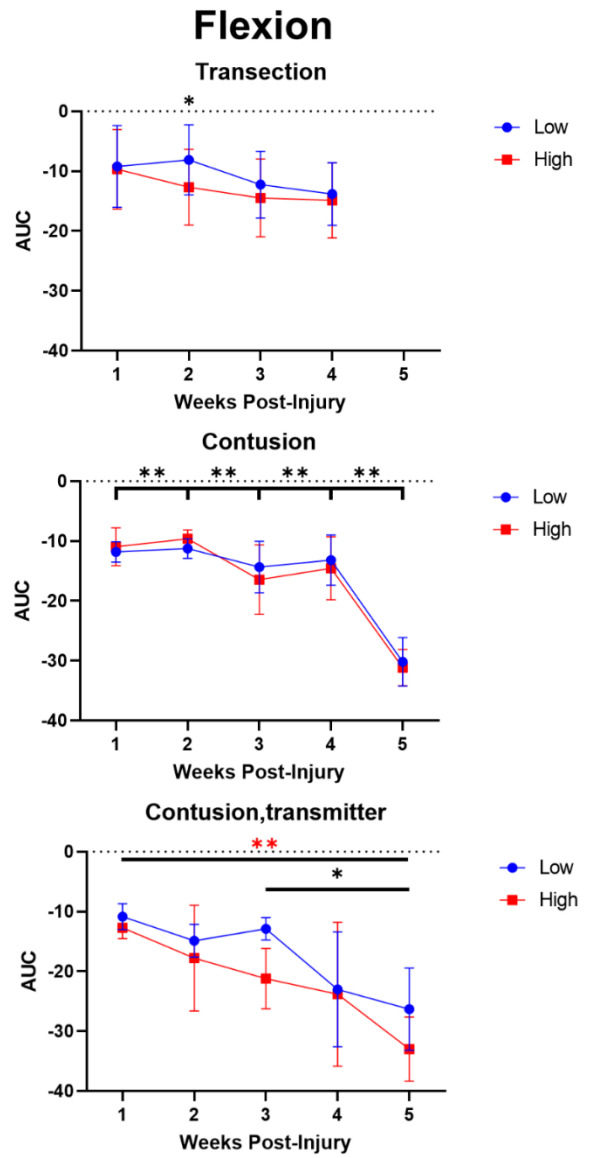
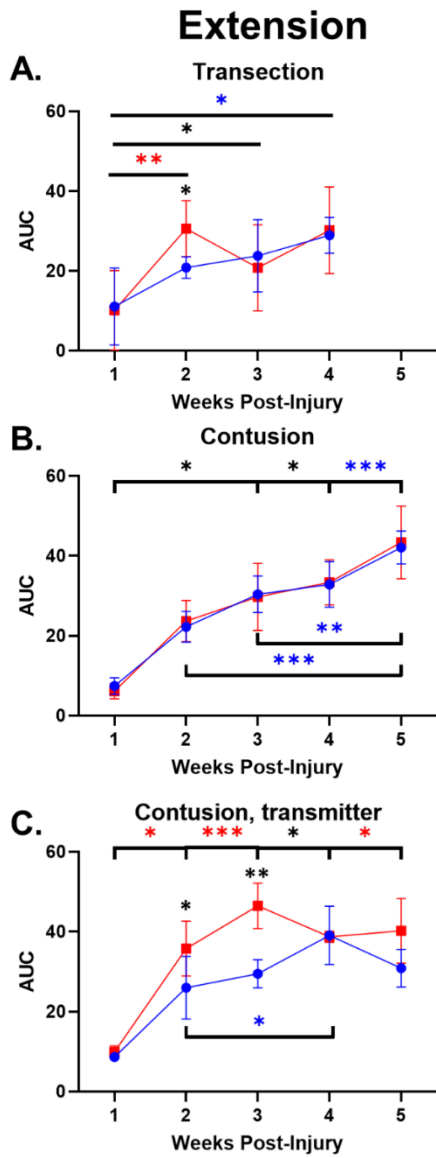


Figure 12. Average non-spastic forces (normalized AUC) for EMG cycling groups.

A) Forces were lowest during week 1, then increased in the subsequent weeks during extension. Although forces were also the during week 1 in flexion, no significant difference was found between weeks. Forces were significantly higher during high cadence cycling at week 2 in flexion and extension. **B)** No significant post-hoc differences were found in cadence for the contusion group. Forces were significantly higher at week 5 compared to all other weeks in flexion and extension. **C)** Although forces were higher during high cadence cycling in flexion and extension, significant differences were only found during extension. Forces were lowest during week 1 and increased in subsequent weeks. Data are displayed as group mean \pm SD. Significant differences from Bonferroni corrected post-hoc t-tests are shown, * $p < 0.05$, ** $p < 0.01$, *** $p < 0.001$. Red, blue, and black stars indicate significant differences were found during high, low, and at both cadences, respectively.

Figure 13. Spastic forces over the course of each cycle, pooled and represented as a heatmap.

(A&B) Forces represented as a function of occurrence, where the scale represents the percentage of trials where a force was detected. **(C&D)** Forces normalized to cycling cadence, where the scale represents the amount of force per minute that is recorded. Scales in **(A&C)** and **(B&D)** are to highlight differences between groups and individual cadences, respectively.

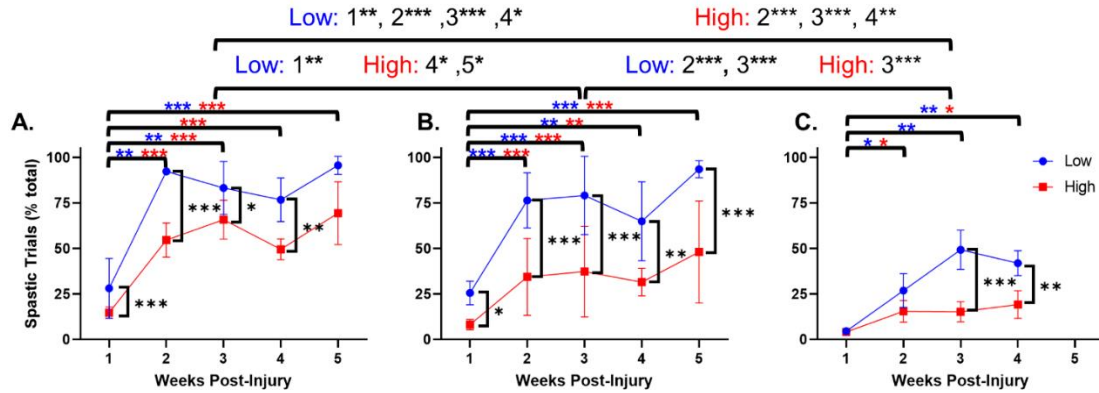


Figure 14. Quantification of trials with spastic forces present.

Results are shown for the (A) contusion/transmitter, (B) contusion, and (C) transection cycling groups. Spasticity was lowest at week 1 for all groups and increased in subsequent weeks. Low cadence trials were significantly more likely to contain a spasm for all injury groups, although this difference was only observed at weeks 3 and 4 in the transected animals. The contusion group contained more spasms than the transection group, while the contusion/transmitter group contained more spasms than contusion or transection groups. Data are displayed as group mean \pm SD. Significant differences from Bonferroni corrected post-hoc t-tests are shown, * $p < 0.05$, ** $p < 0.01$, *** $p < 0.001$. Red, blue, and black stars indicate significant differences were found during high, low, and at both cadences, respectively.

Spastic forces are represented as heatmaps over the course of a gait cycle in Figure 13, where Figure 13 A&B represent the percentages of trials with a spasm present, while Figure 13 C&D represent the number of spasms per minute. A quantification of spasticity occurrence is shown in Figure 14, where cadences were divided into low and high groups. RMANOVA revealed significant effects of group ($F_{2,62}=83.9$, $p<0.001$), cadence ($F_{1,97}=121.8$, $p<0.001$), and week ($F_{4,38}=46.8$, $p<0.001$), but not day. Several significant interactions also occurred: group-cadence ($F_{2,77}=6.5$, $p<0.01$), group-week ($F_{7,43}=2.7$, $p<0.05$), group-day ($F_{2,95}=3.8$, $p<0.05$), week-day ($F_{3,39}=5.1$, $p<0.05$), and group-cadence-week ($F_{7,48}=3.3$, $p<0.01$). All groups showed an effect of cadence, as trials at low cadences were significantly more likely to contain a spastic event. The spasticity mirrors the locomotor recovery in all groups, particularly at week 1 where animals with EMG transmitters had more trials with spasms than transection or contusion cycling groups.

Histological outcomes

The distribution of c-Fos positive neurons did not meet the criteria for normal, therefore Mann-Whitney U test was performed for c-Fos data. As this analysis encompass comparisons between five groups at three spinal levels, significant results are shown in Table 1 for ease of viewing. Significant differences between groups are represented in Figure 15B at individual levels, while heatmaps representing the distribution of c-Fos+ neurons from L2-L4 are shown in Figure 15A. The results of this analysis indicate that cycling upregulated c-Fos expression in the lumbar spinal cord in both contusion and transection groups, although slightly more neurons were found in contusion animals that received cycling. The expression of c-Fos was mostly constrained to the dorsal horn, with most of the expression seen between laminae I-III.

Locomotor function following motorized cycling training

Figure 16 contains BBB scores acquired over the course of the cycling evaluation. Repeated-measures ANOVA revealed an effect of group ($F_{4,117}=80.2$, $p<0.001$), day ($F_{9,27}=26.8$, $p<0.001$), and in the group-day interaction ($F_{32,33}=2.0$, $p<0.05$). Bonferroni post hoc t-tests revealed that most of the differences were between contusion and transection groups, as expected. However, the CT-TR group consistently had higher BBB scores than all other groups, which were significantly higher than the CT-CY group at week 1M/F and week 5F.

Sensory function following motorized cycling training

Sensory function evaluated by tail-flick latency is shown in Figure 17. Repeated-measures ANOVA revealed an effect of GROUP ($F_{4,89}=7.7$, $p<0.001$), DAY ($F_{5,27}=3.5$, $p<0.05$), and in the GROUPxDAY interaction ($F_{18,34}=1.9$, $p<0.05$). Bonferroni post hoc t-tests showed the cycling. Additionally, post hoc testing showed that response latency decreases at 2-, 3-, and 4-weeks post-injury in the TX-NC group compared to baseline.

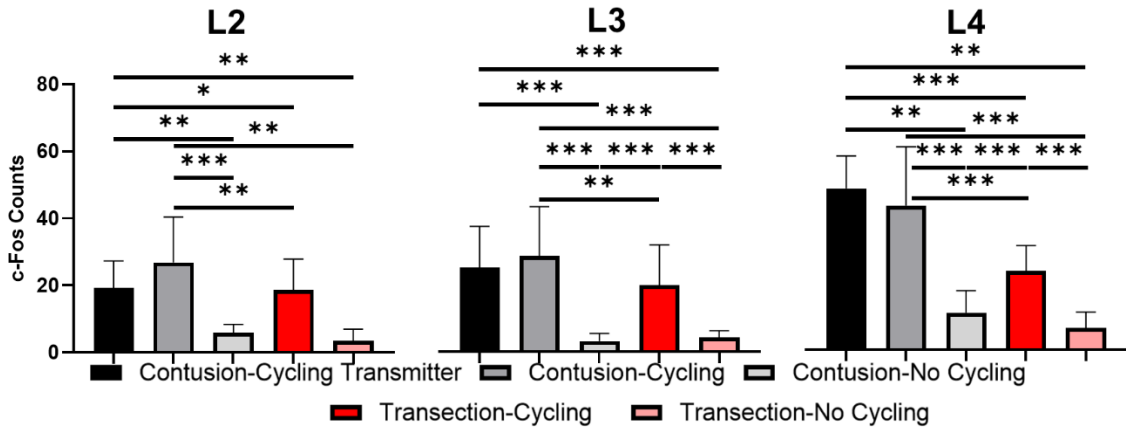
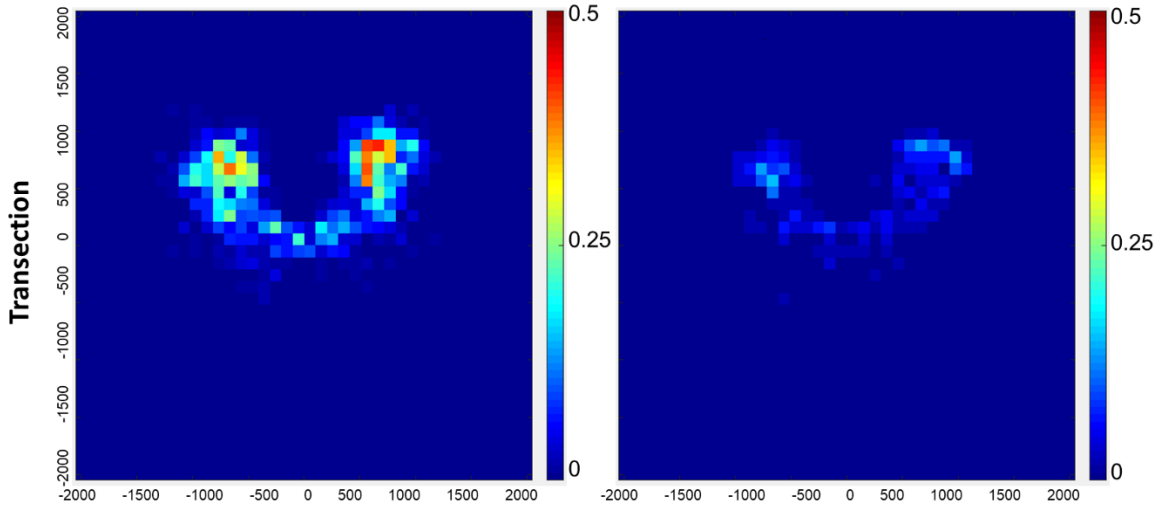
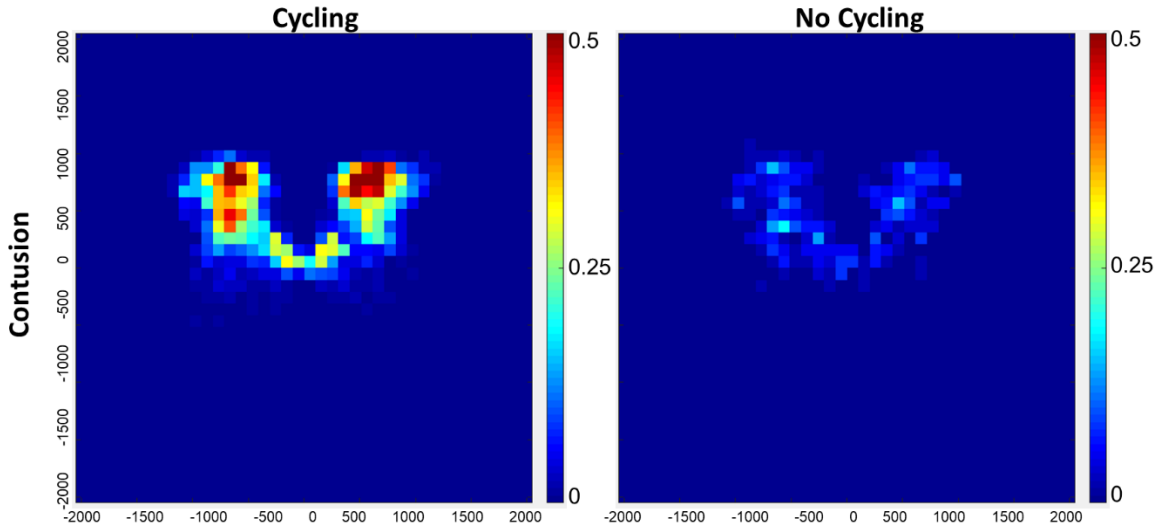


Figure 15. c-Fos expression in the lumbar spinal cord.

A-D) Heatmap visualizations of c-Fos distribution, L2-L4 pooled. No significant differences were found between contusion/cycling groups, which were pooled for visualization. **E-G)** quantifications of neuron counts divided into spinal level, where each bar represents and average number of c-Fos positive neurons from 5 sections at each level. Data are displayed as group mean \pm SD. All data were analyzed using a Mann-Whitney U test, * $p < 0.05$, ** $p < 0.01$, *** $p < 0.001$.

L2	<i>CC</i>	<i>CNC</i>	<i>TC</i>	<i>TNC</i>
<i>CCT</i>	n.s.	U = 53.0, p=0.001	U = 159.0, p<0.01	U = 18.5, p<0.01
<i>CC</i>		U = 46.5, p<0.001	U = 257.0, p<0.01	U = 21.5, p<0.001
<i>CNC</i>			n.s.	n.s.
<i>TC</i>				n.s.
<i>TNC</i>				
L3	<i>CC</i>	<i>CNC</i>	<i>TC</i>	<i>TNC</i>
<i>CCT</i>	n.s.	U = 8.0, p<0.001	n.s.	U = 4.0, p<0.001
<i>CC</i>		U = 24.0, p<0.001	U = 289.0, p<0.01	U = 14.5, p<0.001
<i>CNC</i>			U = 121.0, p<0.001	n.s.
<i>TC</i>				U = 64.5, p<0.01
<i>TNC</i>				
L4	<i>CC</i>	<i>CNC</i>	<i>TC</i>	<i>TNC</i>
<i>CCT</i>	n.s.	U = 14.0, p<0.001	U = 107.5, p<0.001	U = 0.0, p<0.001
<i>CC</i>		U = 29.0, p<0.001	U = 169.5, p<0.001	U = 0.0, p<0.001
<i>CNC</i>			U = 167.0, p<0.001	U = 47.0, p<0.05
<i>TC</i>				U = 6.0, p<0.001
<i>TNC</i>				
<p><i>Legend:</i> Contusion-Cycling Transmitter: <i>CCT</i> Contusion-Cycling: <i>CC</i> Contusion-No Cycling: <i>CNC</i> Transection-Cycling: <i>TC</i> Transection-No Cycling: <i>TNC</i></p>				

Table 1. Significant Mann-Whitney U values and their associated p-values.

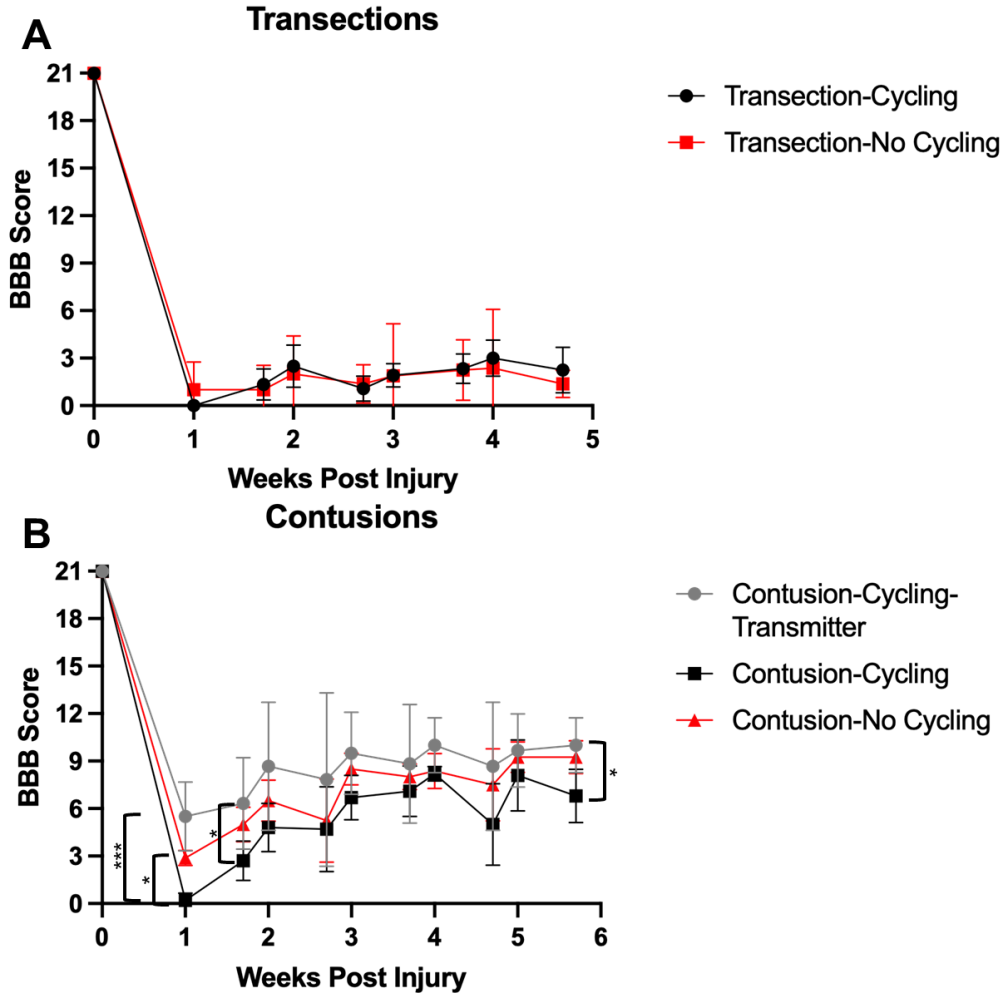


Figure 16. BBB scores during cycling training.

A) Both transection groups predictably lost locomotor function after injury, with slight distal limb movements appearing in the subsequent weeks. No significant difference was found between groups. **B)** Animals in the contusion-cycling group lost more locomotor function than the contusion-no cycling or contusion-cycling-transmitter group at week 1 post-injury, which recovered by week 2. Animals that received a transmitter implantation before injury consistently had higher BBB scores than the other contusion groups, although this only achieved statistical significance on Friday of week 5. Data are displayed as group mean \pm SD.

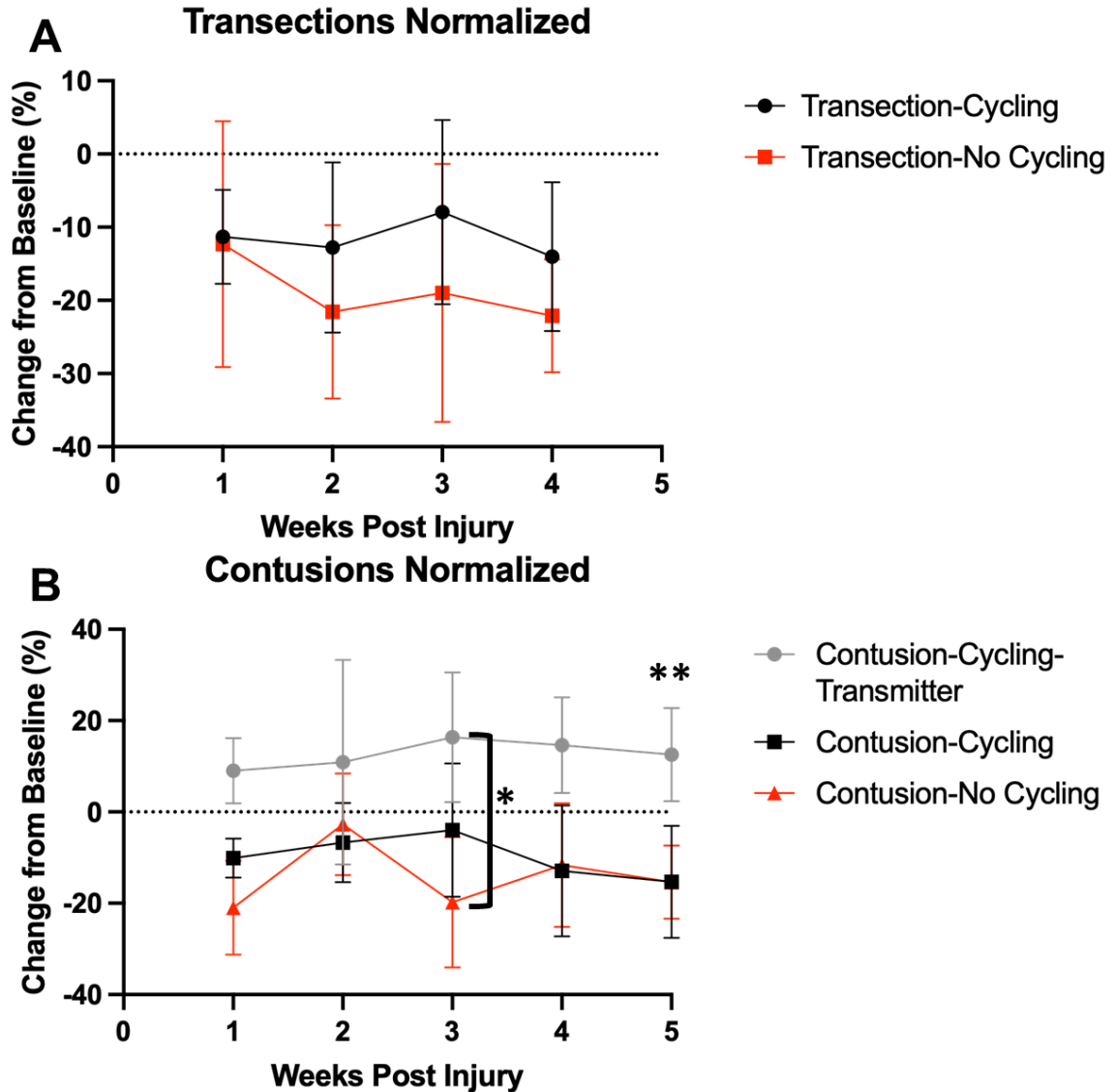


Figure 17. Tail-flick latency during cycling training, normalized to baseline.

A) Both transection groups displayed the same initial decrease at week 1 post injury, however the latency of the cycling group plateaued after this initial decrease while the no cycling group decreased again at week 2 before plateauing. B) Animals that received a transmitter implant before contusion had consistently higher latencies than both groups who did not, with longer latencies compared to baseline. Data are displayed as group mean \pm SD.

Discussion

Although muscle activity has been recorded in a rat model of MC, previous studies did not examine the relationship between PF and cadence in both a transection and contusion model of SCI in rats. Additionally, we developed a technique to separate kicking/spastic forces from non-spastic forces developed with the motion of the pedals. Using this technique, we found that higher cadences (≥ 30 RPM) significantly increase both non-spastic PF and the magnitude/duration of EMG activity, while lower cadences (≤ 15 RPM) increase the likelihood of inducing spastic/kicking forces. Although PF was higher in contusion animals, both spastic and non-spastic forces were present in transected animals. We propose that PF and muscle activity may play a significant role in outcome measures following MC training in rats.

Muscle activity during motorized cycling

SCI causes a disruption of supraspinal pathways projecting onto locomotor centers, which causes locomotor control to disproportionately rely on sensory feedback [210-212]. Although not volitional, MC provides sensory information to the spinal cord (via sources such as cutaneous/ligament mechanoreceptors, muscle spindles, and golgi tendon organs) which can lead to reflexive muscle activation. Evidence from our study suggests that muscle activity can be induced during MC in rats and is modulated strongly by the cycling cadence. Overall, analysis of individual trials demonstrated that higher cadences were more likely to induce longer burst durations and stronger contractions. Of the trials where EMG was higher during low cadences, the majority of these (6/7) were during extension where a higher proportion of spastic forces are seen at lower cadences. Interestingly, muscle activity in biceps femoris and vastus lateralis is increased at higher cadences in both flexion and extension, although the response to

flexion in the vastus is slightly higher than in the biceps. These results suggest that although the monosynaptic stretch reflex likely plays a role, it is not the only factor.

It is important to note that this study primarily investigated the activity of knee flexors/extensors. MC results in a complex movement involving the hip, knee, and ankle joint. Hip extension is known to play a role in activation of central pattern generators [213] and stepping in spinalized treadmill walking [214], implying a key role of the hip in the control of spinal locomotor circuitry. In human SCI, hip oscillations have been shown to drive leg reflex activity in a velocity dependent manner [215]. These multisegmental responses resemble a kicking motion we observed that was primarily induced during extension in addition to pulling or pushing to resist the motion of the pedal. Although rats are capable of hip extension their resting position is far more flexed than humans due to their quadrupedal nature and limb posture at stance [216], suggesting that extension of the hip may play a more pronounced role in rat MC.

Forces during motorized cycling

Interpretation of PF in MC possesses a unique challenge in that a motor provides an external moment that must be considered. Like clinical studies, we record a resting baseline to approximate passive joint moments [217]. However, small kinematic changes in rats lead to different force profiles, making it difficult to justify a simple subtraction of baseline from collected data. Our approach of computationally separating spastic from non-spastic forces offers a solution to this problem, and additionally extends their interpretation in the context of reflex activation. In particular, the stretch reflex in humans contains tonic and phasic components, defined as increased muscle tone and hyperreflexia/clonus, respectively [218, 219]. This definition offers an interesting parallel to the forces developed in our model. As non-spastic forces are developed in resistance to the motion of the pedal while spastic forces are the result of quick

hyperexcitable movements, a possible interpretation of this work is that they provide a representation of the tonic/phasic components of this reflex.

Based on this interpretation, our results suggest that muscle tone increases in response to increasing cadence. While high variability resulted in few differences at discrete timepoints, an overall view of the data showed significant differences between low and high cadences, with transected animals having generally lower non-spastic forces than contusion animals. Spastic forces also showed a difference between cadences; however, it appears that lower cadences increase the occurrence of these forces. Although initially puzzling, it is important to consider that the stretch reflex stimuli are being applied repetitively during cycling. Stretch reflexes are subject to depression following repetitive activation [219], suggesting that more frequently stimulation at higher cadences would lead to different modulation. Heatmaps show an increase in time normalized forces above 30 RPM in all groups (Figure 13D) despite a higher per-trial frequency at lower cadences, particularly 5 RPM (Figure 13B). Interestingly, it has been demonstrated that monosynaptic reflex pathway depression is slightly present at a frequency of 0.1 Hz (6 per minute) but not 0.05 Hz (3 per minute) [220], which may explain why 5 RPM cycling elicits a proportionately higher number of trials containing spastic forces.

Cycle training effects on locomotor and sensory ability

Although sensory information has been shown to affect spinal learning and locomotor output, the effects of passive cycling on locomotion have not been described as most studies use a transection model of spinal cord injury. Here, we performed MC using a moderate contusion model for the first time and describe the effect of MC on locomotion. BBB testing revealed that cycle training had limited effect on locomotor performance, although non-cycled rats had a significantly higher BBB score at Week

5/Friday compared to cycle-trained rats (non-transmitter). A sawtooth pattern emerges starting at week 4 in the contusion (non-transmitter) animals, where the BBB of cycled animals is lower on Friday following 4 days of cycling. This pattern is reminiscent of locomotor deficits caused by daily hindlimb stretching [126, 128], although the effect is much more robust following stretching. However, it has been demonstrated that animals without functional nociceptors have a milder decrease in BBB scores [171], with magnitudes comparable to the mild deficits reported in this study after cycling. This study also reported an increase in c-Fos positive neurons in the lumbar spinal cord of stretched rats, which we also observed in the cycling group. Interestingly, the c-Fos expression after stretching in the nociceptor depleted animals was mostly constrained to the dorsal horn, which we also found in our cycled rats. Taken together, these results suggest the responses we see during cycling are likely not nociceptive in nature.

Finally, it should be noted that animals with transmitter implants were analyzed separately from the other contusion. Although this group had marginally higher BBB scores, we were most surprised to find the injury appeared to have no effect on tail flick latency, even showing a mild increase post-SCI.

Functional Significance

Although MC may show improvements in rats post-SCI such as increased myofiber cross-sectional area [166] or improved cardiovascular function [69], the effectiveness and translatability of these results clinically remains unclear. It has been demonstrated that physiologic responses are only elicited in human cycling when paired with muscle activity, and not during passive movements [155, 157]. Here we demonstrate that EMG can be elicited in response to MC in a rat, and that spastic and non-spastic forces are modulated in a cadence dependent manner in both transection and contusion models of SCI. It may be difficult to directly translate these results as

humans display reduced spinal excitability post-SCI compared to rodents as proprioceptive interneurons depend more on descending input [221]. However, various technologies currently exist that raise excitability in the spinal cord [222, 223] that could be paired with MC in patients that lack the strength for traditional locomotor training. Critically ill but spinally intact patients have shown increased peripheral muscle strength in response to MC [224]. About 20% of these patients showed signs of active muscle contractions during cycling, suggesting this may be an effective therapy if spinal excitability can be raised. Finally, observations from this study may be able to translate into active cycling post-SCI. Although functional electrical stimulation (FES) cycling may provide similar benefits as rodent MC such as increased muscle mass [225] and cardiovascular benefits [226], it quickly subjects patients to fatigue. We noted that many of the muscle contractions in rats are eccentric due to the activation of the stretch reflex. Although intense eccentric exercise has been shown to cause muscle damage [227], mild eccentric exercise can increase muscle strength while putting less stress on the cardiovascular system [228]. Therefore, a milder FES paradigm paired with MC to resist the motion of the pedals may be an alternative to traditional FES cycling in some patients.

CHAPTER IV

INFLUENCE OF RANGE OF MOTION AND CADENCE ON FORCE AND CARDIOVASCULAR OUTCOMES IN A RAT MODEL OF MOTORIZED CYCLING

Introduction

Cardiovascular disease (CVD) is a pervasive issue in the spinal cord injury (SCI) community, as this population is estimated to exhibit a three-fold greater risk of developing CVD relative to the able-bodied population [61, 229]. Lesion level and severity are factors that increase this risk, as individuals with tetraplegia show a 16% greater risk of CVD [62] and elevated risk factors such as blood pressure and serum lipid levels compared to individuals with paraplegia [230]. Physical inactivity plays a key role in the severity and lesion-level dependent development of CVD, as a sedentary lifestyle leads to risk factors such as obesity [231], decreased cardiorespiratory fitness [232], and glucose intolerance [233].

Aerobic exercise is an effective means of improving cardiovascular function, however options for individuals with SCI are limited by the level and severity of paralysis. Although paraplegic individuals can perform upper body exercise there is evidence in humans and rats suggesting that arm/forelimb exercise alone cannot prevent SCI-induced deficits in cardiovascular function [168, 234, 235]. In contrast, lower limb exercise such as body weight supported treadmill training and functional electrical stimulation (FES) cycling have been shown to improve cardiovascular function in individuals with SCI, however these techniques require specialized equipment, trained personnel and are generally cost prohibitive. Motorized cycling (MC) has been proposed

as an alternative to FES cycling as it is considered safe and inexpensive to perform, however the ability of MC to induce meaningful cardiovascular benefits in SCI patients is controversial. Acutely, contradictory evidence has been published showing that passive movements can [158] and cannot [157, 236] induce meaningful changes in femoral artery blood velocity, however any changes seen were limited to an acute training effect. Chronically, it has been demonstrated that a 6-week MC intervention can improve hemodynamic response in the femoral artery, however it has also been demonstrated that MC is unable to induce the physiological responses such as increases in mean oxygen uptake and stroke volume that are seen in FES cycling [155].

Contrary to humans, rodent models of MC have shown significant effects in a variety of cardiovascular outcomes. A pioneering study demonstrated that daily, chronic MC training improved the key functional outcomes of stroke volume and CO, and concomitant improvements in cardiac structure (left ventricular diameter) [69], although these effects does not persist when training was stopped [167]. Furthermore, MC training has been shown to reduce the severity of autonomic dysreflexia and CGRP-positive axon density in the lumbar spinal cord in rats [169]. The effects of MC training on cardiovascular outcomes are not reproduced when rats are subjected to swim training [168] – a forelimb-only exercise post-SCI – suggesting that the larger venous supply and muscle mass in the lower limbs plays a key role.

A possible source of functional benefit during MC is the skeletal muscle pump, a well characterized mechanism whereby skeletal muscle contraction physically compresses blood vessels and promotes venous return [77, 237]. Despite speculation that passive movements could activate the skeletal muscle pump, the evidence is mixed, and direct comparisons show that exercise with skeletal muscle activation has a greater effect on physiological cardiovascular responses [155, 238]. Importantly, it has been

demonstrated that MC in rats elicits rhythmic electromyographical (EMG) bursting coinciding with limb position, suggesting that muscle activity during MC can be triggered by muscle lengthening, presumably via stretch reflexes. Activation of the stretch reflex is dependent on both rate and length of muscle stretch [170], which would be amplified post-SCI due the loss of descending control that manifests as hyperreflexia, spasticity and clonus.

Despite evidence that muscle activity occurs during MC, the hindlimb loading at the pedal and its relation to cardiovascular dynamics has not been described. We speculated that some of the contrasting results between MC studies in humans and rats could be explained by differences in cycling biomechanics, where different muscles were stretched to different lengths and/or at different rates, thus resulting in different cycling loads. It was the goal of this study to characterize the hindlimb kinematics and kinetics (pedal reaction forces) at a variety of cadences and crank lengths in a rat model of MC, and to describe the real-time relationship between pedal reaction forces, blood pressure (BP) and heart rate (HR).

Materials and Methods

Experimental design

Ten adult female Sprague-Dawley rats (280 ± 22 g, Envigo, Indianapolis, IN) were used for this experiment. All procedures involving animals were approved by the Institutional Animal Care and Use Committee at the University of Louisville. Animals were acclimated in their home cages, then handled and exposed to the cycling apparatus for two weeks before evaluations. Handling was continued throughout the experiment on days when the animals did not receive cycling.

A cycling protocol was developed with six cadences (5, 10, 15, 30, 45, and 60 RPM) for 20 cycles/cadence, lasting approximately 8-9 minutes. Blood pressure and electrocardiography (ECG) was recorded in cage for four minutes prior to cycling and six minutes post-cycling, as well as during cycling. Following recovery from SCI, rats underwent this protocol twice per week for six weeks. Additionally, this protocol was performed post-device implantation but pre-SCI, with the cycling taking place under isoflurane (2% in oxygen) to record PF due to non-active muscles.

Transmitter implantation

All animals were instrumented with HD-S11 single pressure/biopotential implants (Data Sciences International, St. Paul, MN) to allow the measurement and recording of arterial pressure and ECG as described previously. Briefly, rats were anesthetized under isoflurane (2% in oxygen) in a sterile surgical environment. A ventral midline incision was made through the skin and abdominal wall, allowing for placement of the transmitter body in the peritoneal cavity. After suturing the transmitter body to the abdominal wall, the abdominal aorta was briefly occluded to allow for insertion of the pressure-sensing cannula. The cannula was inserted into the abdominal aorta slightly rostral to the bifurcation of the iliac arteries, then advanced rostrally to the crossing of the left renal vein over the aorta. The catheter was fixed in place using VetBond tissue adhesive (3M Vetbond Tissue Adhesive, St. Paul, MN). Next, the biopotential leads were fed subcutaneously and sutured in place under the 12th left rib and over the right pectoralis major muscle to allow recording of ECG. After visually inspecting for signs of lower limb damage due to loss of blood flow, the abdominal wall musculature was closed using 4-0 nylon sutures followed by closing of the skin using 4-0 silk sutures. Postoperative care included daily injections of gentamicin sulfate for 7 days post-injury (20 mg/kg, S.C.) and meloxicam for 3 days post-injury or as needed for pain and/or inflammation.

Spinal cord injury

Rats received moderately-severe contusion injuries using the NYU impactor as previously described [239] allowing 4 weeks for recovery. Briefly, animals were anesthetized using a ketamine (50 mg/kg)/xylazine (0.024mg/kg) cocktail to provide a surgical level of anesthesia as confirmed by the absence of paw withdrawal reflexes in response to a strong toe pinch. A dorsal midline incision was made through the skin and muscle to expose the T1-T4 vertebrae. Next, a single level laminectomy was made at the T2 vertebral level, and the spine was prepared for contusion by attaching clamps to the T1 and T4 spinous processes. Contusion injury was performed using a 35 g-cm weight drop, then the muscle and skin were sutured shut separately using 4-0 silk sutures. Rats were single-housed on heating pads and monitored overnight and were double-housed after 7 days of recovery (allowing for the incision to heal) for the remainder of the study.

Pedal design and cycling protocol

Motorized cycles were purchased from the machine shop at Drexel University to ensure the overall dimensions were comparable with previously published studies. The crank length of these cycles is ~22mm (standard cranks), giving a crank to limb ratio of ~1:3. Given that a typical crank to limb ratio in humans is ~1:5, custom cranks were fabricated at a length of 15mm to also be used in this study (short cranks). A custom pedal was designed using SolidWorks software. The goal of this design was to allow for the secure coupling of a single-axis force sensor (LCM100, FUTEK Advanced Sensor Technology, Irvine CA) to the rat's distal limb while maintaining a similar trajectory to the existing pedals (Figure 7B). Rats were evaluated on standard and short cranks once per week each, with the order being switched for alternate weeks. Before cycling, spherical beads (4mm diameter) were placed on the skin over the iliac crest (anterior rim of the

pelvis), hip (head of the greater trochanter), ankle (lateral malleolus), and toe (fifth metatarsophalangeal joint). Additionally, two sagittally-oriented cameras (Basler AG, Ahrensburg, Germany) were positioned and calibrated to allow for triangulation of marked points using the MaxTraQ software package (Innovision Systems Inc; Columbiaville, MI). During cycling, forces from the pedal were acquired at 1000Hz in synchrony with the two cameras at 100Hz using a custom LabView script, which were synchronized to telemetric data recorded at 1000Hz using LabChart8 (ADInstruments, Sydney, Australia).

Euthanasia

Animals were euthanized using a ketamine (50 mg/kg)/xylazine (0.024 mg/kg) cocktail and transcardially perfused with 4% PFA. Spinal cords were dissected and post-fixed in 4% PFA for 2 h, then transferred to 30% sucrose for cryoprotection. Additionally, the femurs and tibias of each rat were dissected out and measured postmortem. These measurements were used to scale custom models of each rat [205] in the OpenSim platform [206].

Data processing

Systolic and diastolic pressures (SP and DP) were calculated by determining maximum and minimum values within each R-R interval in MATLAB. Heart rate (HR) was calculated as $(60 / [\text{beat interval time (s)}])$, where beat intervals were determined using the heart rate analysis module in LabChart 8. Mean values were taken of the entire in-cage recording periods and the on-bike periods where the bike was on. The relationship between mean arterial pressure (MAP) and HR was determined using convergent-cross mapping (CCM) analysis. Briefly, CCM is a nonlinear approach for estimating causality between two time series. The algorithm determines how much

information from one signal is encoded on another based on the degree in which the each signal can be approximated from a time delay series of the other, therefore giving bidirectional information of the strength of coupling between signals. For CCM analysis, beat-by-beat MAP values were determined by averaging the values in each R-R interval. A spline interpolation was applied to MAP and HR time series of 1000 Hz to create evenly sampled signals, and resampled to 10 Hz before CCM analysis [240]. Signals were analyzed using a CCM algorithm in MATLAB based on work from Sugihara et al. [241, 242]. The correlation coefficient value (magnitude from 0-1) was used as an indicator of the degree of causal information between variables.

Forces were processed before analysis using a custom MATLAB script as described in Chapter III. Briefly, a second order zero-lag lowpass filter with a cutoff frequency of 6 Hz was applied to the raw data. The data was then separated into individual cadences and the fundamental frequency (f_0) was identified at each cadence. A notch filter was applied at f_0 , then the subsequent two harmonics ($2*f_0$ and $3*f_0$). The resultant signal described forces that were developed with the motion of the pedals and were termed non-spastic while the spastic force was calculated as the difference between the original and non-spastic forces.

Statistical analyses

Data were analyzed using SPSS (IBM SPSS Statistics for Windows, Versions 26/27. IBM, Armonk, NY). Five animals were lost over the course of the study due to complications from surgery, leaving five animals for analysis. Despite the smaller sample size, distributions were generally normal allowing use of repeated-measures ANOVA for analysis, with strict post hoc t tests (Bonferroni t test for multiple comparisons).

Results

Average hip, knee, and ankle angular range-of-motion (ROM) profiles are represented in Figure 18A, C, and E, respectively. As expected, repeated-measures ANOVA revealed an effect of crank length for the hip ($F_{1,3}=114.2$, $p<0.01$), knee ($F_{1,3}=487.4$, $p<0.001$), and ankle joints ($F_{1,3}=22.7$, $p<0.05$). Although significant, adjustment of crank length had a greater impact on the hip and knee ROM, as compared to the ankle, possibly due to how the foot was affixed to the pedal (weeks 1 and 6 did not show a significant difference in ankle ROM between the two cranks). Interestingly, there was also an effect of time (week) in the knee joint ($F_{5,15}=4.622$, $p<0.01$). As knee ROM increased slightly over time, this is likely an effect of animals recovering and positioning (pushing themselves) further away from the ergometer.

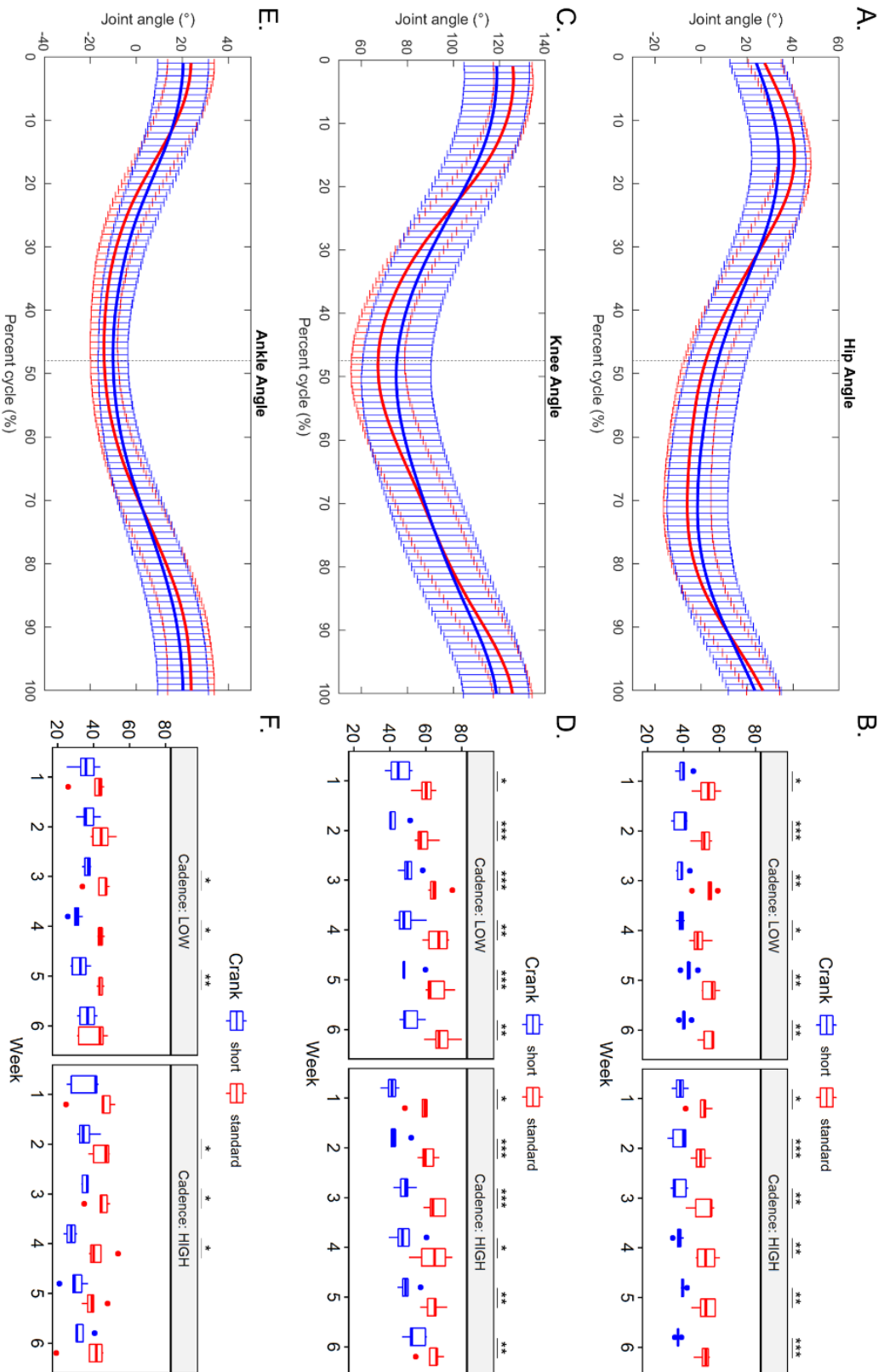


Figure 18. Kinematics and range of motion analysis for the hip, knee, and ankle joints.

A,C,E) Hip, knee, and ankle flexion represented over the course of a gait cycle. Error bars represent standard deviation. **B,D,F)** Boxplot representations of hip, knee, and ankle range of motion for short (blue) and standard (red) cranks. Crank length significantly affected ROM for all joints, although more significant differences were present in the hip and knee joints. All data were analyzed using repeated-measures ANOVA and Bonferroni corrected t-tests, * $p < 0.05$, ** $p < 0.01$, *** $p < 0.001$.

Non-spastic forces were analyzed in flexion and extension using repeated-measures ANOVA. In extension, significant differences were found for crank length ($F_{1,3}=20.6$, $p<0.05$) and cadence, ($F_{1,3}=134.9$, $p=0.001$), as well as the week-cadence interaction ($F_{5,15}=3.0$, $p<0.05$). In flexion, significant differences were only found for cadence ($F_{1,3}=23.0$, $p<0.05$). The results of this analysis are illustrated in Figure 19.

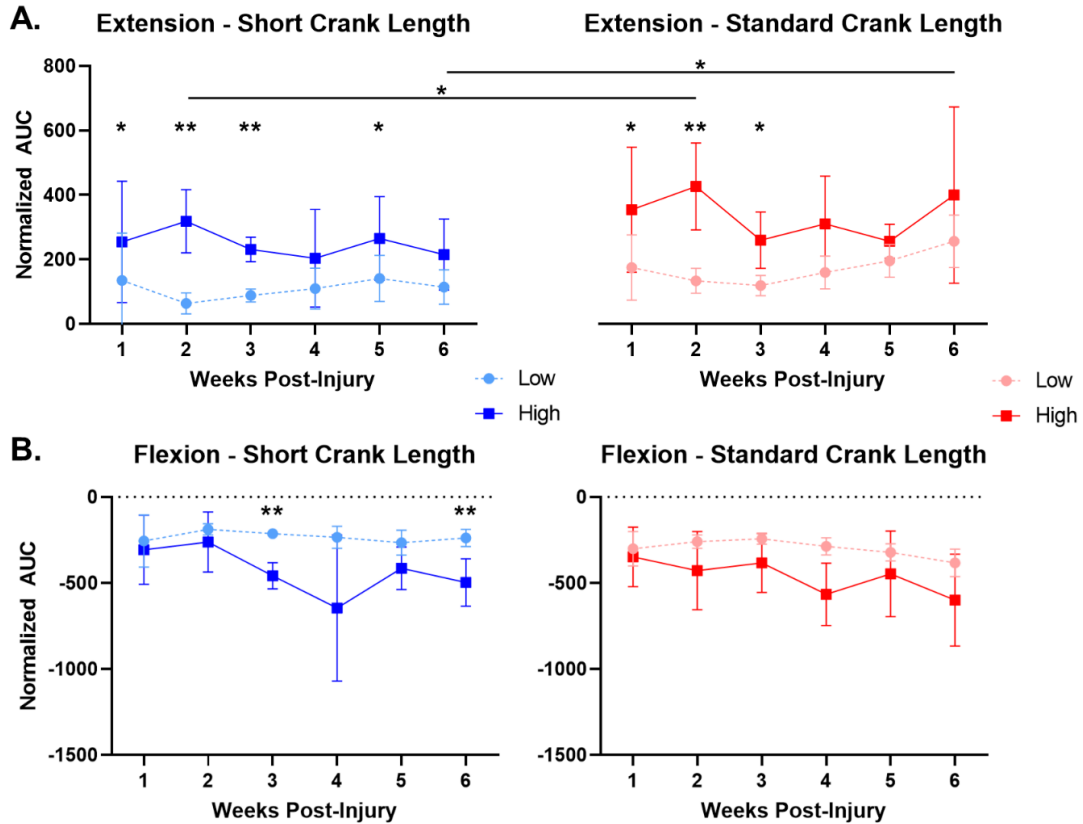


Figure 19. Analysis of non-spastic forces, represent as normalized area under the curve (AUC).

A) Area under the curve measurements for short and standard cranks in extension. **B)** Area under the curve measurements for short and standard cranks in flexion. A significant difference was seen for cadence during both flexion and extension, while crank length was only significant during extension. All data were analyzed using repeated-measures ANOVA and Bonferroni corrected t-tests, * $p < 0.05$, ** $p < 0.01$.

Spastic forces are represented as heatmaps over the course of a gait cycle in Figure 20, where Figure 20 A&C represent the percentages of trials with a spasm present, while Figure 20 B & D represent the number of spasms per minute. In both short and standard crank lengths, 5 RPM cycling overwhelmingly exhibits the most trials with spastic forces present. However, the number of spastic force events per minute was greater at cadences >30 RPM using both short and standard crank lengths, with the standard crank length inducing almost twice as many events at these cadences compared to short. It should be noted that the force patterns are similar between cadences, i.e., starting during extension and peaking during full extension. Despite this similarity, the duration of force during the cycle is longer at 5 RPM cycling (lasting on average ~6 seconds) while lasting between 0.5-1 second at cadences >30RPM.

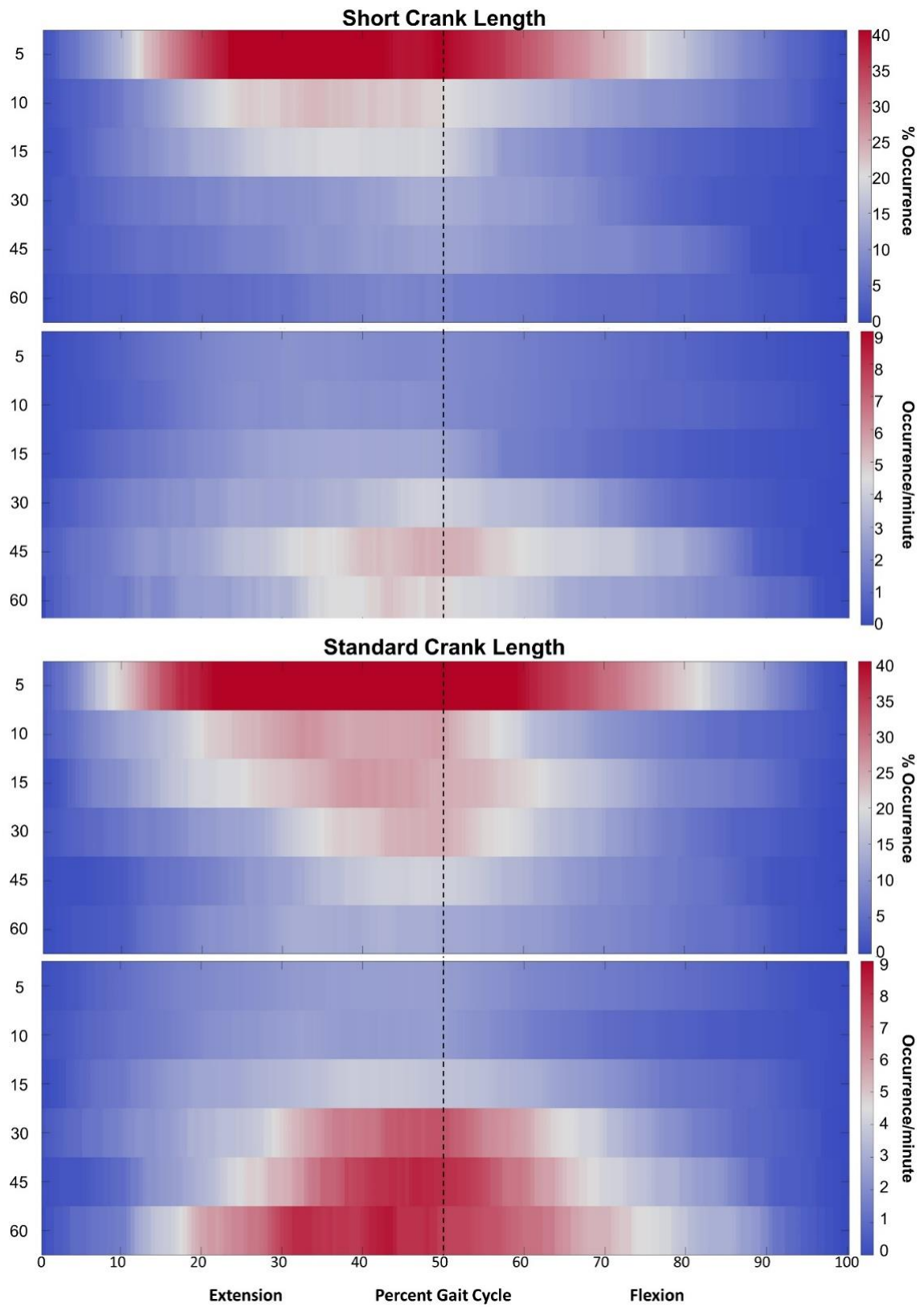


Figure 20. Heatmap visualization of spastic forces averaged over one gait cycle.

A) Spastic forces during short crank cycling **B)** Spastic forces during standard crank cycling. The top graph in each section represents how often a force occurred on a per-trial basis, while the bottom graph represents how often a force was present on a per-minute basis.

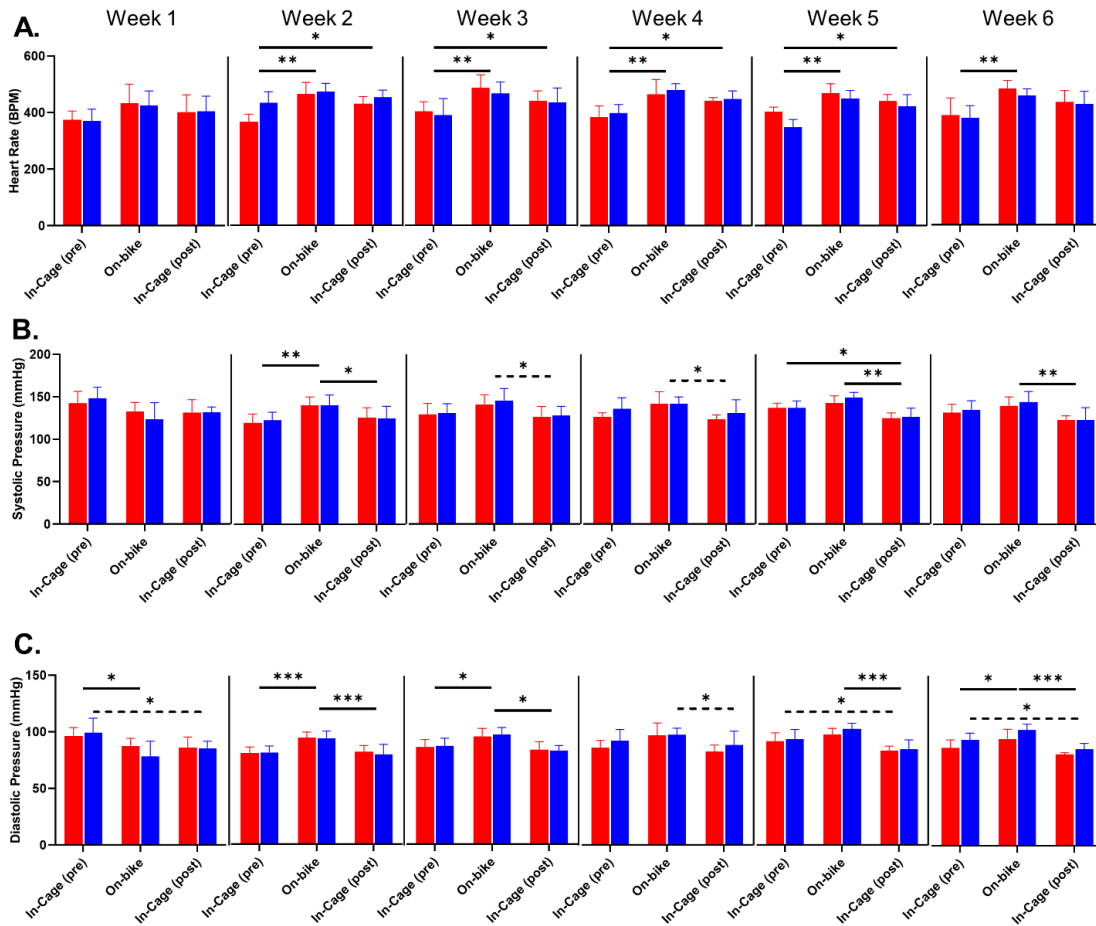


Figure 21. Average heart rate, systolic pressure, and diastolic pressure pre-, during, and post-cycling.

A) HR differences were seen after week 1, where it was elevated during cycling at all timepoints and remained elevated post-cycling except during week 6. **B)** Systolic pressure was elevated during cycling after week 1, however it was only consistently different from post-cycling measures. **C)** Diastolic pressure followed a similar trend to systolic pressure with more significant differences seen between cycling and pre-cycling timepoints. All data were analyzed using mixed-model ANOVA and Bonferroni corrected t-tests, * $p < 0.05$, ** $p < 0.01$, *** $p < 0.001$. Dashed lines indicate significance in the short crank length group only.

Repeated measures ANOVA was used to investigate measurements of heart rate (HR, Figure 21A) and systolic/diastolic pressure (SP/DP, Figure 21B&C) between timepoints and crank lengths along the weeks of cycling. Significant differences were found for all outcome measures in timepoint (HR: $F_{2,76}=73.2$, $p<0.001$; SP: $F_{2,86}=27.5$, $p<0.001$; DP: $F_{2,85}=61.6$, $p<0.001$). This difference was seen as an elevation in heart rate during cycling, which remained elevated post-cycling. Although cycling blood pressure was consistently higher than pre-cycling after week 1, post-hoc Bonferroni corrected t-tests did not find significant differences at all timepoints, rather on-bike blood pressure was consistently higher than post-cycling. In later weeks pre-cycling blood pressure was higher than post-cycling, suggesting a post-exercise hypotension effect. Differences between weeks were found in both blood pressure groups (SP: $F_{5,38}=2.7$, $p<0.05$; DP: $F_{5,36}=5.1$, $p<0.05$) as well as the timepoint x week interaction (SP: $F_{10,36}=3.4$, $p<0.01$; DP: $F_{10,31}=4.8$, $p<0.001$), representing a difference in blood pressures between week 1 and week 2. No direct effect of crank length was found for heart rate or systolic/diastolic pressure. However, it should be noted that the short crank length group showed more significant differences between timepoints in both systolic (significant drop from on-bike to post-bike at weeks 3 and 4) and diastolic pressure (significant drop from on-bike to post-bike at week 4, and from pre-bike to post-bike at weeks 5 and 6).

Although seemingly counter-intuitive, these results highlight the instantaneous effects that force production during cycling has on the cardiovascular system. This relationship is highlighted in the example force, mean arterial pressure (MAP), and HR trace shown in Figure 22. Large, spastic-like force events (indicated by vertical dashed lines) typically lead to a brief spike in, followed by a decrease in MAP with a limited effect on heart rate. It is not until periods of higher cadence cycling without periods of

spasticity that MAP increases and remains elevated. Although heart rate does slightly decrease during the final elevation in MAP it remains above baseline for the duration.

To quantify this relationship, convergent cross-mapping (CCM) was employed. RM AMOVA revealed no differences in either in-cage condition, however significant differences were found in the on-bike condition between HR-MAP/MAP-HR ($F_{1,44}=50.3$, $p<0.001$) and week ($F_{5,18}=6.8$, $p<0.005$). Post-hoc Wilcoxon signed rank testing revealed significant differences between HR-MAP and MAP-HR at five out of six timepoints for standard crank lengths, and four out of six timepoints for short crank lengths during cycling (Figure 23). During cycling, the effect of MAP on HR is consistently lower than HR on MAP, suggesting a one-sided disruption in the relationship. As seen in Figure 22, sharp changes observed in blood pressure that are caused by spastic force events have little effect on heart rate, while the overall effect of heart rate on blood pressure remains consistent.

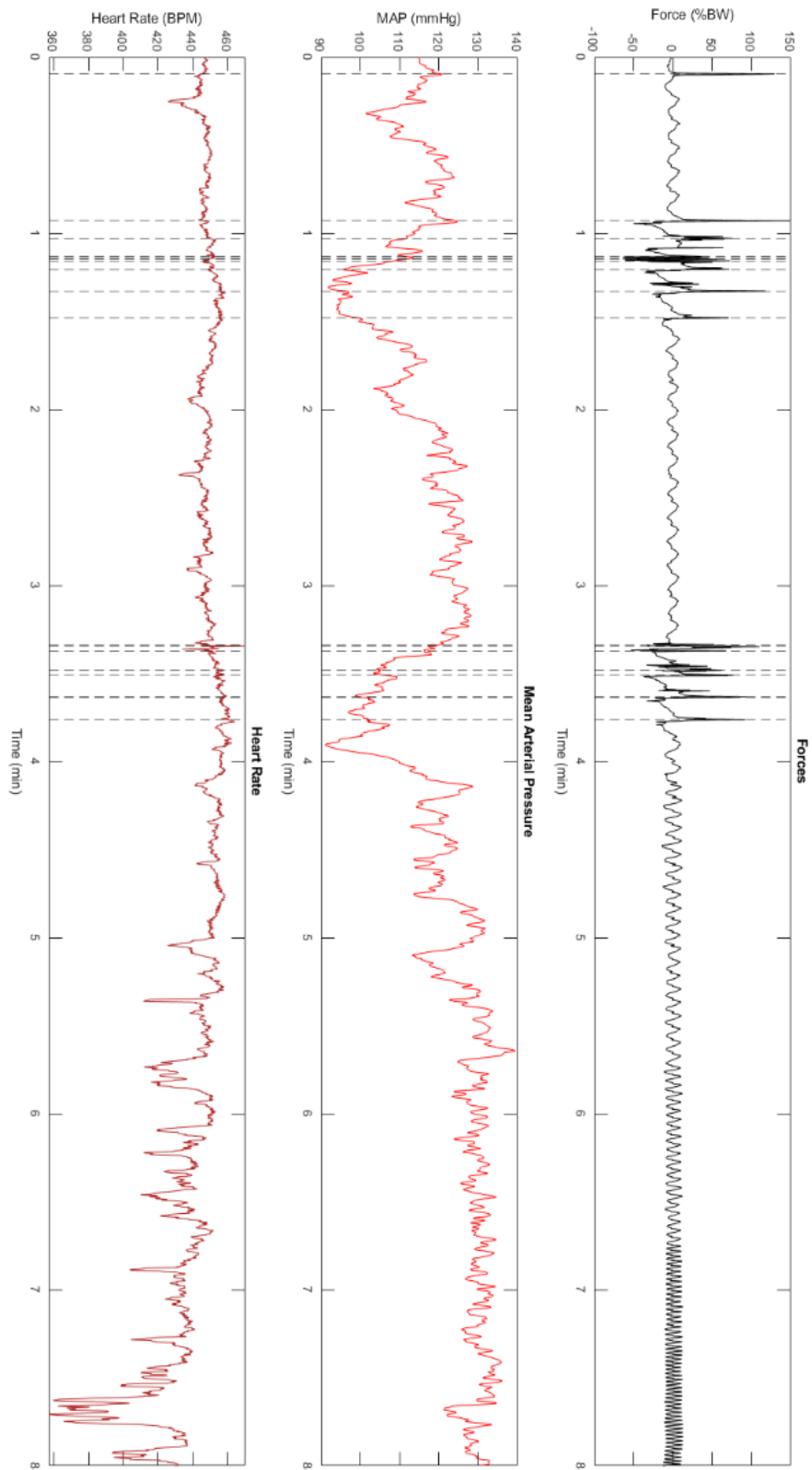


Figure 22. Representative trial demonstrating instantaneous cardiovascular

effects.

A) Forces recorded during cycling, where dashed lines indicate peaks of spastic force activity. **B)** Mean arterial pressure (MAP) during cycling. Notice drops in MAP during spastic force activity. **C)** Heart rate during cycling. Heart rate decreases occur during prolonged periods of elevated MAP, and only responds slightly to drops seen during periods of high intensity spasms.

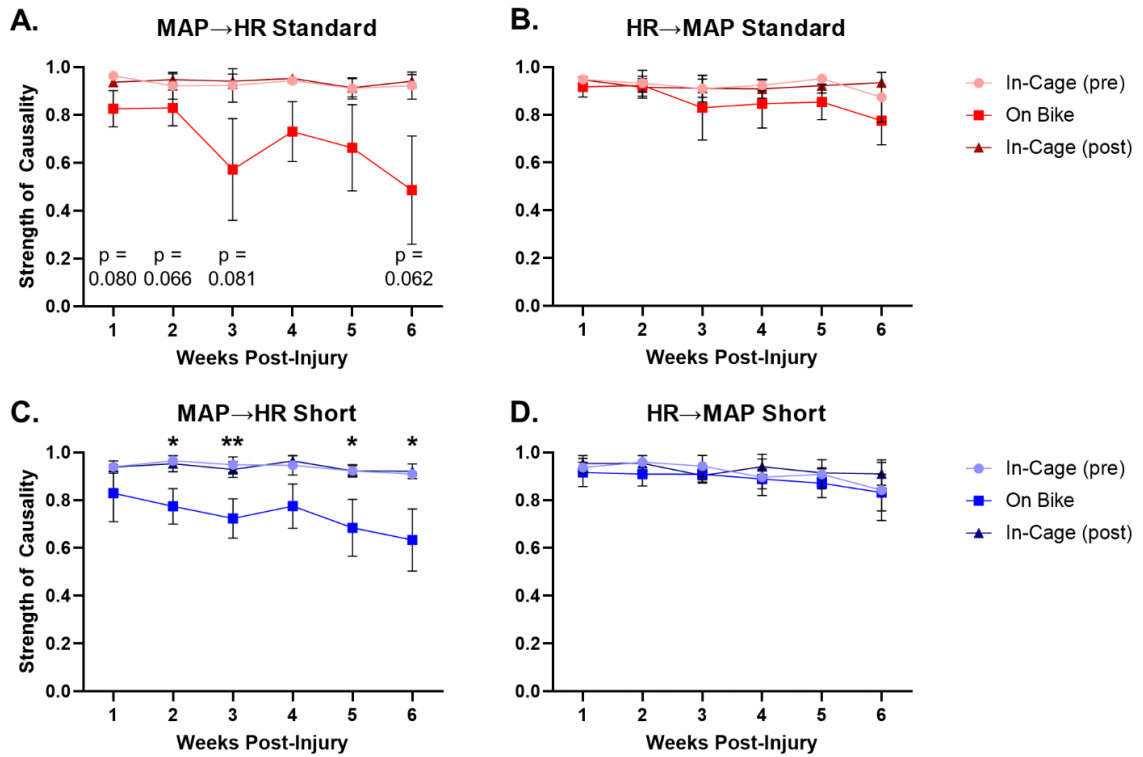


Figure 23. Line graph representations of HR↔MAP causality pre-, during, and post-cycling for standard and short crank lengths.

A&B) Influence of MAP on HR (A) and HR on MAP (B) during cycling under the standard crank condition. Values of the influence of MAP on HR approached statistical significance during cycling compared to both in-cage conditions at weeks 1, 2, 3, and 6 post-injury. **C&D)** Influence of MAP on HR (C) and HR on MAP (D) during cycling under the short crank condition. Values of the influence of MAP on HR approached statistical significance during cycling compared to both in-cage conditions at weeks 2, 3, 5, and 6 post-injury. Statistical significance was found using Bonferroni corrected post-hoc t-tests, * $p < 0.05$, ** $p < 0.01$.

Discussion

The translation of results from animal models to clinical practice is dependent on our understanding of the model system, and specifically the anatomical and/or physiological differences between animal and human that might affect translation. The goal of this study was to expand our understanding of the rat model of MC by investigating the effects PF has on the cardiovascular system, and how cycling ROM and cadence can be used to modulate these effects. Using a lower crank-limb ratio decreased ROM – particularly at the hip and knee – and reduced incidences of high frequency, high force spastic-like responses primarily seen during extension. Although the lower ROM cycling had a slight effect on non-spastic forces in the extension phase there was no effect during flexion, while cadence had a strong effect on non-spastic forces during both flexion and extension.

Overall, MC influenced HR, SP, and DP that extended into the acute post-cycling period. During the first week of cycling rats had difficulty maintaining blood pressure during cycling, likely due to spinal shock [243]. During the remaining evaluation periods cycling consistently induced an elevated heart rate and increased SP, consistent with increased CO and a mild exercise response [244, 245]. However, it should also be noted that DP also increased during cycling, which is atypical in able bodied subjects [246]. DP is dependent on CO and peripheral vascular resistance [247]; the increase in CO during exercise is generally accounted for by vasodilation of vessels in skeletal muscle. In our model, altered vascular dynamics post-SCI may play a role in this response. In cervical and high thoracic injuries, similar to those employed here, stimuli below the level of lesion can lead to spinally mediated reflex activation of sympathetic neurons causing vasoconstriction which may counteract exercise mediated vasodilation. Additionally, chronic stiffening (loss of compliance) of the arterial system can occur within the first 6

weeks post-SCI [248, 249]. Despite the increase in DP during exercise, blood pressure spikes did not reach levels needed to qualify as autonomic dysreflexia and were not associated with bradycardia.

Effects of cycling on CV parameters were found using both short and standard cranks, however short crank length cycling induced more robust changes in both SP and DP compared to standard crank length cycling. Although seemingly counterintuitive, these results may be explained by the relationship of blood pressure to PF. Bursts of spastic muscle activity induced brief spikes followed by decreases in blood pressure, while non-spastic forces were associated with a gradual and prolonged elevation of blood pressure. An increased number of spastic bursts, as seen with the standard crank cycling, may not have an exercise effect, and perhaps may disrupt the balance between heart rate and blood pressure. CCM analysis suggests that while heart rate still maintains an effect on blood pressure during cycling that the effect of blood pressure on heart rate is reduced. As this relationship is further reduced during standard crank cycling, it is likely due to changes in blood pressure that occur too rapidly for a heart rate response to follow.

Unfortunately, direct comparison between rat and human MC is currently difficult. Despite the wealth of information on active cycling biomechanics [250-252] relatively little information exists on MC biomechanics, particularly in-bed cycling. A recent protocol suggests starting knee flexion at 30° for in bed cycling [253] compared to 46° for upright cycling [254], although no other ROM values are reported. PF has been investigated during FES cycling [255, 256], however the purpose of these studies is to calculate muscle torque independent of inertial movement making information on PF during MC limited.

This current study provides insights into the relationship between PF and cardiovascular dynamics during MC in rats, however there are several limitations that must be considered. First, this study was designed to understand how PF was affected by cadence and therefore used a wide range of cadences with a fixed number of cycles. The number of rats used for this aim was low, which was further reduced by post-surgical complications. Future studies should narrow the focus by investigating differences between one low and one high cadence using larger group sizes. Next, the cardiovascular responses were recorded in response to brief (8-10 minute) bouts of cycling, much of which was low cadence. Training studies using MC typically cycle rats in 30-minute bouts, therefore understanding how force affects cardiovascular responses over a longer period is critical. For the current study we did not intend to study the impact of MC training, but rather the changes in PF and CV responses over time post-injury, thus we avoided long periods of high-cadence cycling. Finally, a contusion injury model was chosen for this study, which induced a wide range of PF. We chose the T2 severe injury (35g-cm) due to its perceived clinical relevance, since most SCI patients have some white matter sparing, even if an injury is functionally complete [257]. However, rats with this level of injury are capable of locomotion and may thus exhibit stronger reflex activity in response to MC [258]. Previous work in Chapter III demonstrates that even fully transected rats can generate spastic forces during MC, and that levels of non-spastic forces are only slightly lower than contused rats. Therefore, questions of the clinical relevance of this model remain. An understanding of the magnitudes and causes behind PF during MC in both humans and rats will help future clinical translation.

CHAPTER V

OVERALL DISCUSSION

Summary

The main innovation of this work was the creation of a system to measure the forces during MC in the spinal cord injured rat, which was done in relation to cycle phase at a variety of cadences and two crank lengths. We used six cadences from 5-60 RPM with the intention of creating a “titration curve” of cadence versus force. Much like an actual titration curve, there appeared to be a tipping point between 15 and 30 RPM where forces greatly increased, however a much smaller effect was observed changing cadences from 5-15 RPM and 30-60 RPM. To further understand these forces, a novel filtering technique was developed to separate spastic from non-spastic forces and investigate their relationship to cardiovascular outcomes and hindlimb muscle EMG. Overall, MC in our contusion model caused an elevation of SP, DP, and HR. It appeared that rhythmic cycling with non-spastic forces elevated BP in a prolonged manner, while large magnitude spasms caused a brief elevation in MAP followed by a longer decrease that appeared to disrupt the relationship between HR and MAP. Furthermore, our results suggest that cadences ≥ 30 RPM can increase non-spastic forces that coincide with relatively small, rhythmic bursting of EMG, while cadences ≤ 15 RPM increase spastic forces that are related to high frequency bursting of EMG. Although repeated measures ANOVA revealed significant effects of cadence on non-spastic force in both T2 and T10 injury models there were relatively few post-hoc results due to a larger than expected variability. However, these results overall demonstrate hindlimb loading during cycling

related to muscle activity and provide a possible mechanism for explaining differences between the animal model and clinical MC.

Spasticity During Cycling

This existence of this spasticity raises an obvious question: is it possible to alter cycling parameters and/or other external factors such that the occurrence of spasticity can be modified? Our initial hypothesis was that muscle activity would be driven by velocity-dependent stretch reflexes, which largely appears to be true. A complication to this finding was the relatively large amplitude forces observed in our model of MC characterized by high frequency (4-8 Hz) oscillations. We described these as “spastic” because the frequency component of these forces mimics clonic spasms observed in patients and rats [183], however this is an incomplete view of spasticity. Spasticity after SCI is often broadly divided and defined as tonic or phasic [259], where tonic spasticity is defined as increased muscle tone in response to stretch, while phasic spasticity is oscillatory responses to a muscle stretch. Although we refer to forces in this study as spastic and non-spastic, it may be more appropriate to consider non-spastic forces as tonic given that they are representing a resistance to muscle stretch.

Spastic forces: phasic spasticity?

In humans, phasic spasticity is generally synonymous with tendon hyperreflexia and clonus [260], which is characterized as an involuntary rhythmic contraction with a frequency of 5-8 Hz that is generally thought to be elicited by a rapid stretch of a muscle [261, 262]. Although our spastic forces were often due to EMG patterns in a similar frequency band to clonus, we found that spasms were most likely to occur during 5 RPM cycling, which consistently had the highest occurrence of spastic forces in both our T2 and T10 injury models. This is surprising based on our hypothesis that the activation of

these spasms is stretch reflex dependent, as they bear a similar frequency to clonus in humans. If our spasms are mechanistically related to clonus in humans, there are two schools of thought. The first is the theory of recurrent activation of stretch reflexes [262], where first a rapid muscle stretch activates Ia afferents that results in a brief contraction. As the muscle relaxes, the natural movement of the limb causes the muscle to be stretched again, causing it to enter a phasic stretch-relax-stretch loop. This is possible after SCI as descending inhibition on alpha and gamma motor neurons is disrupted causing the stretch reflex circuit to be hyperexcitable [263]. In addition to seeing spasms more frequently during slow stretch, the spasms in this model generally begin in early to middle extension, meaning that the spasms occur despite the muscle lengthening. However, a second theory postulates that clonus may not be entirely stretch reflex dependent and may depend on central circuitry [261]. This began with work from Geoffrey Walsh, who demonstrated that ankle angle was not a determining factor by using a device to provide a rhythmic force to the foot during clonus, which failed to entrain a superimposed rhythm [264]. This effect was elaborated on by Dimitrijevic et al. who also failed to entrain a rhythm to clonus using tendon taps from 1-15 Hz [265]. Interestingly, it has also been demonstrated that clonus may not need stretch to be activated, as Beres-Jones et al. demonstrated that synchronous clonus-like EMG activity can occur in the soleus, medial gastric, and tibialis anterior during isometric contractions [266].

Recent work in animals supports the theory that spasms are centrally mediated. Notably, Lin et al. demonstrated the role of V3 interneurons by demonstrating that optogenetic activation excitation of this population not only increased spasms in mice but was able to elicit them [267]. The involvement of V3 interneurons in spasticity is intuitive given that they project across the midline [268] and are involved in coordinating

locomotion [269, 270], suggesting that they may play a role in coordinating spasticity as well. It has been demonstrated that V3 interneurons cluster into distinct dorsal and ventral groups (in laminae IV-V and VI-VII, respectively) [271]; the excitatory dorsal V3 interneurons have been shown to receive direct sensory input from Ib and II sensory afferents [272, 273]. Our results demonstrate that c-Fos is upregulated in these areas, particularly in laminae IV-V. However, we also see c-Fos expression in the upper dorsal horn. While low-threshold mechanoreceptors synapse in these areas [274], we see c-Fos expression in Lamina I which is known to receive inputs from nociceptors and modulate pain [275]. Care was taken to ensure the paw was always in contact with a soft surface/was non-irritated and vocalizations during cycling were minimal, however we cannot definitively rule out an effect from skin or muscle nociceptors. It should be noted that decreases in locomotor capacity following MC training were present, although very slight as they only approached significance at week 5 (Figure 16B). These levels are comparable to CGRP+ depleted rats that underwent daily hindlimb stretching [171], suggesting that at least the effect of stretch during cycling is not sufficient to cause c-fiber mediated nociceptive input.

A final caveat is that when normalizing to time it becomes clear that higher cadences elicit more spasms per minute, although it is difficult to interpret this result as stimuli are unevenly applied. Future studies could test this by looking at individual cycles with regular intervals of rest in between. Additionally, future studies could address the issue of possible nociceptive input during cycling. This could be addressed generally by using rats that have depleted nociceptors [171], or target skin specifically by using a topical anesthetic to reduce signal propagation in A δ and C fibers such as lidocaine [276].

Non-spastic forces: tonic spasticity?

Tonic spasticity is thought of as the increase of muscle tone, often in response to a passive stretch and is rate dependent. We hoped to quantify this by filtering out the components of force that were outside of the cycling cadence harmonics. This technique was largely successful, and results suggest that cycling cadence can affect muscle tone during both flexion and extension despite a high degree of variability in the data. The source of this variability is likely from multiple sources, the most obvious being the variable nature of passive cycling itself. Despite our best efforts, rats are naturally adept at escaping tight spaces and were able to move during the recording. Small changes in position can greatly change limb trajectory and therefore alter the rate of stretch between rats. Additionally, there exists a mixed literature regarding the development of increased muscle tone in rats. For example, Chang et al. investigated the development of muscle tension in response to stretch using a similar apparatus to our passive cycle [277], however they used a protocol where the hindlimb was carefully positioned while the rat was under isoflurane and torque was continuously recorded as the rat began to wake up. They then used the amount of torque that was recorded ten seconds prior to the rat struggling against the machine. Despite using this tightly controlled protocol their recorded muscle tension post-SCI (T8 hemisection) was highly variable, ranging from slightly above baseline levels to nearly a 500% increase. Similarly, Bose et al. measured velocity dependent changes in hindlimb torque and EMG of the triceps surae after a moderate T8 contusion [278]. Interestingly, they found a significant increase in torque and EMG at week 1 post-SCI, however the largest percent change from baseline in EMG was observed at the slowest angular velocities. They also observed a marked decrease in torque at weeks 2 and 3 post-SCI, however a velocity dependent increase over baseline was found at week 5 and lasted through week 12. This may explain why we saw a sharp increase in non-spastic forces at week 5 in our T10 contusion model, although our results are not completely comparable as we observed a flaccid paralysis

at week 1. It should also be noted that the T10 transection group had lower non-spastic forces compared to T10 contusions, however that does not mean that transected animals will not experience spasticity. Wind up of stretch reflexes has been demonstrated in the hindlimbs of T10 transected rats [198], while gabapentin sensitive tail spasticity has been demonstrated in both a T4 [279] and S2 transection [280]. It is likely that this reduction in force came from muscular atrophy, as SCI animals had reduced muscle weight that did not reach the levels of animals in the contusion group.

Cardiovascular Effects of Motorized Cycling

We demonstrated a consistent increase in heart rate and blood pressure during MC. HR remained slightly elevated post-cycling while BP tended to drop, suggesting a potential post-exercise hypotension [244]. This is contrary to the results of West et al., who reported no change in SP and a slight decrease in HR during MC [69]. Although they used a different strain and sex (male Wistar rats) than we did the reported body weights are similar suggesting similar biomechanics during cycling, although our use of a force sensing pedal likely altered paw placement slightly. It should also be noted that the largest decrease in heart rate seen in the West et al. study occurred after ~15 minutes of MC, which was longer than any of our sessions. Furthermore, his reported decreased HR was 531 ± 12 b.p.m, which was higher than we ever observed during MC.

Our hypothesis was that the skeletal muscle pump plays a role in cardiovascular improvements seen using MC. This theory is based on the idea that a contraction of skeletal muscle increases venous pressure and ventricular filling, which increases pre-load and CO. The pressure measurements in our study do not directly measure venous pressure, as the pressure cannula resided in the abdominal aorta. Additionally, the BP/HR changes we observed in response to spastic and rhythmic contractions were

different; these responses should be considered individually although some mechanistic overlap may exist.

Rats generally exhibited an increase in BP/HR during MC, which occurred during periods of non-spastic cycling. This is consistent with a healthy exercise response where an initial sympathetic outflow increases HR, which then leads to a gradual increase in SP [281]. However, we also observed an increase in DP which is atypical during exercise and likely results from an excessively high CO or impaired vasodilation in skeletal muscles [282]. Although we cannot definitively state the mechanism that is causing this, it is well known that stimulation of afferents below the lesion after high thoracic/cervical injury leads to unregulated activation of sympathetic pre-ganglionic neurons that can cause exaggerated vasoconstriction in the peripheral vasculature, a phenomenon known as autonomic dysreflexia (AD) [283]. Contraction of skeletal muscle during exercise normally results in local vasodilation due to a combination of multiple factors which blunts sympathetic vasoconstriction, allowing an increase of blood flow to the contracting muscle [284]. Metabolic factors are thought to play a role, such as the release of potassium ions [285], nitric oxide [286], and prostaglandins [287] that are generated and released by contracting skeletal muscle [284]. It is possible that release of metabolic factors is limited during MC as muscle contractions are relatively weak, therefore elevated sympathetic activity limits any vasodilatory effect. However, we observed a sharp decline in MAP during large spastic contractions which could also be related to vasculature. For example, one theory suggests that muscle contraction induces vasodilation by activating mechanosensors in the vasculature [288]. Supporting this hypothesis, it has been demonstrated that pharmacological blockade of integrin receptors can mitigate the effects of compression induced vasodilation [289]. Interestingly, this study demonstrated an increase in dilation during periods of increased

transmural pressure that peaked after compression and lasted ~30 seconds like our observed time course of contraction induced hypotension.

Overall, it appears as though MC may induce an exercise response, although some aspects of the response are abnormal, and the mechanisms causing the response are not fully understood. The potential involvement of vascular regulation has important clinical implications. Although no rats in our study exhibited signs of AD, the stimulation of cutaneous or muscular afferents during MC is a potential trigger for patients and further investigations are warranted.

Effects of Transmitter Implant on SCI Recovery

An interesting observation we made, which, while not the focus of this work, deserves a brief mention, is the apparent impact of transmitter implantation on functional recovery. In our final experiment the locomotor and sensory response to MC training was investigated using weekly BBB and tail-flick evaluations, respectively. Transmitter implanted animals had higher BBB scores compared to the non-implanted transmitter group, but perhaps more surprisingly the injury appeared to have no effect on tail-flick latency, even showing a mild increase post-SCI. Although we allowed the animals three weeks between implantation and SCI, it is possible that there was still a lingering inflammatory response to the initial incision/surgery and/or the foreign body. It has been shown that trauma disrupts the homeostasis of the immune system leading to a decrease in circulating immune cells [290, 291]. Normally this is associated with negative outcomes; for example, non-SCI patients with polytrauma exhibit poor wound healing, which has been associated with a decrease in circulating leukocytes [292, 293]. Although this is an undesirable outcome for peripheral wound healing the contributions of inflammatory mediators to SCI are mixed [294], and the general consensus is that inflammatory damage is a large contributor to secondary injury [295]. In this way, the

transmitter implantation may have inadvertently directed immune response away from the SCI resulting in better functional outcomes. Unfortunately, our study was not designed to measure circulating immune cells or any related outcomes and therefore any relationship between prior immune response and outcome post-SCI is purely conjecture. Still, future studies involving chronic device implantation and SCI should be mindful of the order in which surgeries are performed.

Clinical translation: potential hurdles

One of the most obvious hurdles for overcoming the translation of animal models of exercise to humans is the biomechanical differences, as humans are bipedal while animals are quadrupedal thus inherently making comparisons difficult. As a starting point, one might consider how joint ranges of motion (ROM) compare between cycling and overground walking in rats and humans. In rats, it has been reported that hip, knee, and ankle ROM during overground walking are $39.2 \pm 7.0^\circ$, $52.9 \pm 10.2^\circ$, and $53.9 \pm 10.1^\circ$, respectively [296]. Hip and knee ROM are higher than overground approximately 10 degrees each ($52.0 \pm 5.1^\circ$ and $63.4 \pm 6.9^\circ$, respectively) during standard crank cycling while remaining comparable using the short crank ($38.9 \pm 3.3^\circ$ and $47.9 \pm 6.4^\circ$, respectively), while ankle flexion is reduced in both standard ($42.3 \pm 6.7^\circ$) and short ($34.0 \pm 5.5^\circ$) crank cycling compared to overground locomotion. Active cycling in humans reportedly produces a similar ROM (38° hip, 66° knee, and 24° ankle flexion) compared to overground locomotion for all joints [254]. Based on this information alone, one might conclude that since the ROM of short crank cycling is roughly equivalent to that observed during overground walking in rats then it must be roughly equivalent to human cycling, where the same statement is true.

However, this view is omitting key differences which can be conceptualized through threshold control theory. This can be thought of in terms of the steady state

interaction between an organism and the external environment, where motor actions occur when some component of the system is disturbed [297]. These perturbations can originate from the organism itself (e.g., your brain giving a neural command to lift your arm) or from the environment (an external force acting on a limb, such as the pedal of a MC ergometer) [298]. In this view there is a threshold in which an external force can break the equilibrium point of the system and elicit a motor action, for example the length at which a muscle begins to be excited while being passively stretched [299]. Taking this theory into account, consider the neutral hip position of rats (neutral at $\sim 90^\circ$ and limited by the skeletal and muscular structure around the ischia [216], Figure 24A) to that of humans (neutral closer to 0° , Figure 24C). In rat MC, hip extension often reaches or slightly exceeds 90° (Figure 24B), while in human cycling the hip typically does not exceed 40° (Figure 24D). Therefore, MC in rats may be inherently more likely to move beyond an equilibrium point in the hip that would trigger stretch reflexes. Hip extension is especially important as it has been shown to activate stretch reflexes that are known to facilitate locomotion post-SCI [214].

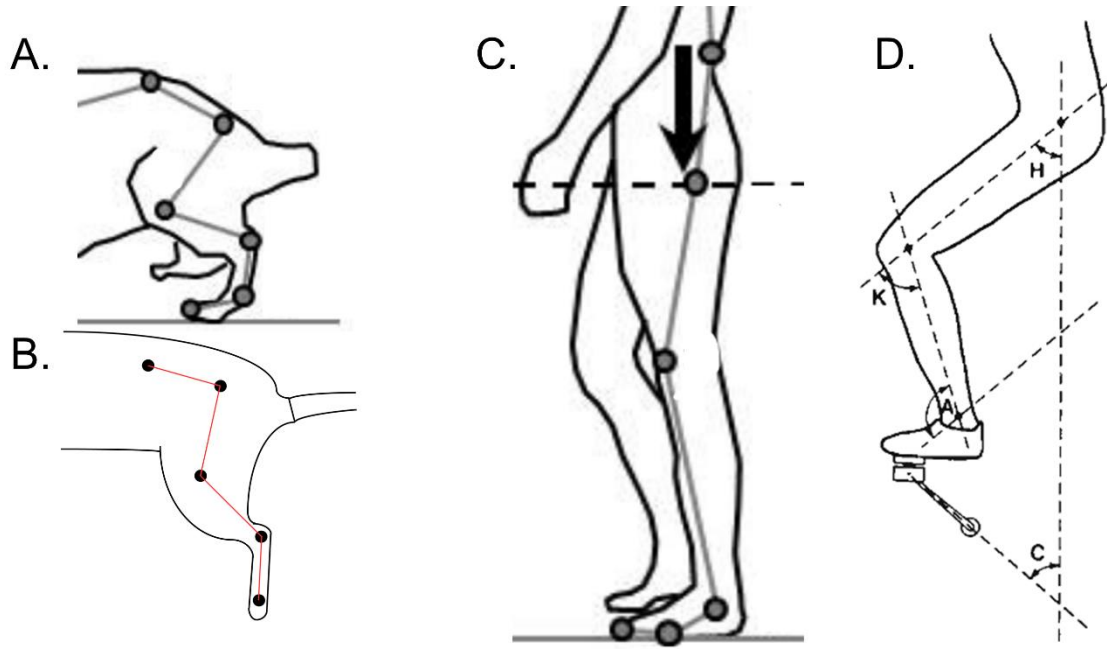


Figure 24. Illustration of relative differences in neutral and cycling hip positions of rats and humans.

A) Neutral position of a rat hindlimb. **B)** Rat hindlimb during MC. **C)** Neutral position of a human lower limb. **D)** Human hindlimb during cycling. **A&C** and **D** were adapted from [216] and [300], respectively.

The points above reflect the effect of the environment on the organism; additionally, the organism itself is able to adjust the threshold at which muscle is activated by stretch [301]. The ability to modulate reflexes is governed by a combination of factors and interactions between primary afferents, interneurons, motor neurons, and the descending pathways that influence them [302]. This is particularly relevant to SCI, as the disruption of descending input causes drastic temporal changes in reflex sensitivity [303]. Although gamma motor neurons that control the gain of the stretch reflex do not appear to directly contribute to hyperexcitability after SCI, it has been suggested that the intrinsic properties of larger alpha motor neurons may play a role in spasticity through changes in persistent inward currents (PIC) [304]. These changes are mediated by a loss of descending serotonergic input that increases the expression of constitutively active 5-HT_{2C} receptors, which causes increased PIC that create an exaggerated response to synaptic afferent inputs such as those from muscle stretch [305]. As this phenomenon occurs in rats [306] and humans [307], it is important to consider when attempting to translate results from MC studies as increased excitability could lead to increased reflex activation during cycling. In rats, these reflexes have been shown to increase after only two weeks post-transection and coincide with the development of spasticity [308]. This corresponds to our results, which demonstrate an increase in force starting at two weeks post-injury. Although reflexes may reappear as early as two weeks after injury in humans, clinical signs of spasticity usually do not appear until two to six months after injury [123, 309]. Therefore, it may be difficult to translate the results of a rat model of MC to acute cycling in humans as there is only a narrow window where the cycling itself is relevant, although this needs to be validated by examining force and EMG during human MC. Additionally, some consideration should be given to the injury model itself. While we primarily used a contusion model of SCI due to the relevance of this kind of injury to humans, some evidence suggests that

transected rather than contused rats exhibit more spasticity, which is the opposite of what occurs in humans [308, 310, 311]. Although the contusion group in our study exhibited more spastic forces during cycling it also showed little cadence dependent changes in non-spastic forces, suggesting that the tonic component of the stretch reflex may not have been activated. Additionally, the spastic forces in this study could also be due to a kicking or fighting of the bike due to input from the brain as some locomotor capacity was retained in the contusion group, therefore the relevance of these forces to human MC is unlikely. In summary, the choice of SCI model must be from a balance between the pathology of the injury with how clinically relevant the response to treatment is. The increase in tonic spasticity, immobility resulting in no in-cage hindlimb loading, and lack of large forces observed may make a transection injury of MC more clinically relevant despite differences in the injury profile.

Future Directions and Potential Clinical Translations

This discussion has considered the relationship between human and rat MC, however without an understanding of the forces, EMG, and cardiovascular response during clinical MC any conclusions will remain speculation. There is progress being made in this regard, as a promising method to assess clinical MC acutely post-SCI has been developed at the Université de Montréal [253], and our labs are working closely to devise comparable outcome measures. In the meantime, one of the main lessons that can be immediately adapted from this work is the idea of eccentric cycle training – targeting activation of the muscles during lengthening – specifically applied to FES cycling. A substantial limitation to FES cycling is rapid muscle fatigue given that patients with SCI have reduced capacity for exercise [312] and FES recruits fatigable fast-twitch fibers, opposite from that of a volitional contraction [313]. As eccentric cycling has been shown to be less metabolically demanding at the same work [314, 315], clinicians could

utilize a procedure where a milder stimulation is applied during the lengthening phase while patients are on a motorized ergometer. Stimulated resistance training has already been performed on SCI patients using weighted knee extensions and has shown benefits in skeletal muscle size [316] and glucose tolerance [317]. Our results demonstrating a BP/HR response to rhythmic MC in rats work suggests that eccentric FES cycling may offer a cardiovascular benefit in addition to the benefits of resistance training.

Although no direct comparison can currently be made between rat and human MC, there are still steps that can be taken to improve our understanding of the rat model due to limitations of the current work. Our study on cardiovascular outcomes was focused on the instantaneous relationship to force and cadence which influenced the design of our evaluation. A consequence of this design was the short time of the evaluation (about one third of published training methods), therefore we do not know how force relates to a possible training effect. Additionally, we do not know what the cardiovascular-force relationship is in a transection model of SCI. Future studies could investigate the relationship between forces, HR, and BP over an extended training session and how differences during cycling relate to long-term cardiovascular outcomes. To induce differences in force production, animals could be trained at different cadences. Additionally, an anti-spastic drug such as baclofen could be administered to separate the contributions of spastic and non-spastic forces.

Finally, our interpretation of EMG results is limited as results were obtained in rats with a contusion injury, and as mentioned previously this group exhibited slightly abnormal recovery following SCI compared to animals that did not receive an implant. While we were able to illustrate EMG patterns at a wide variety of forces, we cannot definitively say that the relationship would be the same in animals with a transection. An

additional limitation was the evaluation design. Our use of six cadences was intended to be thorough, however it reduced statistical power and complicated analyses. As a pattern of low/high cadences was observed, future studies should use one of each as opposed to all six.

This work was performed with the intention of translating benefits of MC seen in rats to the clinic. For this to occur, a deeper understanding of the biomechanics and their relation to physiologic responses in both rats and humans must be attained. It may be that a rat model only applies to chronic SCI, as the timeframe of reflex recovery in rats is too short for meaningful intervention. It is also possible that inherent differences in rat vs. human anatomy require a redesign of the rat cycle to be relevant, or possibly these differences will be such that a direct translation is not possible. Regardless, insights from the animal model can still be used to influence clinical practice in a meaningful way. If MC can be applied clinically in a manner that elicits rhythmic muscle activity and meaningful hindlimb loading it may be a useful rehabilitation strategy for mitigating the loss of muscle mass and cardiovascular function post-SCI.

REFERENCES

1. White, N.-H. and N.-H. Black, *Spinal Cord Injury Facts and Figures at a Glance*. 2017.
2. Hutson, T.H. and S. Di Giovanni, *The translational landscape in spinal cord injury: focus on neuroplasticity and regeneration*. *Nat Rev Neurol*, 2019. **15**(12): p. 732-745.
3. Badhiwala, J.H., et al., *Early vs Late Surgical Decompression for Central Cord Syndrome*. *JAMA Surg*, 2022.
4. Haghnegahdar, A., et al., *A Randomized Controlled Trial of Early versus Late Surgical Decompression for Thoracic and Thoracolumbar Spinal Cord Injury in 73 Patients*. *Neurotrauma Rep*, 2020. **1**(1): p. 78-87.
5. Wilson, J.R., D.W. Cadotte, and M.G. Fehlings, *Clinical predictors of neurological outcome, functional status, and survival after traumatic spinal cord injury: a systematic review*. *J Neurosurg Spine*, 2012. **17**(1 Suppl): p. 11-26.
6. Rowland, J.W., et al., *Current status of acute spinal cord injury pathophysiology and emerging therapies: promise on the horizon*. *Neurosurg Focus*, 2008. **25**(5): p. E2.
7. Tator, C.H. and M.G. Fehlings, *Review of the secondary injury theory of acute spinal cord trauma with emphasis on vascular mechanisms*. *J Neurosurg*, 1991. **75**(1): p. 15-26.
8. Figley, S.A., et al., *Characterization of vascular disruption and blood-spinal cord barrier permeability following traumatic spinal cord injury*. *J Neurotrauma*, 2014. **31**(6): p. 541-52.
9. Ditunno, J.F., et al., *Spinal shock revisited: a four-phase model*. *Spinal Cord*, 2004. **42**(7): p. 383-95.
10. Tator, C.H. and I. Koyanagi, *Vascular mechanisms in the pathophysiology of human spinal cord injury*. *J Neurosurg*, 1997. **86**(3): p. 483-92.
11. Kirichok, Y., G. Krapivinsky, and D.E. Clapham, *The mitochondrial calcium uniporter is a highly selective ion channel*. *Nature*, 2004. **427**(6972): p. 360-4.
12. Pivovarova, N.B. and S.B. Andrews, *Calcium-dependent mitochondrial function and dysfunction in neurons*. *FEBS J*, 2010. **277**(18): p. 3622-36.
13. Fischer, T., et al., *Wallerian degeneration in cervical spinal cord tracts is commonly seen in routine T2-weighted MRI after traumatic spinal cord injury and is associated with impairment in a retrospective study*. *Eur Radiol*, 2021. **31**(5): p. 2923-2932.
14. Zhang, N., et al., *Inflammation & apoptosis in spinal cord injury*. *Indian J Med Res*, 2012. **135**: p. 287-96.
15. Yang, T., et al., *Dissecting the Dual Role of the Glial Scar and Scar-Forming Astrocytes in Spinal Cord Injury*. *Front Cell Neurosci*, 2020. **14**: p. 78.
16. Maynard, F.M., R.S. Karunas, and W.P. Waring, 3rd, *Epidemiology of spasticity following traumatic spinal cord injury*. *Arch Phys Med Rehabil*, 1990. **71**(8): p. 566-9.
17. Lance, J.W., *The control of muscle tone in man*. *Electroencephalogr Clin Neurophysiol*, 1969. **27**(7): p. 713-4.
18. Bhattacharyya, K.B., *The stretch reflex and the contributions of C David Marsden*. *Ann Indian Acad Neurol*, 2017. **20**(1): p. 1-4.
19. Lan, N. and X. He, *Fusimotor control of spindle sensitivity regulates central and peripheral coding of joint angles*. *Front Comput Neurosci*, 2012. **6**: p. 66. .

20. Wright, J. and M. Rang, *The spastic mouse. And the search for an animal model of spasticity in human beings*. Clin Orthop Relat Res, 1990(253): p. 12-9.
21. Leis, A.A., et al., *Spinal motoneuron excitability after acute spinal cord injury in humans*. Neurology, 1996. **47**(1): p. 231-7
22. Bailey, C.S., J.S. Lieberman, and R.L. Kitchell, *Response of muscle spindle primary endings to static stretch in acute and chronic spinal cats*. Am J Vet Res, 1980. **41**(12): p. 2030-6.
23. Wilson, L.R., et al., *Evidence for fusimotor drive in stroke patients based on muscle spindle thixotropy*. Neurosci Lett, 1999. **264**(1-3): p. 109-12.
24. Mannion, R.J., et al., *Collateral sprouting of uninjured primary afferent A-fibers into the superficial dorsal horn of the adult rat spinal cord after topical capsaicin treatment to the sciatic nerve*. J Neurosci, 1996. **16**(16): p. 5189-95.
25. Murray, M. and M.E. Goldberger, *Restitution of function and collateral sprouting in the cat spinal cord: the partially hemisectioned animal*. J Comp Neurol, 1974. **158**(1): p. 19-36.
26. Krenz, N.R. and L.C. Weaver, *Sprouting of primary afferent fibers after spinal cord transection in the rat*. Neuroscience, 1998. **85**(2): p. 443-58.
27. Tan, A.M., et al., *Selective corticospinal tract injury in the rat induces primary afferent fiber sprouting in the spinal cord and hyperreflexia*. J Neurosci, 2012. **32**(37): p. 12896-908.
28. Rudomin, P. and R.F. Schmidt, *Presynaptic inhibition in the vertebrate spinal cord revisited*. Exp Brain Res, 1999. **129**(1): p. 1-37.
29. Hari, K., et al., *GABA facilitates spike propagation through branch points of sensory axons in the spinal cord*. Nat Neurosci, 2022. **25**(10): p. 1288-1299.
30. Li, Y., et al., *Effects of baclofen on spinal reflexes and persistent inward currents in motoneurons of chronic spinal rats with spasticity*. J Neurophysiol, 2004. **92**(5): p. 2694-703.
31. Dario, A. and G. Tomei, *A benefit-risk assessment of baclofen in severe spinal spasticity*. Drug Saf, 2004. **27**(11): p. 799-818.
32. Dugan, E.A., S. Jergova, and J. Sagen, *Mutually beneficial effects of intensive exercise and GABAergic neural progenitor cell transplants in reducing neuropathic pain and spinal pathology in rats with spinal cord injury*. Exp Neurol, 2020. **327**: p. 113208.
33. Mazzone, G.L. and A. Nistri, *Modulation of extrasynaptic GABAergic receptor activity influences glutamate release and neuronal survival following excitotoxic damage to mouse spinal cord neurons*. Neurochem Int, 2019. **128**: p. 175-185.
34. Kang, J., et al., *Regional Hyperexcitability and Chronic Neuropathic Pain Following Spinal Cord Injury*. Cell Mol Neurobiol, 2020. **40**(6): p. 861-878.
35. Rafati, D.S., et al., *Nuclear factor-kappaB decoy amelioration of spinal cord injury-induced inflammation and behavior outcomes*. J Neurosci Res, 2008. **86**(3): p. 566-80.
36. Siddall, P.J., et al., *A longitudinal study of the prevalence and characteristics of pain in the first 5 years following spinal cord injury*. Pain, 2003. **103**(3): p. 249-257.
37. Bryce, T.N., et al., *International spinal cord injury pain classification: part I. Background and description. March 6-7, 2009*. Spinal Cord, 2012. **50**(6): p. 413-7.
38. Goetz, T., et al., *GABA(A) receptors: structure and function in the basal ganglia*. Prog Brain Res, 2007. **160**: p. 21-41.
39. Chamma, I., et al., *Role of the neuronal K-Cl co-transporter KCC2 in inhibitory and excitatory neurotransmission*. Front Cell Neurosci, 2012. **6**: p. 5.
40. Hasbargen, T., et al., *Role of NKCC1 and KCC2 in the development of chronic neuropathic pain following spinal cord injury*. Ann N Y Acad Sci, 2010. **1198**: p. 168-72.

41. Huang, Y.J. and J.W. Grau, *Ionic plasticity and pain: The loss of descending serotonergic fibers after spinal cord injury transforms how GABA affects pain*. *Exp Neurol*, 2018. **306**: p. 105-116.
42. Detloff, M.R., et al., *Remote activation of microglia and pro-inflammatory cytokines predict the onset and severity of below-level neuropathic pain after spinal cord injury in rats*. *Exp Neurol*, 2008. **212**(2): p. 337-47.
43. Song, C., et al., *AMPK/p38/Nrf2 activation as a protective feedback to restrain oxidative stress and inflammation in microglia stimulated with sodium fluoride*. *Chemosphere*, 2020. **244**: p. 125495.
44. Crown, E.D., et al., *Increases in the activated forms of ERK 1/2, p38 MAPK, and CREB are correlated with the expression of at-level mechanical allodynia following spinal cord injury*. *Exp Neurol*, 2006. **199**(2): p. 397-407.
45. Huang, S., et al., *Delayed inhibition of ERK and p38 attenuates neuropathic pain without affecting motor function recovery after peripheral nerve injury*. *Neuropharmacology*, 2022. **202**: p. 108835.
46. Cooper, T.E., et al., *Morphine for chronic neuropathic pain in adults*. *Cochrane Database Syst Rev*, 2017. **5**: p. CD011669.
47. McNicol, E.D., M.C. Ferguson, and R. Schumann, *Methadone for neuropathic pain in adults*. *Cochrane Database Syst Rev*, 2017. **5**: p. CD012499.
48. Woller, S.A. and M.A. Hook, *Opioid administration following spinal cord injury: implications for pain and locomotor recovery*. *Exp Neurol*, 2013. **247**: p. 328-41.
49. Kohno, T., et al., *Peripheral axonal injury results in reduced mu opioid receptor pre- and post-synaptic action in the spinal cord*. *Pain*, 2005. **117**(1-2): p. 77-87.
50. Michael, F.M., et al., *Contusive spinal cord injury up regulates mu-opioid receptor (mor) gene expression in the brain and down regulates its expression in the spinal cord: possible implications in spinal cord injury research*. *Neurol Res*, 2015. **37**(9): p. 788-96.
51. Maduna, T., et al., *Microglia Express Mu Opioid Receptor: Insights From Transcriptomics and Fluorescent Reporter Mice*. *Front Psychiatry*, 2018. **9**: p. 726.
52. Raghavendra, V., M.D. Rutkowski, and J.A. DeLeo, *The role of spinal neuroimmune activation in morphine tolerance/hyperalgesia in neuropathic and sham-operated rats*. *J Neurosci*, 2002. **22**(22): p. 9980-9.
53. Reiss, D., et al., *Mu opioid receptor in microglia contributes to morphine analgesic tolerance, hyperalgesia, and withdrawal in mice*. *J Neurosci Res*, 2022. **100**(1): p. 203-219.
54. Kupfer, M. and C.S. Formal, *Non-opioid pharmacologic treatment of chronic spinal cord injury-related pain*. *J Spinal Cord Med*, 2022. **45**(2): p. 163-172.
55. Burchiel, K.J. and F.P. Hsu, *Pain and spasticity after spinal cord injury: mechanisms and treatment*. *Spine (Phila Pa 1976)*, 2001. **26**(24 Suppl): p. S146-60.
56. Detloff, M.R., et al., *Acute exercise prevents the development of neuropathic pain and the sprouting of non-peptidergic (GDNF- and artemin-responsive) c-fibers after spinal cord injury*. *Exp Neurol*, 2014. **255**: p. 38-48.
57. Detloff, M.R., et al., *Delayed Exercise Is Ineffective at Reversing Aberrant Nociceptive Afferent Plasticity or Neuropathic Pain After Spinal Cord Injury in Rats*. *Neurorehabil Neural Repair*, 2016. **30**(7): p. 685-700.
58. Nees, T.A., et al., *Early-onset treadmill training reduces mechanical allodynia and modulates calcitonin gene-related peptide fiber density in lamina III/IV in a mouse model of spinal cord contusion injury*. *Pain*, 2016. **157**(3): p. 687-697.

59. Sliwinski, C., et al., *Sensorimotor Activity Partially Ameliorates Pain and Reduces Nociceptive Fiber Density in the Chronically Injured Spinal Cord*. J Neurotrauma, 2018. **35**(18): p. 2222-2238.
60. Tashiro, S., et al., *The Amelioration of Pain-Related Behavior in Mice with Chronic Spinal Cord Injury Treated with Neural Stem/Progenitor Cell Transplantation Combined with Treadmill Training*. J Neurotrauma, 2018. **35**(21): p. 2561-2571.
61. Myers, J., M. Lee, and J. Kiratli, *Cardiovascular disease in spinal cord injury: an overview of prevalence, risk, evaluation, and management*. Am J Phys Med Rehabil, 2007. **86**(2): p. 142-52.
62. Groah, S.L., et al., *The relationship between neurological level of injury and symptomatic cardiovascular disease risk in the aging spinal injured*. Spinal Cord, 2001. **39**(6): p. 310-7.
63. Wecht, J.M., et al., *Cardiovascular Autonomic Dysfunction in Spinal Cord Injury: Epidemiology, Diagnosis, and Management*. Semin Neurol, 2020. **40**(5): p. 550-559.
64. Biering-Sorensen, F., et al., *Alterations in cardiac autonomic control in spinal cord injury*. Auton Neurosci, 2018. **209**: p. 4-18.
65. Furlan, J.C., et al., *Descending vasomotor pathways in humans: correlation between axonal preservation and cardiovascular dysfunction after spinal cord injury*. J Neurotrauma, 2003. **20**(12): p. 1351-63.
66. Biering-Sorensen, F., et al., *Alterations in cardiac autonomic control in spinal cord injury*. Auton Neurosci, 2017.
67. Convertino, V.A., *Blood volume response to physical activity and inactivity*. Am J Med Sci, 2007. **334**(1): p. 72-9.
68. Bertoli, S., et al., *Nutritional status and dietary patterns in disabled people*. Nutr Metab Cardiovasc Dis, 2006. **16**(2): p. 100-12.
69. West, C.R., et al., *Passive hind-limb cycling improves cardiac function and reduces cardiovascular disease risk in experimental spinal cord injury*. J Physiol, 2014. **592**(8): p. 1771-83.
70. Williams, A.M., et al., *Cardiac consequences of spinal cord injury: systematic review and meta-analysis*. Heart, 2019. **105**(3): p. 217-225.
71. Ong, B., J.R. Wilson, and M.K. Henzel, *Management of the Patient with Chronic Spinal Cord Injury*. Med Clin North Am, 2020. **104**(2): p. 263-278.
72. Howard-Quijano, K., et al., *Spinal Cord Stimulation Reduces Ventricular Arrhythmias by Attenuating Reactive Gliosis and Activation of Spinal Interneurons*. JACC Clin Electrophysiol, 2021. **7**(10): p. 1211-1225.
73. Wei, X., X. Liu, and A. Rosenzweig, *What do we know about the cardiac benefits of exercise?* Trends Cardiovasc Med, 2015. **25**(6): p. 529-36.
74. Ding, S., et al., *C/EBPB-CITED4 in Exercised Heart*. Adv Exp Med Biol, 2017. **1000**: p. 247-259.
75. Calvert, J.W., et al., *Exercise protects against myocardial ischemia-reperfusion injury via stimulation of beta(3)-adrenergic receptors and increased nitric oxide signaling: role of nitrite and nitrosothiols*. Circ Res, 2011. **108**(12): p. 1448-58.
76. Hamann, J.J., et al., *Muscle pump does not enhance blood flow in exercising skeletal muscle*. J Appl Physiol (1985), 2003. **94**(1): p. 6-10.
77. Miller, J.D., et al., *Skeletal muscle pump versus respiratory muscle pump: modulation of venous return from the locomotor limb in humans*. J Physiol, 2005. **563**(Pt 3): p. 925-43.
78. Laughlin, M.H., *Skeletal muscle blood flow capacity: role of muscle pump in exercise hyperemia*. Am J Physiol, 1987. **253**(5 Pt 2): p. H993-1004.

79. Pollack, A.A. and E.H. Wood, *Venous pressure in the saphenous vein at the ankle in man during exercise and changes in posture*. J Appl Physiol, 1949. **1**(9): p. 649-62.
80. Chaudhry, R., J.H. Miao, and A. Rehman, *Physiology, Cardiovascular*, in StatPearls. 2022, StatPearls Publishing

Copyright © 2022, StatPearls Publishing LLC.: Treasure Island (FL).

81. Bronzino, J.D. and D.R. Peterson, *The Biomedical Engineering Handbook: Four Volume Set*. 2018: CRC Press.
82. Wunsch, S.A., J. Muller-Delp, and M.D. Delp, *Time course of vasodilatory responses in skeletal muscle arterioles: role in hyperemia at onset of exercise*. Am J Physiol Heart Circ Physiol, 2000. **279**(4): p. H1715-23.
83. White, N., *National Spinal Cord Injury Statistical Center, Facts and Figures at a Glance*. University of Alabama at Birmingham, Birmingham, AL, 2017.
84. MacKay-Lyons, M., *Central pattern generation of locomotion: a review of the evidence*. Phys Ther, 2002. **82**(1): p. 69-83.
85. Hammell, K.R., *Spinal cord injury rehabilitation research: patient priorities, current deficiencies and potential directions*. Disabil Rehabil, 2010. **32**(14): p. 1209-18.
86. Lo, C., et al., *Functional Priorities in Persons with Spinal Cord Injury: Using Discrete Choice Experiments To Determine Preferences*. J Neurotrauma, 2016. **33**(21): p. 1958-1968.
87. Jacobs, P.L. and M.S. Nash, *Exercise recommendations for individuals with spinal cord injury*. Sports Med, 2004. **34**(11): p. 727-51.
88. Ilha, J., et al., *Overground gait training promotes functional recovery and cortical neuroplasticity in an incomplete spinal cord injury model*. Life Sci, 2019. **232**: p. 116627.
89. States, R.A., E. Pappas, and Y. Salem, *Overground physical therapy gait training for chronic stroke patients with mobility deficits*. Cochrane Database Syst Rev, 2009(3): p. CD006075.
90. Mehrholz, J., et al., *Is body-weight-supported treadmill training or robotic-assisted gait training superior to overground gait training and other forms of physiotherapy in people with spinal cord injury? A systematic review*. Spinal Cord, 2017. **55**(8): p. 722-729.
91. Lam, T., et al., *A systematic review of the efficacy of gait rehabilitation strategies for spinal cord injury*. Top Spinal Cord Inj Rehabil, 2007. **13**(1): p. 32-57.
92. Mehrholz, J., J. Kugler, and M. Pohl, *Locomotor training for walking after spinal cord injury*. Spine (Phila Pa 1976), 2008. **33**(21): p. E768-77.
93. Mehrholz, J., J. Kugler, and M. Pohl, *Locomotor training for walking after spinal cord injury*. Cochrane Database Syst Rev, 2012. **11**: p. CD006676.
94. Field-Fote, E.C. and K.E. Roach, *Influence of a locomotor training approach on walking speed and distance in people with chronic spinal cord injury: a randomized clinical trial*. Phys Ther, 2011. **91**(1): p. 48-60.
95. Edwards, D.J., et al., *Walking improvement in chronic incomplete spinal cord injury with exoskeleton robotic training (WISE): a randomized controlled trial*. Spinal Cord, 2022. **60**(6): p. 522-532.
96. Fang, C.Y., et al., *Effects of Robot-Assisted Gait Training in Individuals with Spinal Cord Injury: A Meta-analysis*. Biomed Res Int, 2020. **2020**: p. 2102785.
97. Nam, K.Y., et al., *Robot-assisted gait training (Lokomat) improves walking function and activity in people with spinal cord injury: a systematic review*. J Neuroeng Rehabil, 2017. **14**(1): p. 24.

98. Loy, K. and F.M. Bareyre, *Rehabilitation following spinal cord injury: how animal models can help our understanding of exercise-induced neuroplasticity*. *Neural Regen Res*, 2019. **14**(3): p. 405-412.
99. Shah, P.K., et al., *Use of quadrupedal step training to re-engage spinal interneuronal networks and improve locomotor function after spinal cord injury*. *Brain*, 2013. **136**(Pt 11): p. 3362-77.
100. Bonizzato, M., et al., *Brain-controlled modulation of spinal circuits improves recovery from spinal cord injury*. *Nat Commun*, 2018. **9**(1): p. 3015.
101. Song, Y.S., et al., *Soft robot for gait rehabilitation of spinalized rodents*.
102. Gruner, J.A., *A monitored contusion model of spinal cord injury in the rat*. *J Neurotrauma*, 1992. **9**(2): p. 123-6; discussion 126-8.
103. Brownstone, R.M., T.V. Bui, and N. Stifani, *Spinal circuits for motor learning*. *Curr Opin Neurobiol*, 2015. **33**: p. 166-73.
104. Takeoka, A., et al., *Muscle spindle feedback directs locomotor recovery and circuit reorganization after spinal cord injury*. *Cell*, 2014. **159**(7): p. 1626-39.
105. Takeoka, A. and S. Arber, *Functional Local Proprioceptive Feedback Circuits Initiate and Maintain Locomotor Recovery after Spinal Cord Injury*. *Cell Rep*, 2019. **27**(1): p. 71-85 e3.
106. Harnie, J., et al., *The recovery of standing and locomotion after spinal cord injury does not require task-specific training*. *Elife*, 2019. **8**.
107. McGuigan, M.R., G.A. Wright, and S.J. Fleck, *Strength training for athletes: does it really help sports performance?* *Int J Sports Physiol Perform*, 2012. **7**(1): p. 2-5.
108. Cormie, P., M.R. McGuigan, and R.U. Newton, *Developing maximal neuromuscular power: Part 1--biological basis of maximal power production*. *Sports Med*, 2011. **41**(1): p. 17-38.
109. Douglas, J., et al., *Chronic Adaptations to Eccentric Training: A Systematic Review*. *Sports Med*, 2017. **47**(5): p. 917-941.
110. Hody, S., et al., *Eccentric Muscle Contractions: Risks and Benefits*. *Front Physiol*, 2019. **10**: p. 536.
111. Friden, J., M. Sjoström, and B. Ekblom, *A morphological study of delayed muscle soreness*. *Experientia*, 1981. **37**(5): p. 506-7.
112. Julian, V., et al., *Eccentric Training Improves Body Composition by Inducing Mechanical and Metabolic Adaptations: A Promising Approach for Overweight and Obese Individuals*. *Front Physiol*, 2018. **9**: p. 1013.
113. Kim, H.E., D.M. Corcos, and T.G. Hornby, *Increased spinal reflex excitability is associated with enhanced central activation during voluntary lengthening contractions in human spinal cord injury*. *J Neurophysiol*, 2015. **114**(1): p. 427-39.
114. Stone, W.J., et al., *Strength and Step Activity After Eccentric Resistance Training in Those With Incomplete Spinal Cord Injuries*. *Top Spinal Cord Inj Rehabil*, 2018. **24**(4): p. 343-352.
115. Faw, T.D., et al., *Eccentric rehabilitation induces white matter plasticity and sensorimotor recovery in chronic spinal cord injury*. *Exp Neurol*, 2021. **346**: p. 113853.
116. Hansen, C.N., et al., *Characterization of recovered walking patterns and motor control after contusive spinal cord injury in rats*. *Brain Behav*, 2012. **2**(5): p. 541-52.
117. Duncan, G.J., et al., *Locomotor recovery following contusive spinal cord injury does not require oligodendrocyte remyelination*. *Nat Commun*, 2018. **9**(1): p. 3066.
118. Harvey, L.A., et al., *Contracture management for people with spinal cord injuries*. *NeuroRehabilitation*, 2011. **28**(1): p. 17-20.

119. Mizuno, T., *Effect of different stretch amplitudes of dynamic stretching on joint range of motion*. The Journal of Physical Fitness and Sports Medicine, 2019. **8**(3): p. 137-142.
120. Iwata, M., et al., *Dynamic Stretching Has Sustained Effects on Range of Motion and Passive Stiffness of the Hamstring Muscles*. J Sports Sci Med, 2019. **18**(1): p. 13-20.
121. Pompe, B., S. Filipidis, and P. Dovc, *Impact of Static Progressive Stretch on Range of Motion after Total Knee Replacement in Patients with Haemophilia*. J Rehabil Med Clin Commun, 2022. **5**: p. 2285.
122. Williams, P.E., *Use of intermittent stretch in the prevention of serial sarcomere loss in immobilised muscle*. Ann Rheum Dis, 1990. **49**(5): p. 316-7.
123. Billington, Z.J., A.M. Henke, and D.R. Gater, Jr., *Spasticity Management after Spinal Cord Injury: The Here and Now*. J Pers Med, 2022. **12**(5).
124. Harvey, L.A., et al., *Stretch for the treatment and prevention of contractures*. Cochrane Database Syst Rev, 2017. **1**: p. CD007455.
125. Bhilwade, A. and S. Ganvir, *EFFECT OF STRETCHING TO RELIEVE SPASTICITY IN NEUROLOGICAL CONDITIONS- A SYSTEMATIC REVIEW: STRETCHING TO RELIEVE SPASTICITY*. VIMS JOURNAL OF PHYSICAL THERAPY, 2020. **2**: p. 3-12.
126. Caudle, K.L., et al., *Hindlimb stretching alters locomotor function after spinal cord injury in the adult rat*. Neurorehabil Neural Repair, 2015. **29**(3): p. 268-77.
127. Keller, A.V., et al., *Disruption of Locomotion in Response to Hindlimb Muscle Stretch at Acute and Chronic Time Points after a Spinal Cord Injury in Rats*. J Neurotrauma, 2017. **34**(3): p. 661-670.
128. Keller, A., et al., *Dynamic "Range of Motion" Hindlimb Stretching Disrupts Locomotor Function in Rats with Moderate Subacute Spinal Cord Injuries*. J Neurotrauma, 2017. **34**(12): p. 2086-2091.
129. Keller, A.V., *Stretching adversely modulates locomotor capacity following spinal cord injury via activation of nociceptive afferents.*, in *Physiology and Biophysics*. 2017, University of Louisville.
130. Grau, J.W., *Learning from the spinal cord: how the study of spinal cord plasticity informs our view of learning*. Neurobiol Learn Mem, 2014. **108**: p. 155-71.
131. Grau, J.W., D.G. Barstow, and R.L. Joynes, *Instrumental learning within the spinal cord: I. Behavioral properties*. Behav Neurosci, 1998. **112**(6): p. 1366-86.
132. Crown, E.D. and J.W. Grau, *Preserving and restoring behavioral potential within the spinal cord using an instrumental training paradigm*. J Neurophysiol, 2001. **86**(2): p. 845-55.
133. Forssberg, H., et al., *The locomotion of the low spinal cat. II. Interlimb coordination*. Acta Physiol Scand, 1980. **108**(3): p. 283-95.
134. Dietz, V., W. Zijlstra, and J. Duysens, *Human neuronal interlimb coordination during split-belt locomotion*. Exp Brain Res, 1994. **101**(3): p. 513-20.
135. Prokop, T., et al., *Adaptational and learning processes during human split-belt locomotion: interaction between central mechanisms and afferent input*. Exp Brain Res, 1995. **106**(3): p. 449-56.
136. Peng, C.-W., et al., *Clinical benefits of functional electrical stimulation cycling exercise for subjects with central neurological impairments*. J. Med. Biol. Eng., 2011. **31**(1): p. 1-11.
137. Atkins, D., et al., *Grading quality of evidence and strength of recommendations*. BMJ, 2004. **328**(7454): p. 1490.
138. van der Scheer, J.W., et al., *Effects of exercise on fitness and health of adults with spinal cord injury: A systematic review*. Neurology, 2017. **89**(7): p. 736-745.

139. van der Scheer, J.W., et al., *Functional electrical stimulation cycling exercise after spinal cord injury: a systematic review of health and fitness-related outcomes*. J Neuroeng Rehabil, 2021. **18**(1): p. 99.
140. Galea, M.P., et al., *SCIPA Switch-On: A Randomized Controlled Trial Investigating the Efficacy and Safety of Functional Electrical Stimulation-Assisted Cycling and Passive Cycling Initiated Early After Traumatic Spinal Cord Injury*. Neurorehabil Neural Repair, 2017. **31**(6): p. 540-551.
141. Ralston, K.E., et al., *Functional electrical stimulation cycling has no clear effect on urine output, lower limb swelling, and spasticity in people with spinal cord injury: a randomised cross-over trial*. J Physiother, 2013. **59**(4): p. 237-43.
142. Panisset, M.G., et al., *Factors influencing thigh muscle volume change with cycling exercises in acute spinal cord injury - a secondary analysis of a randomized controlled trial*. J Spinal Cord Med, 2022. **45**(4): p. 510-521.
143. Baldi, J.C., et al., *Muscle atrophy is prevented in patients with acute spinal cord injury using functional electrical stimulation*. Spinal Cord, 1998. **36**(7): p. 463-9.
144. Demchak, T.J., et al., *Effects of functional electric stimulation cycle ergometry training on lower limb musculature in acute sci individuals*. J Sports Sci Med, 2005. **4**(3): p. 263-71.
145. Phillips, C.A., et al., *Muscular, respiratory and cardiovascular responses of quadriplegic persons to an F. E. S. bicycle ergometer conditioning program*. Int J Rehabil Res, 1989. **12**(2): p. 147-57.
146. Petrofsky, J.S. and R. Stacy, *The effect of training on endurance and the cardiovascular responses of individuals with paraplegia during dynamic exercise induced by functional electrical stimulation*. Eur J Appl Physiol Occup Physiol, 1992. **64**(6): p. 487-92.
147. Berry, H.R., et al., *Cardiorespiratory and power adaptations to stimulated cycle training in paraplegia*. Med Sci Sports Exerc, 2008. **40**(9): p. 1573-80.
148. Miller, R. and W. Brown, *Steps and sitting in a working population*. Int J Behav Med, 2004. **11**(4): p. 219-24.
149. Healy, G.N., et al., *Breaks in sedentary time: beneficial associations with metabolic risk*. Diabetes Care, 2008. **31**(4): p. 661-6.
150. Healy, G.N., et al., *Sedentary time and cardio-metabolic biomarkers in US adults: NHANES 2003-06*. Eur Heart J, 2011. **32**(5): p. 590-7.
151. Peterman, J.E., et al., *Motor-Driven (Passive) Cycling: A Potential Physical Inactivity Countermeasure?* Med Sci Sports Exerc, 2016. **48**(9): p. 1821-8.
152. Nobrega, A.C., et al., *Cardiovascular responses to active and passive cycling movements*. Med Sci Sports Exerc, 1994. **26**(6): p. 709-14.
153. Muraki, S., Y. Ehara, and M. Yamasaki, *Cardiovascular responses at the onset of passive leg cycle exercise in paraplegics with spinal cord injury*. Eur J Appl Physiol, 2000. **81**(4): p. 271-4.
154. Muraki, S., et al., *Cardiovascular and respiratory responses to passive leg cycle exercise in people with spinal cord injuries*. Eur J Appl Physiol Occup Physiol, 1996. **74**(1-2): p. 23-8.
155. Figoni, S.F., et al., *Physiologic responses of paraplegics and quadriplegics to passive and active leg cycle ergometry*. J Am Paraplegia Soc, 1990. **13**(3): p. 33-9.
156. Thomas, A.J., G.M. Davis, and J.R. Sutton, *Cardiovascular and metabolic responses to electrical stimulation-induced leg exercise in spinal cord injury*. Methods Inf Med, 1997. **36**(4-5): p. 372-5.
157. Ter Woerds, W., et al., *Passive leg movements and passive cycling do not alter arterial leg blood flow in subjects with spinal cord injury*. Phys Ther, 2006. **86**(5): p. 636-45.

158. Ballaz, L., et al., *Acute peripheral blood flow response induced by passive leg cycle exercise in people with spinal cord injury*. Arch Phys Med Rehabil, 2007. **88**(4): p. 471-6.
159. Groothuis, J.T. and M.T. Hopman, *Does passive cycling induce changes in peripheral blood flow in persons with spinal cord injury?* Arch Phys Med Rehabil, 2007. **88**(12): p. 1740; author reply 1740-1.
160. Udina, E., A. Puigdemasa, and X. Navarro, *Passive and active exercise improve regeneration and muscle reinnervation after peripheral nerve injury in the rat*. Muscle Nerve, 2011. **43**(4): p. 500-9.
161. Arbat-Plana, A., X. Navarro, and E. Udina, *Effects of forced, passive, and voluntary exercise on spinal motoneurons changes after peripheral nerve injury*. Eur J Neurosci, 2017. **46**(12): p. 2885-2892.
162. Keeler, B.E., et al., *Acute and prolonged hindlimb exercise elicits different gene expression in motoneurons than sensory neurons after spinal cord injury*. Brain Res, 2012. **1438**: p. 8-21.
163. Chopek, J.W., et al., *Serotonin receptor and KCC2 gene expression in lumbar flexor and extensor motoneurons posttransection with and without passive cycling*. J Neurophysiol, 2015. **113**(5): p. 1369-76.
164. Chopek, J.W., et al., *Daily passive cycling attenuates the hyperexcitability and restores the responsiveness of the extensor monosynaptic reflex to quipazine in the chronic spinally transected rat*. J Neurotrauma, 2014. **31**(12): p. 1083-7.
165. Beaumont, E., et al., *Passive exercise and fetal spinal cord transplant both help to restore motoneuronal properties after spinal cord transection in rats*. Muscle Nerve, 2004. **29**(2): p. 234-42.
166. Houle, J.D., et al., *Effects of fetal spinal cord tissue transplants and cycling exercise on the soleus muscle in spinalized rats*. Muscle Nerve, 1999. **22**(7): p. 846-56.
167. Popok, D.W., et al., *Effects of early and delayed initiation of exercise training on cardiac and haemodynamic function after spinal cord injury*. Exp Physiol, 2017. **102**(2): p. 154-163.
168. DeVeau, K.M., et al., *A comparison of passive hindlimb cycling and active upper-limb exercise provides new insights into systolic dysfunction after spinal cord injury*. Am J Physiol Heart Circ Physiol, 2017. **313**(5): p. H861-H870.
169. West, C.R., et al., *Passive Hind-Limb Cycling Reduces the Severity of Autonomic Dysreflexia After Experimental Spinal Cord Injury*. Neurorehabil Neural Repair, 2016. **30**(4): p. 317-27.
170. Takano, K. and H.D. Henatsch, *The effect of the rate of stretch upon the development of active reflex tension in hind limb muscles of the decerebrate cat*. Exp Brain Res, 1971. **112**(4): p. 422-34.
171. Keller, A.V., et al., *Nociceptor-dependent locomotor dysfunction after clinically-modeled hindlimb muscle stretching in adult rats with spinal cord injury*. Exp Neurol, 2019. **318**: p. 267-276.
172. Zajac, F.E., *Muscle and tendon: properties, models, scaling, and application to biomechanics and motor control*. Crit Rev Biomed Eng, 1989. **17**(4): p. 359-411.
173. Blackburn, T.P., et al., *Autoradiographic localization of delta opiate receptors in rat and human brain*. Neuroscience, 1988. **27**(2): p. 497-506.
174. Corder, G., et al., *Endogenous and Exogenous Opioids in Pain*. Annu Rev Neurosci, 2018. **41**: p. 453-473.
175. Taylor, B.K. and G. Corder, *Endogenous analgesia, dependence, and latent pain sensitization*. Curr Top Behav Neurosci, 2014. **20**: p. 283-325.

176. Walters, E.T., *Nociceptors as chronic drivers of pain and hyperreflexia after spinal cord injury: an adaptive-maladaptive hyperfunctional state hypothesis*. *Front Physiol*, 2012. **3**: p. 309.
177. Corder, G., et al., *Constitutive mu-opioid receptor activity leads to long-term endogenous analgesia and dependence*. *Science*, 2013. **341**(6152): p. 1394-9.
178. Scherrer, G., et al., *Dissociation of the opioid receptor mechanisms that control mechanical and heat pain*. *Cell*, 2009. **137**(6): p. 1148-59.
179. Snyder, L.M., et al., *Kappa Opioid Receptor Distribution and Function in Primary Afferents*. *Neuron*, 2018. **99**(6): p. 1274-1288 e6.
180. Magnuson, D.S., et al., *Comparing deficits following excitotoxic and contusion injuries in the thoracic and lumbar spinal cord of the adult rat*. *Exp Neurol*, 1999. **156**(1): p. 191-204.
181. Joynes, R.L. and J.W. Grau, *Instrumental learning within the spinal cord: III. Prior exposure to noncontingent shock induces a behavioral deficit that is blocked by an opioid antagonist*. *Neurobiol Learn Mem*, 2004. **82**(1): p. 35-51.
182. Willette, R.E., et al., *Narcotic Antagonists: Naltrexone Pharmacology and Sustained-release Preparations*. 1981: Department of Health and Human Services, Public Health Service, Alcohol, Drug Abuse, and Mental Health Administration, National Institute on Drug Abuse, Division of Research.
183. Keller, A.V., et al., *Electromyographic patterns of the rat hindlimb in response to muscle stretch after spinal cord injury*. *Spinal Cord*, 2018. **56**(6): p. 560-568.
184. Basso, D.M., M.S. Beattie, and J.C. Bresnahan, *A sensitive and reliable locomotor rating scale for open field testing in rats*. *J Neurotrauma*, 1995. **12**(1): p. 1-21.
185. Besse, D., et al., *Pre- and postsynaptic distribution of mu, delta and kappa opioid receptors in the superficial layers of the cervical dorsal horn of the rat spinal cord*. *Brain Res*, 1990. **521**(1-2): p. 15-22.
186. Stein, C., *Opioid Receptors*. *Annu Rev Med*, 2016. **67**: p. 433-51.
187. Xu, Q., W.Y. Li, and Y. Guan, *Mu-opioidergic modulation differs in deep and superficial wide-dynamic range dorsal horn neurons in mice*. *Neurosci Lett*, 2013. **549**: p. 157-62.
188. Caudle, R.M., et al., *Spinal kappa1 and kappa2 opioid binding sites in rats, guinea pigs, monkeys and humans*. *Neuroreport*, 1998. **9**(11): p. 2523-5.
189. Washburn, S.N., et al., *Opioid regulation of spinal cord plasticity: evidence the kappa-2 opioid receptor agonist GR89696 inhibits learning within the rat spinal cord*. *Neurobiol Learn Mem*, 2008. **89**(1): p. 1-16.
190. Lee, H.J., et al., *Central Plasticity of Cutaneous Afferents Is Associated with Nociceptive Hyperreflexia after Spinal Cord Injury in Rats*. *Neural Plast*, 2019. **2019**: p. 6147878.
191. Brackett, N.L., et al., *Systemic naloxone infusion may trigger spasticity in patients with spinal cord injury: case series*. *J Spinal Cord Med*, 2007. **30**(3): p. 272-5.
192. Hemstapat, K., et al., *Comparative studies of the neuro-excitatory behavioural effects of morphine-3-glucuronide and dynorphin A(2-17) following spinal and supraspinal routes of administration*. *Pharmacol Biochem Behav*, 2009. **93**(4): p. 498-505.
193. Long, J.B., et al., *Endogenous opioids in spinal cord injury: a critical evaluation*. *Cent Nerv Syst Trauma*, 1986. **3**(4): p. 295-315.
194. Kakebeeke, T.H., H.E. Lechner, and P.A. Knapp, *The effect of passive cycling movements on spasticity after spinal cord injury: preliminary results*. *Spinal Cord*, 2005. **43**(8): p. 483-8.

195. Krause, P., J. Szecsi, and A. Straube, *Changes in spastic muscle tone increase in patients with spinal cord injury using functional electrical stimulation and passive leg movements*. Clin Rehabil, 2008. **22**(7): p. 627-34.
196. Burns, K.J., et al., *Passive limb movement intervals results in repeated hyperemic responses in those with paraplegia*. Spinal Cord, 2018. **56**(10): p. 940-948.
197. Ollivier-Lanvin, K., et al., *Proprioceptive neuropathy affects normalization of the H-reflex by exercise after spinal cord injury*. Exp Neurol, 2010. **221**(1): p. 198-205.
198. Garrison, M.K., et al., *Wind-up of stretch reflexes as a measure of spasticity in chronic spinalized rats: The effects of passive exercise and modafinil*. Exp Neurol, 2011. **227**(1): p. 104-9.
199. Walkowski, A.D. and S. Munakomi, *Monosynaptic Reflex*, in StatPearls. 2022, StatPearls Publishing

Copyright © 2022, StatPearls Publishing LLC.: Treasure Island (FL).

200. Weiss, P.L., R.E. Kearney, and I.W. Hunter, *Position dependence of stretch reflex dynamics at the human ankle*. Exp Brain Res, 1986. **63**(1): p. 49-59.
201. Wu, Y.N., et al., *Position as Well as Velocity Dependence of Spasticity-Four-Dimensional Characterizations of Catch Angle*. Front Neurol, 2018. **9**: p. 863.
202. Liu, G., et al., *Exercise modulates microRNAs that affect the PTEN/mTOR pathway in rats after spinal cord injury*. Exp Neurol, 2012. **233**(1): p. 447-56.
203. Crown, E.D., et al., *Instrumental learning within the spinal cord: IV. Induction and retention of the behavioral deficit observed after noncontingent shock*. Behav Neurosci, 2002. **116**(6): p. 1032-51.
204. Fouad, K., et al., *Treadmill training in incomplete spinal cord injured rats*. Behav Brain Res, 2000. **115**(1): p. 107-13.
205. Johnson, W.L., et al., *A three-dimensional model of the rat hindlimb: musculoskeletal geometry and muscle moment arms*. J Biomech, 2008. **41**(3): p. 610-9.
206. Delp, S.L., et al., *OpenSim: open-source software to create and analyze dynamic simulations of movement*. IEEE Trans Biomed Eng, 2007. **54**(11): p. 1940-50.
207. Sinha, N. *EMG-onset-detection*. 2022; Available from: <https://github.com/NirvikNU/EMG-onset-detection/releases/tag/1.1.0>.
208. Yang, D., et al., *Accurate EMG onset detection in pathological, weak and noisy myoelectric signals*. Biomedical Signal Processing and Control, 2017. **33**: p. 306-315.
209. States, G.J.R., et al., *Broad opioid antagonism amplifies disruption of locomotor function following therapy-like hindlimb stretching in spinal cord injured rats*. Spinal Cord, 2022. **60**(4): p. 312-319.
210. Edgerton, V.R., et al., *Retraining the injured spinal cord*. J Physiol, 2001. **533**(Pt 1): p. 15-22.
211. Lam, T. and K.G. Pearson, *Proprioceptive modulation of hip flexor activity during the swing phase of locomotion in decerebrate cats*. J Neurophysiol, 2001. **86**(3): p. 1321-32.
212. Markin, S.N., et al., *Afferent control of locomotor CPG: insights from a simple neuromechanical model*. Ann N Y Acad Sci, 2010. **1198**: p. 21-34.
213. Andersson, O. and S. Grillner, *Peripheral control of the cat's step cycle. II. Entrainment of the central pattern generators for locomotion by sinusoidal hip movements during "fictive locomotion."*. Acta Physiol Scand, 1983. **118**(3): p. 229-39.
214. Grillner, S. and S. Rossignol, *On the initiation of the swing phase of locomotion in chronic spinal cats*. Brain Res, 1978. **146**(2): p. 269-77.

215. Onushko, T. and B.D. Schmit, *Reflex Response to Imposed Bilateral Hip Oscillations in Human Spinal Cord Injury*. Journal of Neurophysiology, 2007. **98**(4): p. 1849-1861.
216. Hosoido, T., et al., *Qualitative Comparison between Rats and Humans in Quadrupedal and Bipedal Locomotion*. Journal of Behavioral and Brain Science, 2013. **Vol.03No.01**: p. 13.
217. Szecsi, J., A. Straube, and C. Fornusek, *A biomechanical cause of low power production during FES cycling of subjects with SCI*. J Neuroeng Rehabil, 2014. **11**: p. 123.
218. Sheean, G., *The pathophysiology of spasticity*. Eur J Neurol, 2002. **9 Suppl 1**: p. 3-9; discussion 53-61.
219. Dietz, V., *Spastic movement disorder*. Spinal Cord, 2000. **38**(7): p. 389-93.
220. Lloyd, D.P. and V.J. Wilson, *Reflex depression in rhythmically active monosynaptic reflex pathways*. J Gen Physiol, 1957. **40**(3): p. 409-26.
221. Ni, Y., et al., *Characterization of Long Descending Premotor Propriospinal Neurons in the Spinal Cord*. The Journal of Neuroscience, 2014. **34**(28): p. 9404.
222. Sayenko, D.G., et al., *Self-Assisted Standing Enabled by Non-Invasive Spinal Stimulation after Spinal Cord Injury*. J Neurotrauma, 2019. **36**(9): p. 1435-1450.
223. Harkema, S., et al., *Effect of epidural stimulation of the lumbosacral spinal cord on voluntary movement, standing, and assisted stepping after motor complete paraplegia: a case study*. Lancet, 2011. **377**(9781): p. 1938-47.
224. Machado, A.D.S., et al., *Effects that passive cycling exercise have on muscle strength, duration of mechanical ventilation, and length of hospital stay in critically ill patients: a randomized clinical trial*. J Bras Pneumol, 2017. **43**(2): p. 134-139.
225. Allison, D.J., et al., *Effects of a Functional Electrical Stimulation-Assisted Cycling Program on Immune and Cardiovascular Health in Persons with Spinal Cord Injury*. Top Spinal Cord Inj Rehabil, 2016. **22**(1): p. 71-78.
226. Sadowsky, C.L., et al., *Lower extremity functional electrical stimulation cycling promotes physical and functional recovery in chronic spinal cord injury*. J Spinal Cord Med, 2013. **36**(6): p. 623-31.
227. Call, J.A. and D.A. Lowe, *Eccentric Contraction-Induced Muscle Injury: Reproducible, Quantitative, Physiological Models to Impair Skeletal Muscle's Capacity to Generate Force*. Methods Mol Biol, 2016. **1460**: p. 3-18.
228. Meyer, K., et al., *Eccentric Exercise in Coronary Patients: Central Hemodynamic and Metabolic Responses*. Medicine & Science in Sports & Exercise, 2003. **35**(7).
229. Cragg, J.J., et al., *Cardiovascular disease and spinal cord injury: results from a national population health survey*. Neurology, 2013. **81**(8): p. 723-8.
230. Raguindin, P.F., et al., *The neurological level of spinal cord injury and cardiovascular risk factors: a systematic review and meta-analysis*. Spinal Cord, 2021. **59**(11): p. 1135-1145.
231. Gordon, P.S., G.J. Farkas, and D.R. Gater, Jr., *Neurogenic Obesity-Induced Insulin Resistance and Type 2 Diabetes Mellitus in Chronic Spinal Cord Injury*. Top Spinal Cord Inj Rehabil, 2021. **27**(1): p. 36-56.
232. Itodo, O.A., et al., *Physical activity and cardiometabolic risk factors in individuals with spinal cord injury: a systematic review and meta-analysis*. Eur J Epidemiol, 2022. **37**(4): p. 335-365.
233. Raymond, J., et al., *Glucose tolerance and physical activity level in people with spinal cord injury*. Spinal Cord, 2010. **48**(8): p. 591-6.
234. Davis, G.M., R.J. Shephard, and F.H. Leenen, *Cardiac effects of short term arm crank training in paraplegics: echocardiographic evidence*. Eur J Appl Physiol Occup Physiol, 1987. **56**(1): p. 90-6.

235. Nash, M.S. and P.L. Jacobs, *Cardiac structure and function in exercise trained and sedentary persons with paraplegia*. Med Sci Sports Exerc, 1998. **30**(8): p. 1336-8.
236. Svensson, M., et al., *Influence of physiotherapy on leg blood flow in patients with complete spinal cord injury lesions*. Physiotherapy Theory and Practice, 1995. **11**(2): p. 97-107.
237. Laughlin, M.H. and W.G. Schrage, *Effects of muscle contraction on skeletal muscle blood flow: when is there a muscle pump?* Med Sci Sports Exerc, 1999. **31**(7): p. 1027-35.
238. Nash, M.S., et al., *Effects of electrically-stimulated exercise and passive motion on echocardiographically-derived wall motion and cardiodynamic function in tetraplegic persons*. Paraplegia, 1995. **33**(2): p. 80-9.
239. Harman, K.A., et al., *Temporal analysis of cardiovascular control and function following incomplete T3 and T10 spinal cord injury in rodents*. Physiol Rep, 2018. **6**(6): p. e13634.
240. Verma, A.K., et al., *Skeletal Muscle Pump Drives Control of Cardiovascular and Postural Systems*. Sci Rep, 2017. **7**: p. 45301.
241. Jakubik, J. *Convergent cross mapping*. 2016 [cited 2019; Available from: <https://www.mathworks.com/matlabcentral/fileexchange/52964-convergent-cross-mapping>].
242. Sugihara, G., et al., *Detecting causality in complex ecosystems*. Science, 2012. **338**(6106): p. 496-500.
243. Silver, J.R., *Vascular reflexes in spinal shock*. Paraplegia, 1971. **8**(4): p. 231-42.
244. Guidry, M.A., et al., *The influence of short and long duration on the blood pressure response to an acute bout of dynamic exercise*. Am Heart J, 2006. **151**(6): p. 1322 e5-12.
245. Pescatello, L.S., et al., *Short-term effect of dynamic exercise on arterial blood pressure*. Circulation, 1991. **83**(5): p. 1557-61.
246. MacDonald, J.R., *Potential causes, mechanisms, and implications of post exercise hypotension*. J Hum Hypertens, 2002. **16**(4): p. 225-36.
247. Rowell, L.B., *Human cardiovascular control*. 1993: Oxford University Press, USA.
248. Miyatani, M., et al., *Pulse wave velocity for assessment of arterial stiffness among people with spinal cord injury: a pilot study*. J Spinal Cord Med, 2009. **32**(1): p. 72-8.
249. Wecht, J.M., et al., *Arterial stiffness in persons with paraplegia*. J Spinal Cord Med, 2004. **27**(3): p. 255-9.
250. Bini, R.R. and F. Diefenthaler, *Kinetics and kinematics analysis of incremental cycling to exhaustion*. Sports Biomechanics, 2010. **9**(4): p. 223-235.
251. Carpes, F.P., R.R. Bini, and J.I.P. Quesada, *Joint Kinematics*, in *Biomechanics of Cycling*, R.R. Bini and F.P. Carpes, Editors. 2014, Springer International Publishing: Cham. p. 33-42.
252. Wozniak Timmer, C.A., *Cycling Biomechanics: A Literature Review*. Journal of Orthopaedic & Sports Physical Therapy, 1991. **14**(3): p. 106-113.
253. Mac-Thiong, J.M., et al., *Protocol for rapid onset of mobilisation in patients with traumatic spinal cord injury (PROMPT-SCI) study: a single-arm proof-of-concept trial of early in-bed leg cycling following acute traumatic spinal cord injury*. BMJ Open, 2021. **11**(11): p. e049884.
254. Ericson, M.O., R. Nisell, and G. Németh, *Joint Motions of the Lower Limb During Ergometer Cycling*. Journal of Orthopaedic & Sports Physical Therapy, 1988. **9**(8): p. 273-278.
255. Kawai, H., et al., *Closed-Loop Position and Cadence Tracking Control for FES-Cycling Exploiting Pedal Force Direction With Antagonistic Biarticular Muscles*. IEEE Transactions on Control Systems Technology, 2019. **27**(2): p. 730-742.

256. Gfohler, M. and P. Lugner, *Dynamic simulation of FES-cycling: influence of individual parameters*. IEEE Transactions on Neural Systems and Rehabilitation Engineering, 2004. **12**(4): p. 398-405.
257. Kakulas, B.A., *Neuropathology: the foundation for new treatments in spinal cord injury*. Spinal Cord, 2004. **42**(10): p. 549-63.
258. Boyce, V.S., et al., *Differential effects of brain-derived neurotrophic factor and neurotrophin-3 on hindlimb function in paraplegic rats*. Eur J Neurosci, 2012. **35**(2): p. 221-32.
259. De Gail, P., J.W. Lance, and P.D. Neilson, *Differential effects on tonic and phasic reflex mechanisms produced by vibration of muscles in man*. J Neurol Neurosurg Psychiatry, 1966. **29**(1): p. 1-11.
260. Adams, M.M. and A.L. Hicks, *Spasticity after spinal cord injury*. Spinal Cord, 2005. **43**(10): p. 577-86.
261. Boyraz, I., et al., *Clonus: definition, mechanism, treatment*. Med Glas (Zenica), 2015. **12**(1): p. 19-26.
262. Rossi, A., R. Mazzocchio, and C. Scarpini, *Clonus in man: a rhythmic oscillation maintained by a reflex mechanism*. Electroencephalogr Clin Neurophysiol, 1990. **75**(2): p. 56-63.
263. Zimmerman, B. and J.B. Hubbard, *Clonus*. 2018.
264. Walsh, E.G., *Clonus: beats provoked by the application of a rhythmic force*. J Neurol Neurosurg Psychiatry, 1976. **39**(3): p. 266-74.
265. Dimitrijevic, M.R., P.W. Nathan, and A.M. Sherwood, *Clonus: the role of central mechanisms*. J Neurol Neurosurg Psychiatry, 1980. **43**(4): p. 321-32.
266. Beres-Jones, J.A., T.D. Johnson, and S.J. Harkema, *Clonus after human spinal cord injury cannot be attributed solely to recurrent muscle-tendon stretch*. Exp Brain Res, 2003. **149**(2): p. 222-36.
267. Lin, S., et al., *Locomotor-related V3 interneurons initiate and coordinate muscles spasms after spinal cord injury*. J Neurophysiol, 2019. **121**(4): p. 1352-1367.
268. Grillner, S. and T.M. Jessell, *Measured motion: searching for simplicity in spinal locomotor networks*. Curr Opin Neurobiol, 2009. **19**(6): p. 572-86.
269. Zhang, H., et al., *The role of V3 neurons in speed-dependent interlimb coordination during locomotion in mice*. Elife, 2022. **11**.
270. Zhang, Y., et al., *V3 spinal neurons establish a robust and balanced locomotor rhythm during walking*. Neuron, 2008. **60**(1): p. 84-96.
271. Borowska, J., et al., *V3 interneuron subpopulations in the mouse spinal cord undergo distinctive postnatal maturation processes*. Neuroscience, 2015. **295**: p. 221-8.
272. Bannatyne, B.A., et al., *Excitatory and inhibitory intermediate zone interneurons in pathways from feline group I and II afferents: differences in axonal projections and input*. J Physiol, 2009. **587**(2): p. 379-99.
273. Jankowska, E. and S.A. Edgley, *Functional subdivision of feline spinal interneurons in reflex pathways from group Ib and II muscle afferents; an update*. Eur J Neurosci, 2010. **32**(6): p. 881-93.
274. Olson, W., et al., *The specification and wiring of mammalian cutaneous low-threshold mechanoreceptors*. Wiley Interdiscip Rev Dev Biol, 2016. **5**(3): p. 389-404.
275. Graham, B.A. and D.I. Hughes, *Defining populations of dorsal horn interneurons*. Pain, 2020. **161**(11): p. 2434-2436.
276. Voute, M., V. Morel, and G. Pickering, *Topical Lidocaine for Chronic Pain Treatment*. Drug Des Devel Ther, 2021. **15**: p. 4091-4103.

277. Chang, C.H., et al., *Reversible Spasticity Suppression and Locomotion Change After Pulsed Radiofrequency on the Dorsal Root Ganglia of Rats With Spinal Cord Injury*. *Neuromodulation*, 2019. **22**(1): p. 53-60.
278. Bose, P., R. Parmer, and F.J. Thompson, *Velocity-dependent ankle torque in rats after contusion injury of the midthoracic spinal cord: time course*. *J Neurotrauma*, 2002. **19**(10): p. 1231-49.
279. Rabchevsky, A.G., et al., *Effects of gabapentin on muscle spasticity and both induced as well as spontaneous autonomic dysreflexia after complete spinal cord injury*. *Front Physiol*, 2012. **3**: p. 329.
280. Kitzman, P.H., T.L. Uhl, and M.K. Dwyer, *Gabapentin suppresses spasticity in the spinal cord-injured rat*. *Neuroscience*, 2007. **149**(4): p. 813-21.
281. Myers, J.N., *The physiology behind exercise testing*. *Prim Care*, 1994. **21**(3): p. 415-37.
282. Brett, S.E., J.M. Ritter, and P.J. Chowienczyk, *Diastolic blood pressure changes during exercise positively correlate with serum cholesterol and insulin resistance*. *Circulation*, 2000. **101**(6): p. 611-5.
283. Krassioukov, A. and V.E. Claydon, *The clinical problems in cardiovascular control following spinal cord injury: an overview*. *Prog Brain Res*, 2006. **152**: p. 223-9.
284. Hong, K.S. and K. Kim, *Skeletal muscle contraction-induced vasodilation in the microcirculation*. *J Exerc Rehabil*, 2017. **13**(5): p. 502-507.
285. Eckman, D.M. and M.T. Nelson, *Potassium ions as vasodilators: role of inward rectifier potassium channels*. *Circ Res*, 2001. **88**(2): p. 132-3.
286. Maiorana, A., et al., *Exercise and the nitric oxide vasodilator system*. *Sports Med*, 2003. **33**(14): p. 1013-35.
287. Aiku, A.O. and J.M. Marshall, *Contribution of prostaglandins to exercise hyperaemia: workload, ethnicity and sex matter!* *J Physiol*, 2019. **597**(19): p. 4887-4900.
288. Clifford, P.S., et al., *Mechanical compression elicits vasodilatation in rat skeletal muscle feed arteries*. *J Physiol*, 2006. **572**(Pt 2): p. 561-7.
289. Lu, X. and G.S. Kassab, *Integrins mediate mechanical compression-induced endothelium-dependent vasodilation through endothelial nitric oxide pathway*. *J Gen Physiol*, 2015. **146**(3): p. 221-32.
290. Dong, X., et al., *The Trajectory of Alterations in Immune-Cell Counts in Severe-Trauma Patients Is Related to the Later Occurrence of Sepsis and Mortality: Retrospective Study of 917 Cases*. *Front Immunol*, 2020. **11**: p. 603353.
291. Heffernan, D.S., et al., *Failure to normalize lymphopenia following trauma is associated with increased mortality, independent of the leukocytosis pattern*. *Crit Care*, 2012. **16**(1): p. R12.
292. Bastian, O.W., et al., *Impaired bone healing in multitrauma patients is associated with altered leukocyte kinetics after major trauma*. *J Inflamm Res*, 2016. **9**: p. 69-78.
293. Muire, P.J., L.H. Mangum, and J.C. Wenke, *Time Course of Immune Response and Immunomodulation During Normal and Delayed Healing of Musculoskeletal Wounds*. *Front Immunol*, 2020. **11**: p. 1056.
294. Trivedi, A., A.D. Olivas, and L.J. Noble-Haeusslein, *Inflammation and Spinal Cord Injury: Infiltrating Leukocytes as Determinants of Injury and Repair Processes*. *Clin Neurosci Res*, 2006. **6**(5): p. 283-292.
295. Kwiecien, J.M., et al., *Prolonged inflammation leads to ongoing damage after spinal cord injury*. *PLoS One*, 2020. **15**(3): p. e0226584.
296. Dienes, J.A., et al., *Analysis and Modeling of Rat Gait Biomechanical Deficits in Response to Volumetric Muscle Loss Injury*. *Front Bioeng Biotechnol*, 2019. **7**: p. 146.

297. Feldman, A.G. and M.F. Levin, *The equilibrium-point hypothesis--past, present and future*. Adv Exp Med Biol, 2009. **629**: p. 699-726.
298. Feldman, A.G., *Equilibrium Point Control*, in *Encyclopedia of Neuroscience*, M.D. Binder, N. Hirokawa, and U. Windhorst, Editors. 2009, Springer Berlin Heidelberg: Berlin, Heidelberg. p. 1145-1153.
299. Sainburg, R.L., *Should the Equilibrium Point Hypothesis (EPH) be Considered a Scientific Theory?* Motor Control, 2015. **19**(2): p. 142-8.
300. Ercison, M.O., R. Nisell, and G. Nemeth, *Joint Motions of the Lower Limb during Ergometer Cycling*. J Orthop Sports Phys Ther, 1988. **9**(8): p. 273-8.
301. Feldman, A.G. and M.L. Latash, *Testing hypotheses and the advancement of science: recent attempts to falsify the equilibrium point hypothesis*. Exp Brain Res, 2005. **161**(1): p. 91-103.
302. Frigon, A. and S. Rossignol, *Functional plasticity following spinal cord lesions*. Prog Brain Res, 2006. **157**: p. 231-260.
303. Ko, H.Y., *Revisit Spinal Shock: Pattern of Reflex Evolution during Spinal Shock*. Korean J Neurotrauma, 2018. **14**(2): p. 47-54.
304. Hamm, T.M., et al., *Persistent currents and discharge patterns in rat hindlimb motoneurons*. J Neurophysiol, 2010. **104**(3): p. 1566-77.
305. Murray, K.C., et al., *Recovery of motoneuron and locomotor function after spinal cord injury depends on constitutive activity in 5-HT_{2C} receptors*. Nat Med, 2010. **16**(6): p. 694-700.
306. Li, Y., M.A. Gorassini, and D.J. Bennett, *Role of persistent sodium and calcium currents in motoneuron firing and spasticity in chronic spinal rats*. J Neurophysiol, 2004. **91**(2): p. 767-83.
307. Gorassini, M.A., et al., *Role of motoneurons in the generation of muscle spasms after spinal cord injury*. Brain, 2004. **127**(Pt 10): p. 2247-58.
308. Bennett, D.J., et al., *Spasticity in rats with sacral spinal cord injury*. J Neurotrauma, 1999. **16**(1): p. 69-84.
309. Hiersemenzel, L.P., A. Curt, and V. Dietz, *From spinal shock to spasticity: neuronal adaptations to a spinal cord injury*. Neurology, 2000. **54**(8): p. 1574-82.
310. Cote, M.P., M. Murray, and M.A. Lemay, *Rehabilitation Strategies after Spinal Cord Injury: Inquiry into the Mechanisms of Success and Failure*. J Neurotrauma, 2017. **34**(10): p. 1841-1857.
311. Eaton, M., *Common animal models for spasticity and pain*. J Rehabil Res Dev, 2003. **40**(4 Suppl 1): p. 41-54.
312. Ibitoye, M.O., et al., *Strategies for Rapid Muscle Fatigue Reduction during FES Exercise in Individuals with Spinal Cord Injury: A Systematic Review*. PLoS One, 2016. **11**(2): p. e0149024.
313. Fazio, C., *Functional electrical stimulation for incomplete spinal cord injury*. Proc (Bayl Univ Med Cent), 2014. **27**(4): p. 353-5.
314. Abbott, B.C., B. Bigland, and J.M. Ritchie, *The physiological cost of negative work*. J Physiol, 1952. **117**(3): p. 380-90.
315. Penailillo, L., A.J. Blazevich, and K. Nosaka, *Factors contributing to lower metabolic demand of eccentric compared with concentric cycling*. J Appl Physiol (1985), 2017. **123**(4): p. 884-893.
316. Dudley, G.A., et al., *A simple means of increasing muscle size after spinal cord injury: a pilot study*. Eur J Appl Physiol Occup Physiol, 1999. **80**(4): p. 394-6.

317. Mahoney, E.T., et al., *Changes in skeletal muscle size and glucose tolerance with electrically stimulated resistance training in subjects with chronic spinal cord injury*. Arch Phys Med Rehabil, 2005. **86**(7): p. 1502-4.

LIST OF ABBREVIATIONS AND SYMBOLS

AD	autonomic dysreflexia
ANOVA	analysis of variance
AUC	area under the curve
BBB	Basso, Beattie, and Bresnahan locomotor rating scale
BF	biceps femoris
BP	blood pressure
BSA	bovine serum albumin
BWS	body weight support
BWSTT	body weight supported treadmill training
CGRP	calcitonin gene related peptide
CO	cardiac output
CPG	central pattern generator
CV	cardiovascular
CVD	cardiovascular disease
DAPI	4-,6-diamidino-2-phenylindole
DP	diastolic pressure
DRG	dorsal root ganglia
EMG	electromyography
EtOH	ethanol
f ₀	fundamental frequency
FES	functional electrical stimulation
FITC	fluorescein isothiocyanate
GABA	gamma-aminobutyric acid
HR	heart rate
Hz	hertz

IGF-1	insulin-like growth factor 1
j	scale factor
KCC2	potassium chloride cotransporter 2
l	length
L1-L5	lumbar level one-five
MAP	mean arterial pressure
MAP-kinase	mitogen-activated protein kinase
MC	motorized cycling
n	sample number
NDS	normal donkey serum
NF- κ B	nuclear factor kappa b
NRG-1	neuregulin-1
O.C.T	optimal cutting temperature
P_a	arterial pressure
PBS	phosphate-buffered saline
PBST	phosphate-buffered saline with Triton
PF	pedal force
PFA	paraformaldehyde
PIC	persistent inward currents
P_v	venous pressure
Q	blood flow
r	radius
R	resistance
RAST	robot assisted gait training
RMANOVA	repeated measures analysis of variance
RMS	root mean square
ROM	range of motion
RPM	rotations per minute
SCI	spinal cord injury
SD	standard deviation

T	threshold
T10	thoracic level ten
T2	thoracic level two
T5	thoracic level five
TKE	Teager-Kaiser Energy
TRPV1	transient receptor potential cation channel subfamily V member 1
VL	vastus lateralis
x	electromyography signal
δ_0	standard deviation
Δp	change in pressure
η	viscosity
μ_0	mean
ψ	Teager-Kaiser energy operator

CURRICULUM VITA
Gregory States, MEng

CONTACT INFORMATION:

Office Address:

Medical Dental Research Building
511 S. Floyd Street, RM 422
Louisville, KY 40202

Home Address:

1006 Carolyn Ave.
Nashville, TN 37216-3612

Telephone: C: 502-235-8304

E-mail: gregory.states@louisville.edu

ORCID: 0000-0001-7883-357X

EDUCATION:

2014 University of Louisville, Louisville, KY; B. S. in Bioengineering

2016 University of Louisville, Louisville, KY; MEng. in Bioengineering

2022 (anticipated) University of Louisville, Louisville, KY; PhD in Anatomical Sciences and Neurobiology

HONORS & AWARDS:

2013 Jerry and Pat Sturgeon Award, University of Louisville, Louisville, KY

2014 Departmental Alumni Award, University of Louisville, Louisville, KY

MAJOR PROFESSIONAL SOCIETIES (currently active):

Society for Neuroscience

PUBLICATIONS:

Articles published in refereed journals:

1. Carrasquer CA, Malik N, States G, Qamar S, Cunningham SL, and Cunningham AR. "Chemical Structure Determines Target Organ Carcinogenesis in Rats." SAR QSAR Environ Res. 2012 Oct;23(7-8):775-95. doi: 10.1080/1062936X.2012.728996.
2. Pocratsky AM, Burke DA, Morehouse JR, Beare JE, Riegler AS, Tsoufas P, States GJR, Whittemore SR and Magnuson DSK. "Reversible silencing of lumbar spinal interneurons unmasks a flexible, task-specific network for securing hindlimb alternation". Nature Comm. 2017 Dec 6;8(1):1963. doi: 10.1038/s41467-017-02033-x.
3. Harman KA, States G, Wade A, Stepp C, Wainwright G, DeVeau K, King N, Shum-Siu A, and Magnuson DSK. "Temporal analysis of cardiovascular control and function following incomplete T3 and T10 spinal cord injury in rodents". Physiol Rep. 2018 Mar;6(6):e13634. doi: 10.14814/phy2.13634.
4. Brown NP, Bertocci GE, States GJR, Levine GJ, Levine JM, Howland DR. "Development of a Canine Rigid Body Musculoskeletal Computer Model to Evaluate Gait". Front Bioeng Biotechnol. 2020;8:150. doi: 10.3389/fbioe.2020.00150.
5. Pocratsky AM, Shepard CT, Morehouse JR, Burke DA, Riegler AS, Hardin JT, Beare JE, Hainline C, States GJ, Brown BL, Whittemore SR, Magnuson DS. "Long ascending propriospinal neurons provide flexible, context-specific control of interlimb coordination". Elife. 2020 Sep 9;9. doi: 10.7554/eLife.53565.
6. States, G.J.R., Keller, A., Shum-Siu, A. et al. Broad opioid antagonism amplifies disruption of locomotor function following therapy-like hindlimb stretching in spinal cord injured rats. Spinal Cord (2021). <https://doi.org/10.1038/s41393-021-00705-6>

Published Abstracts:

1. States G, Keller A, Buckley C, Shum-Siu A, Magnuson D, "Naltrexone Amplifies Disruption in Locomotor Function Following Hindlimb Stretching in Rats with Spinal Cord Injuries" The 3rd Joint Symposium of the International and National Neurotrauma Societies and AANS/CNS Section on Neurotrauma and Critical Care, Toronto, Canada (2018)
2. States G, Buckley C, Shum-Siu A, Magnuson D, "Development of an Instrumented Passive Cycle to Measure Pedal Reaction Forces in Rats" The 18th International Symposium on Neural Regeneration, Asilomar, Pacific Grove, CA, United States (2020)
3. States, G.J.R, Shum-Siu, A.H, Roussel, T, Rouffet, D.M, Magnuson, D.S.K, "Interpretation of Pedal Reaction Forces During Motorized Cycling in a Rat Model of Spinal Cord Injury" The 50th Annual Neuroscience Meeting, Online, (2021)
4. States G, Magnuson D, "Interpretation of Pedal Reaction Forces in a Rat Model of Motorized Cycling " The 39th Annual Symposium of the National Neurotrauma Society,

including the AANS/CNS Joint Section on Neurotrauma and Critical Care, Atlanta, GA, United States (2022)

PRESENTATIONS:

Invited internationally or nationally:

1. States G, Keller A, Buckley C, Shum-Siu A, Magnuson D, "Naltrexone Amplifies Disruption in Locomotor Function Following Hindlimb Stretching in Rats with Spinal Cord Injuries" The 3rd Joint Symposium of the International and National Neurotrauma Societies and AANS/CNS Section on Neurotrauma and Critical Care (Data Blitz), Toronto, Canada (2018)
2. States G, Magnuson D, "Interpretation of Pedal Reaction Forces in a Rat Model of Motorized Cycling" I-OSCIRS and the International Spinal Research Trust, Online (2021)

Abstracts at local/regional meetings:

1. States G, Brown N, Levine G, Levine J, Howland D, Bertocci G, "Development of a Neuromusculoskeletal Model to Quantify Recovery Following Canine Intervertebral Disc Herniation" Research!Louisville, Louisville, KY (2014)
2. States G, Keller A, Buckley C, Shum-Siu A, Magnuson D, "Naltrexone amplifies disruption in locomotor function following hindlimb stretching in rats with spinal cord injuries" Research!Louisville, Louisville, KY (2018)
3. States G, Magnuson D, "Interpretation of Pedal Reaction Forces in a Rat Model of Motorized Cycling" 27th Annual Kentucky Spinal Cord and Head Injury Research Trust Symposium (2022)